AN INTEGRATION OF SEQUENCE STRATIGRAPHIC AND PETROPHYSICAL ANALYSIS IN THE BAKKEN FORMATION, NORTH DAKOTA

A Thesis

Presented to

the Faculty of the Department of Earth and Atmospheric Sciences

University of Houston

In Partial Fulfillment

of the Requirements for the Degree

Master of Science

By

Eren Dongel

July 2014

AN INTEGRATION OF SEQUENCE STRATIGRAPHIC AND PETROPHYSICAL ANALYSIS IN THE BAKKEN FORMATION, NORTH DAKOTA

____

Eren Dongel

APPROVED:

____

Dr. Julia Smith Wellner, Chairman

____

Dr. Robert R. Stewart, Member

____

Dr. Alison Henning, Member

____

Dean, College of Natural Sciences and Mathematics

Acknowledgements

I would like to thank people who supported, encouraged and believed in me throughout my academic education at the University of Houston.

I would like to express my sincere gratitude to my advisor, Dr. Julia Wellner for her support, guidance, encouragement, patience and advice during my research. I feel very lucky to be a part of your research group. Extended special thanks are given to Dr. Robert Stewart for his invaluable support, advice and encouragement. I would like to thank Dr. Alison Henning for being my committee member and her valuable guidance. I would like to give special thanks to Dr. Paul Mann and Dr. Peter Bartok for their suggestions and timely assistance.

I would like to thank Turkish Petroleum Corporation for financial support and giving me the opportunity to study abroad. I would like to extend my personal gratitude to my friends Mehmet Sahin and Ricardo Zavala for their help and advice on using the software.

I also want to express my appreciation for Audrey Stanley, who stuck with me during the long months of researching and writing this thesis. Thank you for endless patience and help.

Finally, I would like to thank my mother, Gulbin Dongel and my father, Recep Dongel for their support. Even though you are far away, you have had a place here in my heart.

AN INTEGRATION OF SEQUENCE STRATIGRAPHIC AND PETROPHYSICAL ANALYSIS IN THE BAKKEN FORMATION, NORTH DAKOTA

A Thesis

Presented to

the Faculty of the Department of Earth and Atmospheric Sciences

University of Houston

In Partial Fulfillment

of the Requirements for the Degree

Master of Science

By

Eren Dongel

July 2014

Abstract

A decrease in the discovery of reserves in conventional reservoirs has led to a focus on unconventional reservoirs. New techniques, such as hydraulic fracturing, provide better production conditions and allow the development of new reservoirs. The Bakken unconventional play is one of the most important oil plays since it has the largest crude oil accumulation in the United States.

During the study, 86 wells with the digitized format (log ASCII standard) were used for depositional environment analysis and petrophysical interpretation of the Bakken Formation in the northwest part of North Dakota. The Bakken Formation is subdivided into six facies which show diversity in thicknesses over the study area. The thicker parts of the Bakken Formation correlate to higher oil production.

Petrophysical and elastic properties of the Bakken Formation was examined in terms of their effects on productivity. The best calculation methods for these properties such as water saturation, effective porosity, brittleness, were tested according to the best match of log data calculations and core data results. Log data calculations show a harmonious trend with the core data.

It has been questioned as to whether brittleness can, in and of itself, be a key indicator of the productivity of a well. Brittleness, an important factor in hydraulic fracturing, was calculated by using log and mineralogy data. These results were used to estimate how the facies would respond to hydraulic fracturing, and were compared with petrophysical calculations for the determination of possible horizontal targets. High

brittle conditions allow the rock to be fractured resulting in a smoother production process.

The brittleness analysis shows that an increase in brittleness also results in an increase of productivity. Even though there were some areas with high resistivity and low water saturation conditions, which are key points for oil production, due to unsufficient brittleness, these areas are not ideal for drilling. Therefore, the brittleness has been concluded to be a key factor of how productive a well can and will be.

Table of Contents

List of Figures

List of Tables

1. INTRODUCTION

In the past, tight, impermeable formations, like shale, were considered uneconomical for oil and gas production. This aspect has been changed dramatically by the technology development in directional well drilling and reservoir stimulation. Production from unconventional plays has changed the United States' energy posture and global energy markets since 2007 (Bellelli, 2013). The use of new techniques, such as directional drilling and hydraulic fracturing, contributed to the United States becoming the largest natural-gas producer and the third-largest oil producer in the world in 2009, according to the U.S. Energy Information Administration. Texas and North Dakota are the main contributors to skyrocketing crude-oil production from shale and related tight oil formations. Other tight oil plays are also assisting to raise energy independence (Figure 1.1).

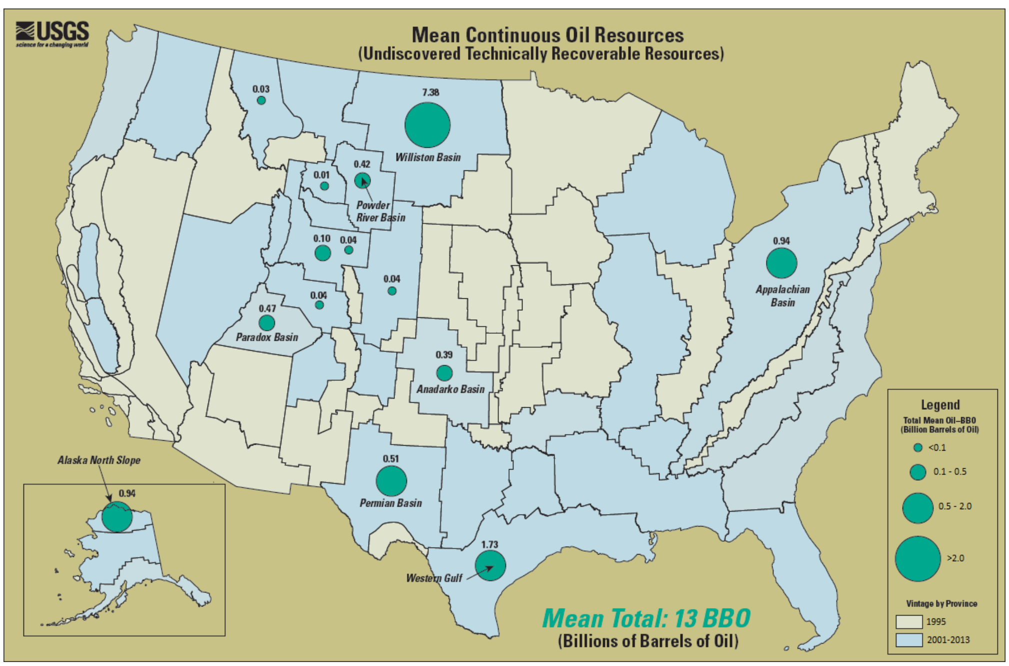

Figure 1.1. Mean Continuous Oil Resources in the United States (USGS, 2013)

For assessment purposes, oil and gas resources are commonly divided into two prominent types: conventional and unconventional. Conventional formations are characterized by discontinuous structural, stratigraphic, or combination traps where water, gaseous hydrocarbons, and liquid hydrocarbons are separated according to their immiscible and relative buoyancy features (Milici and Swezey, 2006).

Unconventional formations, “continuous-type deposits” or “tight formations”, consist of fine grained, organically rich, sedimentary rocks that are usually shales or similar impermeable rocks such as mudrocks. The rocks for unconventional petroleum systems, can be both the source and reservoir for oil and natural gas (Ratner and Tiemann, 2014). Continuous-type deposits are not affected by hydrodynamic influences such as oil/water or gas/water contacts (Attanasi et al., 1995).

The Williston Basin has been important in terms of horizontal drilling since 1987, when the first horizontal wells were drilled into the Bakken Formation. Though the horizontal drilling activity declined in the Bakken in the early 90’s, a variety of formations, such as Red River and Mission Canyon plays, have been targeted for horizontal drilling in the Williston Basin. After the shale play in the early 90’s, the Bakken Formation again became a possible target for horizontal drilling. An increase in thickness of the Bakken towards the center of the basin increases the potential for drilling (LeFever, 2006).

According to the United States Geological Survey (USGS) oil assessment, the Bakken Formation is the largest continuous crude oil accumulation in the United States. The Bakken Formation of the Williston Basin, in Montana and North Dakota, has undiscovered volumes of 3.65 billion barrels of oil, 1.85 trillion cubic feet of associated/dissolved natural gas, and 148 million barrels of natural gas liquids (Pollastro et al., 2008).

The purpose of this study is to find a link between stratigraphy, petrophysical and elastic parameters and productivity in the Bakken Formation. Different well locations were chosen and analyzed for their depositional environment and their stratigraphy. Well logs were used for calculation of petrophysical parameters (shale volume, effective porosity, and saturation) and elastic properties (Poisson's ratio, Young's modulus, and brittleness index) of the Bakken Formation. Accuracy of these properties was tested by comparing them with analyzed core data. Different methods were applied to calculate these parameters and applicability of these methods for the Bakken Formation was tested. Each parameter was analyzed and interpreted in terms of their contribution to productivity. The results were compared with the monthly production data to check the accuracy of the calculations.

2. GEOLOGIC BACKGROUND

2.1. The Williston Basin

The Williston Basin, in central North America, is a broad, circular, intracratonic basin that covers portions of North Dakota, South Dakota and Montana in the United States, in addition to southwest Manitoba and southeast Saskatchewan in Canada (Figure 2.1) (Ahern and Mrkvicka, 1984; Price et. al, 1986). The basin reaches 560 km (350 mi) in diameter with an area of 250,000 km^2 (96,500 mi^2) and 4900 m (16,000 ft) maximum stratal thickness (Kent and Christropher, 1994). The sediment deposition took place from the Cambrian to the Tertiary periods. From the Cambrian to Middle Mississippian, predominantly carbonate rocks were formed; after the Middle Mississippian, clastic sediments were deposited. The basin is structurally simple, and sediments thicken toward the center and thin as it extends to the edges (Flannery, 2006).

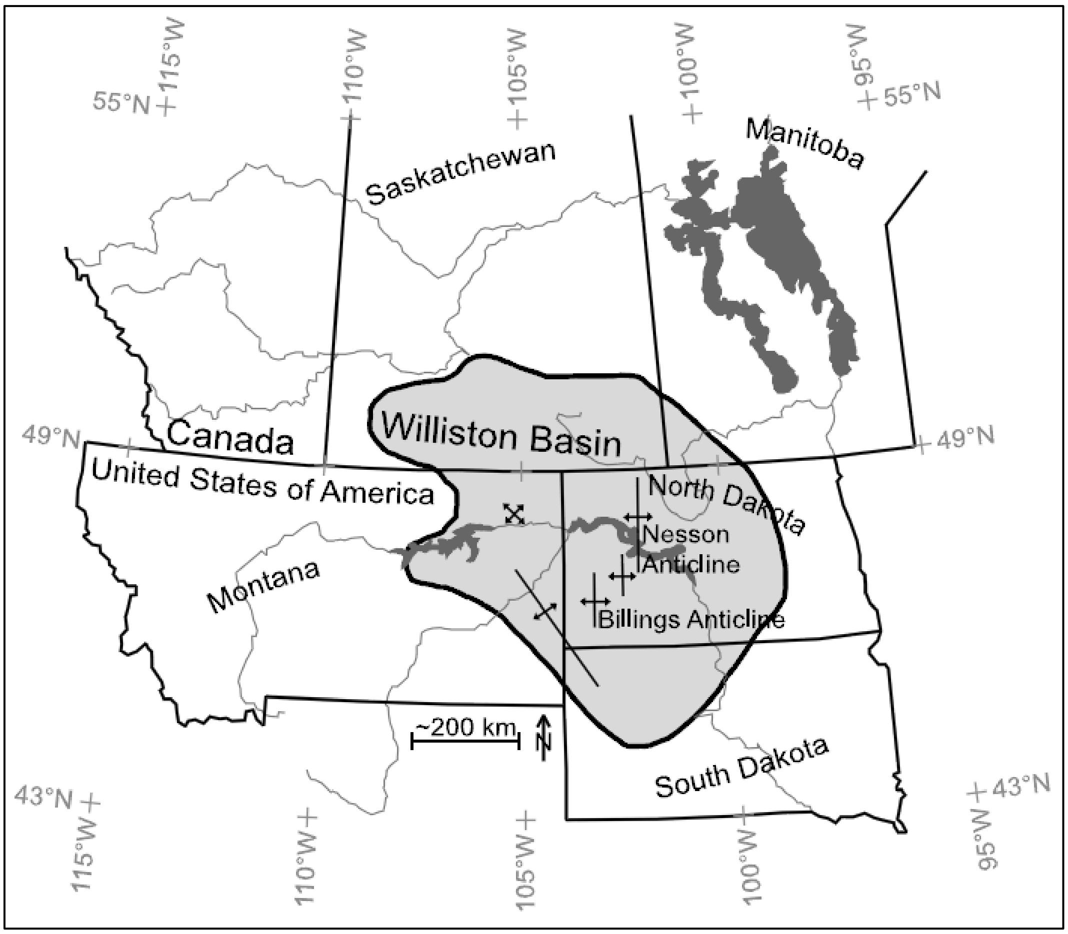

Figure 2.1. Location of the Williston Basin in the United States and Canada (Kuhn et. al., 2012)

The Williston Basin first originated as a cratonic-margin basin, initially filled by Upper Cambrian strata, which became intracratonic after the Cordilleran orogeny (Burgess, 2008; Gerhard et al., 1990). The basin was created with a steady and slow subsidence. Major gaps in the basin's stratigraphy are related to eustatic variations in sea-level. From the Cambrian to the early Cretaceous, the basin was filled with sediments near sea-level. Therefore, small falls in sea-level led to erosion (Figure 2.2). Other factors affecting sediment facies changes and thickness variations include a varying distribution of the sediment load, local accidents of erosion, and deposition influencing the flexural history of the lithosphere (Nisbet and Fowler, 1984).

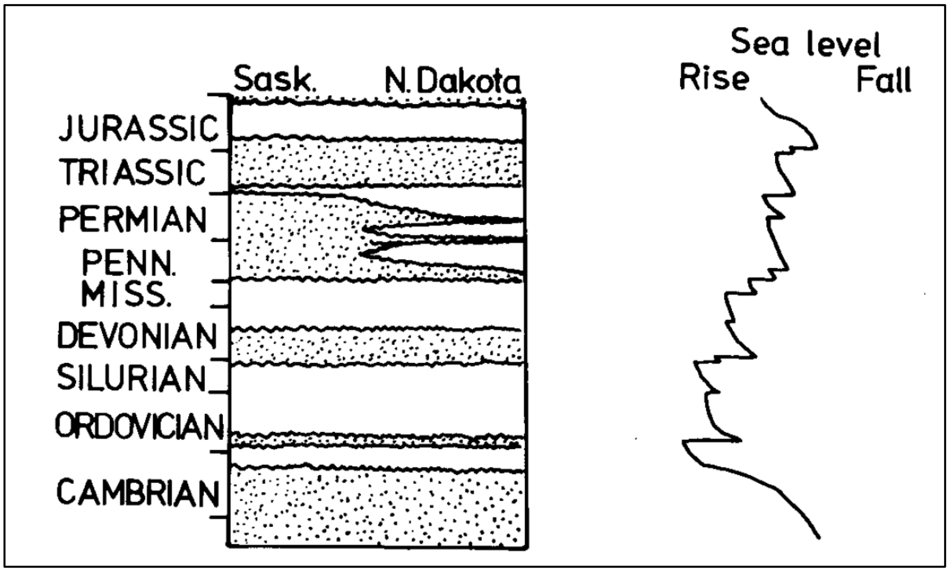

Figure 2.2. Stratigraphic record of the Williston Basin. Each low sea-level correlates with erosional gaps which are shown as stippled (Nisbet and Fowler, 1984).

The rocks of the Williston Basin (cratonic or cratonic-margin originated) can be divided into continental-scale packages corresponding to when the sea level increases, the subsequent sedimentation, and then a subsequent drop in sea-level with accompanying unconformity. Sloss (1963) called these packages “sequences”. The Bakken Formation took form as a result of a major transgression during the Late Devonian in the Kaskaskia sequence (Anna et. al., 2010) (Figure 2.3). Upper Kaskaskia sequence rocks (Mississippian and uppermost Devonian) have the most petroleum of the Williston Basin (Gerhard et. al, 1991).

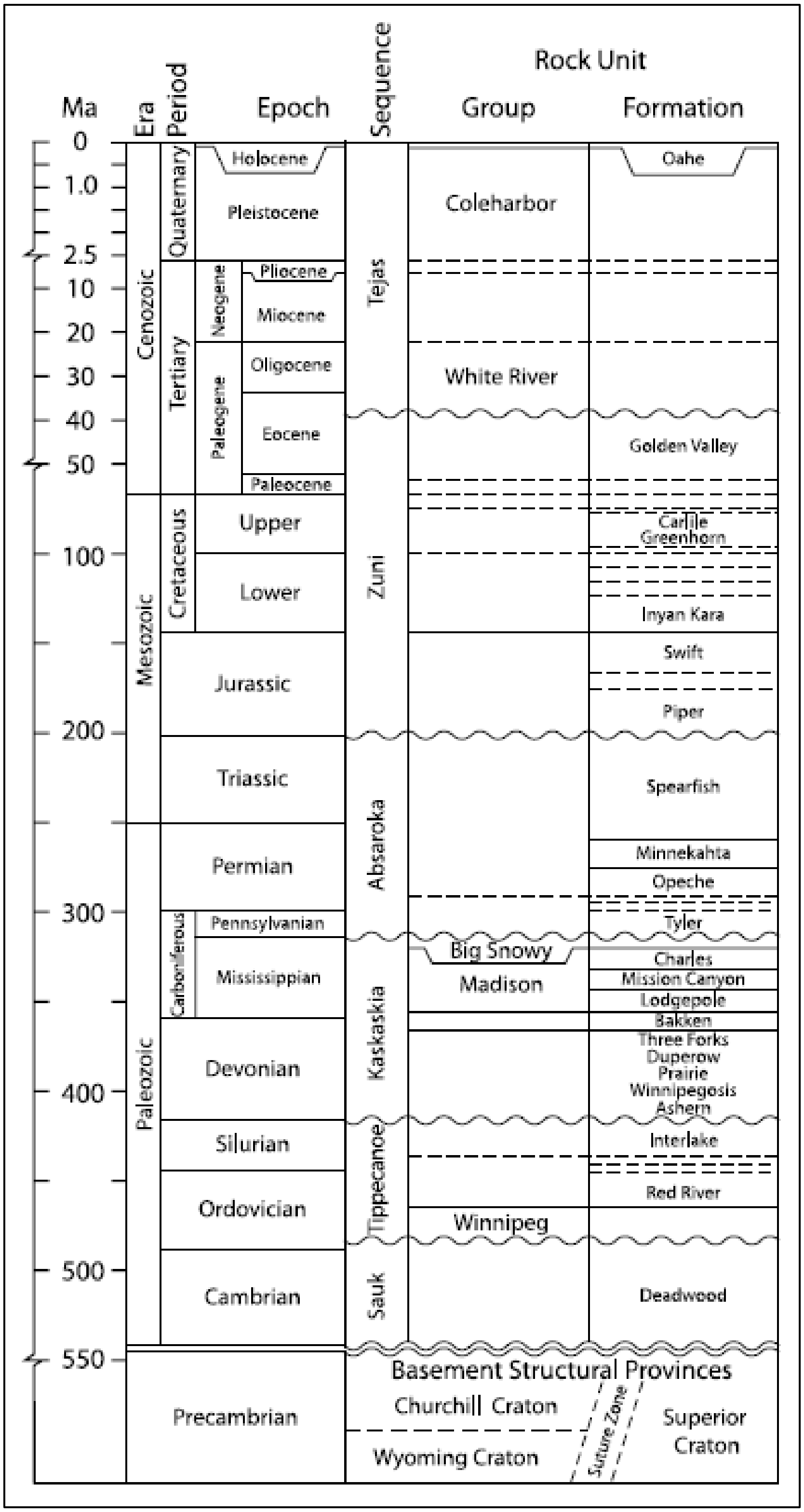

Figure 2.3. Stratigraphic column of the Williston Basin (Kuhn et. al., 2012)

There are several remarkable structures in the U.S. portion of the Williston Basin, which are oriented predominantly to the north or northwest. The north-trending structures consist of the Nesson, Billings, and Little Knife anticlines. Northwest-trending structures include the Cedar Creek, Antelope, and Poplar anticlines (Figure 2.4). Currently, all of these structures are capable of producing oil (LeFever, 1992).

The Nesson anticline is the largest anticlinal structure in the North Dakota part of the Williston Basin (Gerhard et al., 1987). It is also the largest producing structural feature in North Dakota (LeFever et al., 1987). Nesson anticline was initiated with Precambrian. Lower-Cambrian sediments were deposited around, but not over the present anticline. Upper-Cambrian rocks are present where they onlap the top of the structure. Abrupt changes in thickness across the structure are indicator of fault movement on the west flank of the Nesson. Renewed activity along the fault affected Winnipeg deposition during early Ordovician. Thinning of the post-Winnipeg – pre-Devonian section is caused by renewed uplift without faulting. Second vertical fault movement took place in the pre-Pennsylvanian, post-Mississippian Big Snowy section. The stress regime was changed with the mid-Permian event. The former normal fault changed direction of movement, up on the west, instead of down on the west. There is reversal of movement along the Nesson fault in the pre-Late Cretaceous. Since that time, little evidence was found for major fault movement. Cretaceous rocks are folded across the structure and may also be faulted (Gerhard et al., 1982).

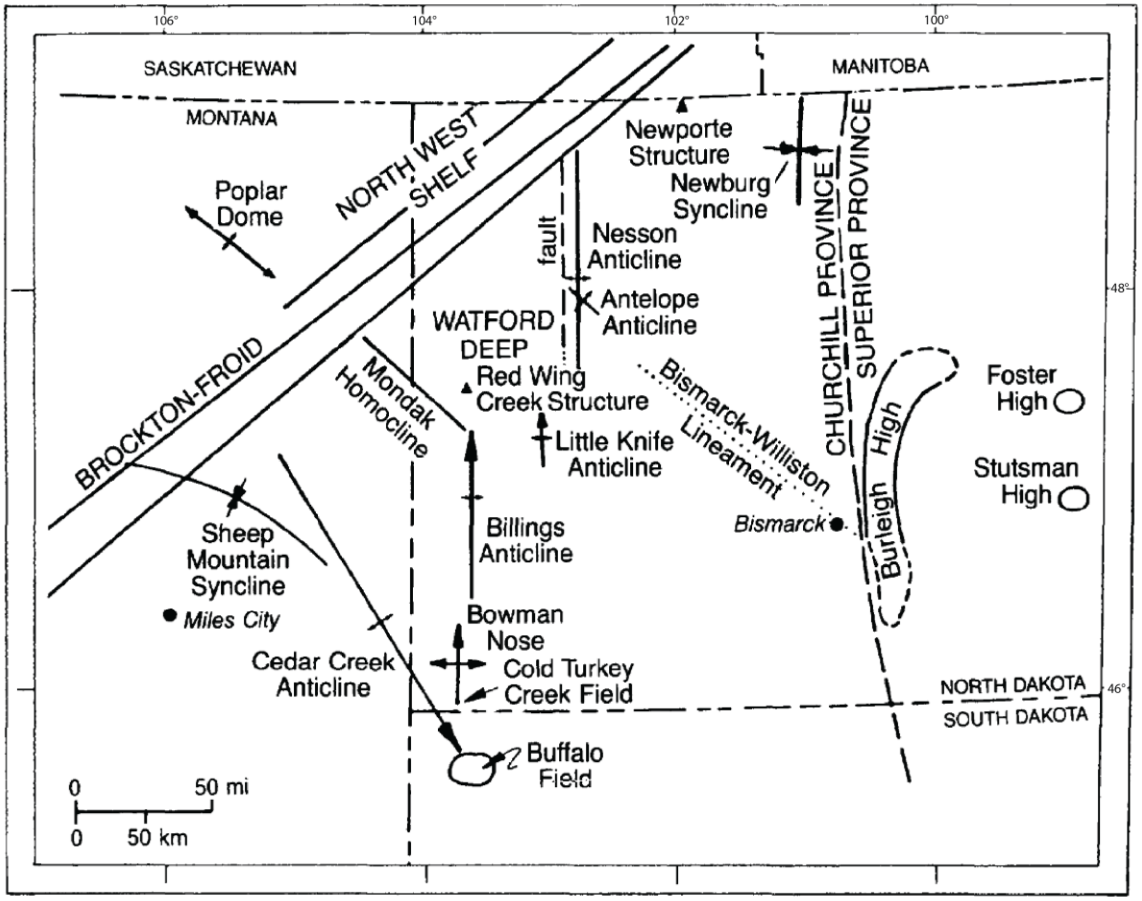

Figure 2.4. Major Structures of the Williston Basin (Gerhard et al., 1990)

2.2. The Bakken Formation

2.2.1. Bakken Formation Geology

The Lower Mississippian – Upper Devonian Bakken Formation consists of a highly organic rich and siliciclastic rock sequence that is only present within the central and deeper parts of the basin. Maximum thickness of the formation is about 160 ft. (48 m) in the U.S. part of the basin. The total formation thickness reaches the maximum value near the center of the Williston Basin and becomes nonexistent reaching the edge of the eastern, southern and southeastern flanks (Meissner, 1978) (Figure 2.5). Although the thickness seems small compared to the 16,000 ft. thickness of the basin, the formation has high quality petroleum source and reservoir rock potential which can produce huge amounts of undiscovered hydrocarbons (Pollastro et. al., 2010).

The Bakken Formation is stratigraphically between the Three Forks Formation and The Lodgepole Formation. The Bakken overlays the upper Devonian Three Forks Formation conformably in the basin center and unconformably toward the basin margin. The Bakken Formation is conformably overlain by the Lower Mississippian Lodgepole Formation which is the basal unit of the Madison Group (LeFever 1991, Meissner 1978).

The Bakken Formation consists of three members: the upper shale member, the middle siltstone member and the lower shale member (Webster, 1984). Hayes and Holland (1983) used conodonts to date the formation in North Dakota. Conodonts from the lower shale affirm a late Devonian (Famennian) age, however, conodont evidence from the upper shale suggests a Mississippian age. In the middle member, only rare, fragmentary conodonts have been found.

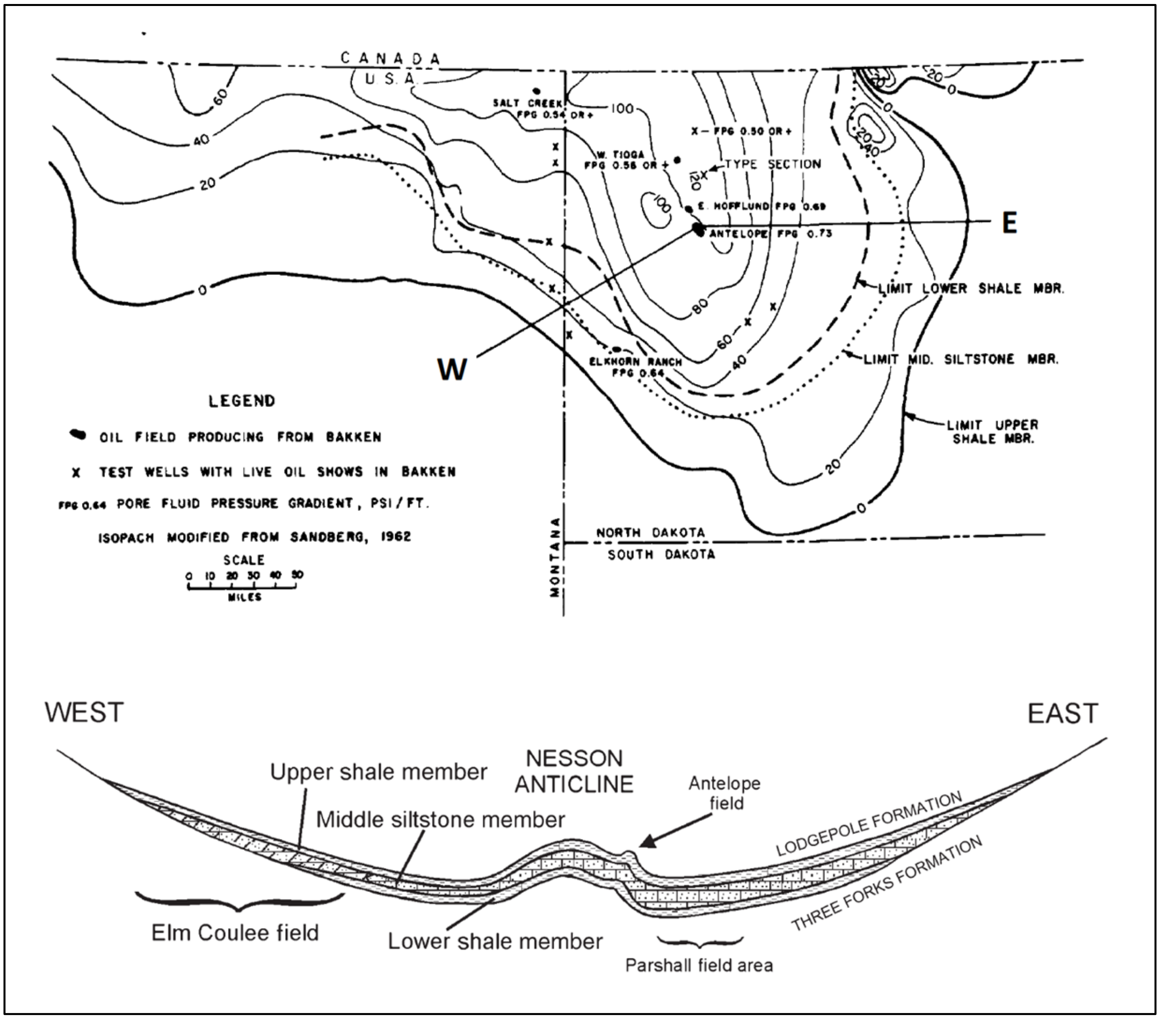

Figure 2.5. The limit of the Bakken members in the U.S. (modified from Meissner, 1978) and west-east schematic cross section of the Bakken Formation (Sonnenberg and Pramudito, 2009, modified from Meissner, 1978).

The Bakken Formation can be easily recognized using wireline logs in the subsurface of the Williston Basin. The Bakken reflects unique log responses in the Paleozoic rock section of the basin which is widely used as a marker. The upper and lower shales show abnormally high gamma-ray readings (>200 API), low resistivity (ohm-m) readings in the shallower parts of the basin, high resistivity readings in the deeper portion of the basin, and high interval transit times (80 to 120 microsec/ft)

(Meissner, 1978; Webster, 1984; LeFever et al., 1991). The middle member has normal log characteristics for carbonates and clastics. Figure 2.6 shows the well log readings for the Bakken lithology. When the lower shale becomes absent towards the basin margins, it becomes difficult to distinguish the middle member from the underlying Three Forks Formation (LeFever et al., 1991).

The upper and lower shale members are the source rocks of the Bakken Formation. The maximum thickness of the lower shale reaches 50 ft (15.2 m) (Webster, 1984). The lower shale varies from dark-gray to brown-black to black, competent and massive to fissile, slightly to highly organic rich shale and locally calcareous at its base. The upper shale, which reaches a maximum thickness of 23 ft (7 m), is lithologically similar to the lower shale and can be described as dark-gray to brownish-black to black, fissile, slightly calcareous, and organically rich. It differs from the lower shale with a higher organic content, and a lack of crystallized limestones and greenish-gray beds (Webster 1984; Pitman et al., 2001). The shale members develop into a kerogen-rich (type-II kerogen), mature source rock with evenly distributed organic material through the deeper portion of the basin. The middle Bakken member, which is the reservoir rock of the formation, reaches a maximum thickness of 90 ft (27 m) (LeFever, 2008). The lithology of the middle member varies from light to medium gray, very dolomitic fine-grained siltstone to a very silty, fine-crystalline dolomite (Meissner, 1978).

The three members of the Bakken Formation display an onlapping relationship; each successively higher member has a larger areal distribution (LeFever et al., 1991). The lower shale overlies the Three Forks Formation conformably in the central part of the

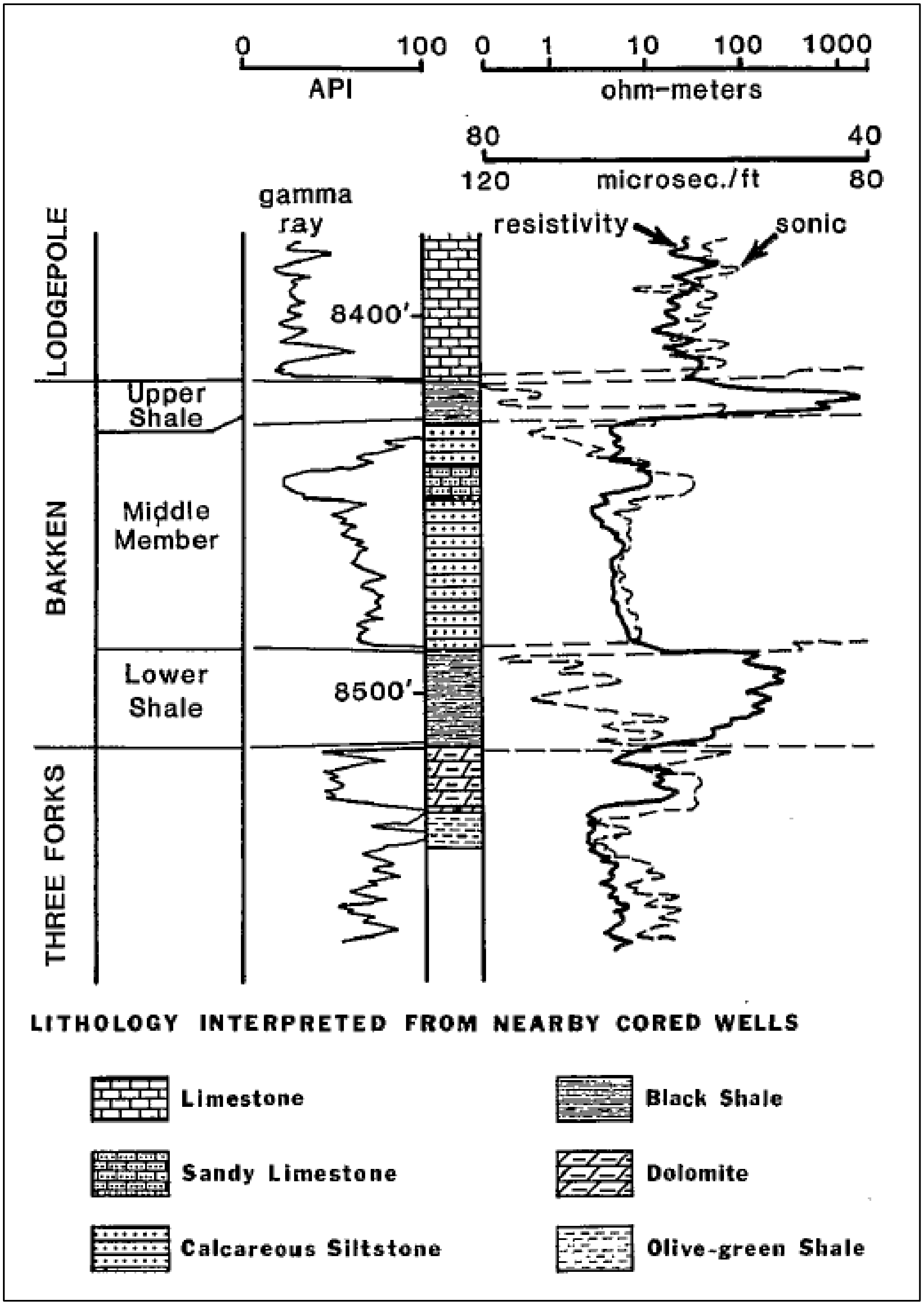

Figure 2.6. Well logs and interpreted lithology of the Tipperary Oil and Gas Corporation Olsen No. 1 well, SE-SW Sec 26, T160N, R97W. Divide County (Webster, 1987).

basin with an angular conformity along the margins. The middle member is conformable with the lower shale in the central part of the basin and oversteps it and lies unconformably on the Three Forks Formation along the basin margin. The upper shale has the greatest distribution of the three members. Extension of the upper member is considered to represent the general depositional limit of the Bakken. It conformably overlies the middle member. Along the depositional edge, the upper shale unconformably overlies the Three Forks Formation. The member is conformably overlain by the Lodgepole Formation (LeFever, 1991) (Figure 2.7).

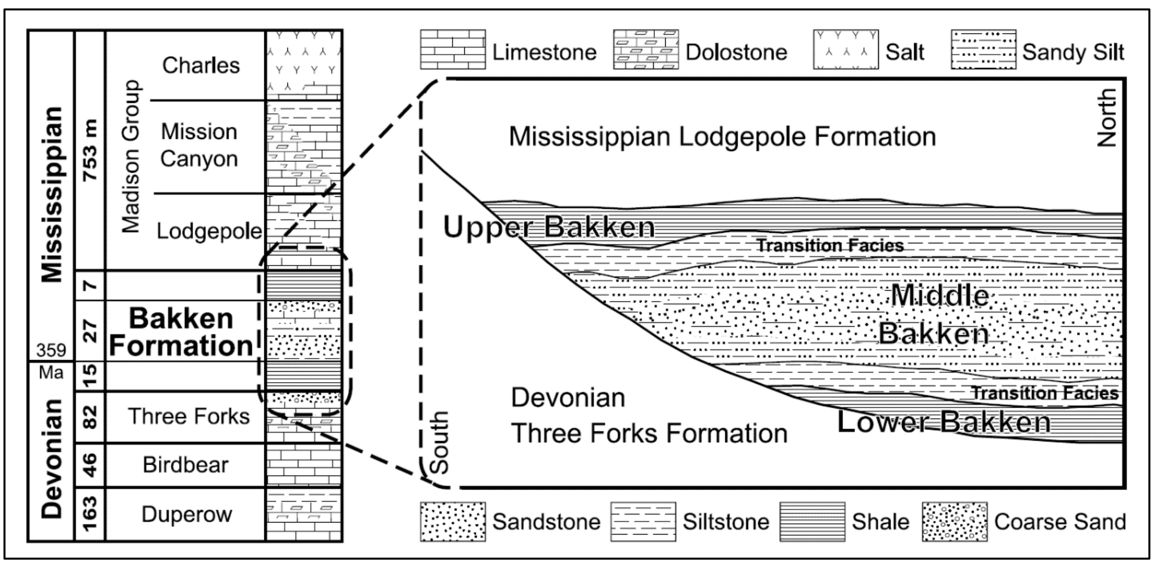

Figure 2.7. Stratigraphic column and schematic profile of the Bakken Formation (Kuhn et al., 2012).

The total organic carbon (TOC) of the Bakken shales ranges between 3 and 25 wt. % (average of 11.33 wt. %) and are composed of amorphous, sapropelic kerogen (Schmoker and Hester, 1983; Price et al., 1984). The upper Bakken shale has a higher TOC (average 12.1 wt. %) than the lower Bakken shale (average 11.5 wt. %). The TOC is depleted near to the oil window since the organic matter is converted to oil and expelled from the source rocks. The Bakken source rocks can be divided into three zones in terms of maturation in North Dakota (Figure 2.8). In the first zone, referred to as 'immature', the Bakken shales have low hydrocarbon content in the eastern region. The second zone reflects that shales are entering the stage of oil generation. Hydrocarbon content slightly increases and the breakdown of kerogen begins. The third zone shows an intense hydrocarbon generation which corresponds to the deepest part of the basin. This zone is considered as an effective source area of the Bakken where enough hydrocarbons have been generated to charge oil reservoirs (Webster, 1987).

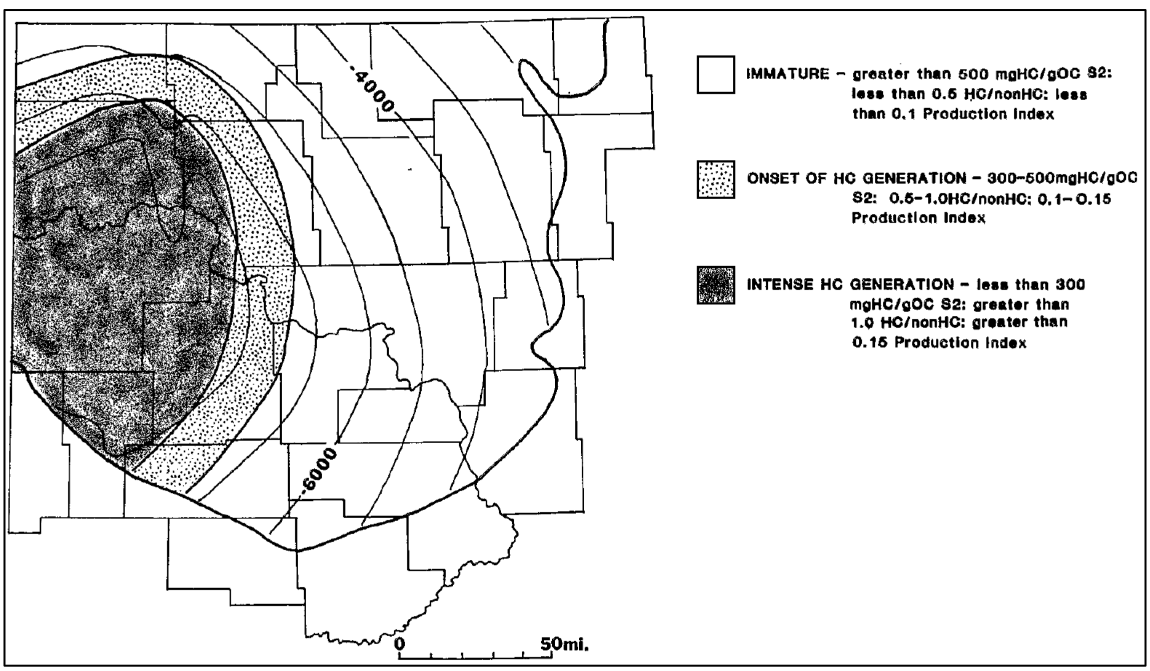

Figure 2.8. Map of source rock maturity zones in the Bakken shales with superimposed structure contours on top of the Bakken Formation. Numbers on contours the subsea depth of the Bakken. (modified from Webster, 1987).

Porosity in both the lower and the upper Bakken shales ranges from nonexistent to an average of 3.6 % (Meissner, 1978; Kuhn et al., 2012). The middle Bakken porosities are generally low, ranging from 1 to 16% with an average of 5% (Pitman et al., 2001). The vertical permeability ranges from 0.01 to 0.001 μd (Burrus et al., 1996a) whereas the middle Bakken has the permeability, ranges from 0 to 20 md, with an average of 0.04 md (Pitman et al., 2001). Permeability is also depends on the thermal maturity of the source shales. With the increase of burial depth, permeability of sandstones decreases from a range of about 0.06 to 0.01 md with the adjacent immature shale, to a range of about ≤0.01 to 0.01 md where these shales are mature. Reservoir sandstones and siltstones, where the adjacent shales are thermally immature and kerogen-poor, typically are devoid of fractures and have lower permeabilities. On the other hand, reservoir rocks, where the adjacent shales are thermally mature and kerogen-rich, generally have a high fracture density with a large residual oil content and therefore significant permeability enhancement (Pitman et al., 2001).

2.2.2. Facies Descriptions

In previous studies, different facies naming methods were applied for the Bakken Formation. Although the shale units have been mostly named as the upper and lower shale members, the middle Bakken was named alphabetically or numerically (Figure 2.9).

Holland et al. (1987) and Thrasher (1987) divided the middle Bakken member into three units by using conodonts and macrofossils which allowed more accurate biozonation in North Dakota. These three units are a Late Famennian aged lower unit

(Unit 1), poorly fossiliferous middle unit (Unit 2), and Mississippian aged upper unit (Unit 3).

LeFever et al. (1991), described seven lithofacies (lithofacies units range from 1 to 7 moving upward) in the cores of the middle member in northern North Dakota. These facies are correlative with the cores from Manitoba and Saskatchewan.

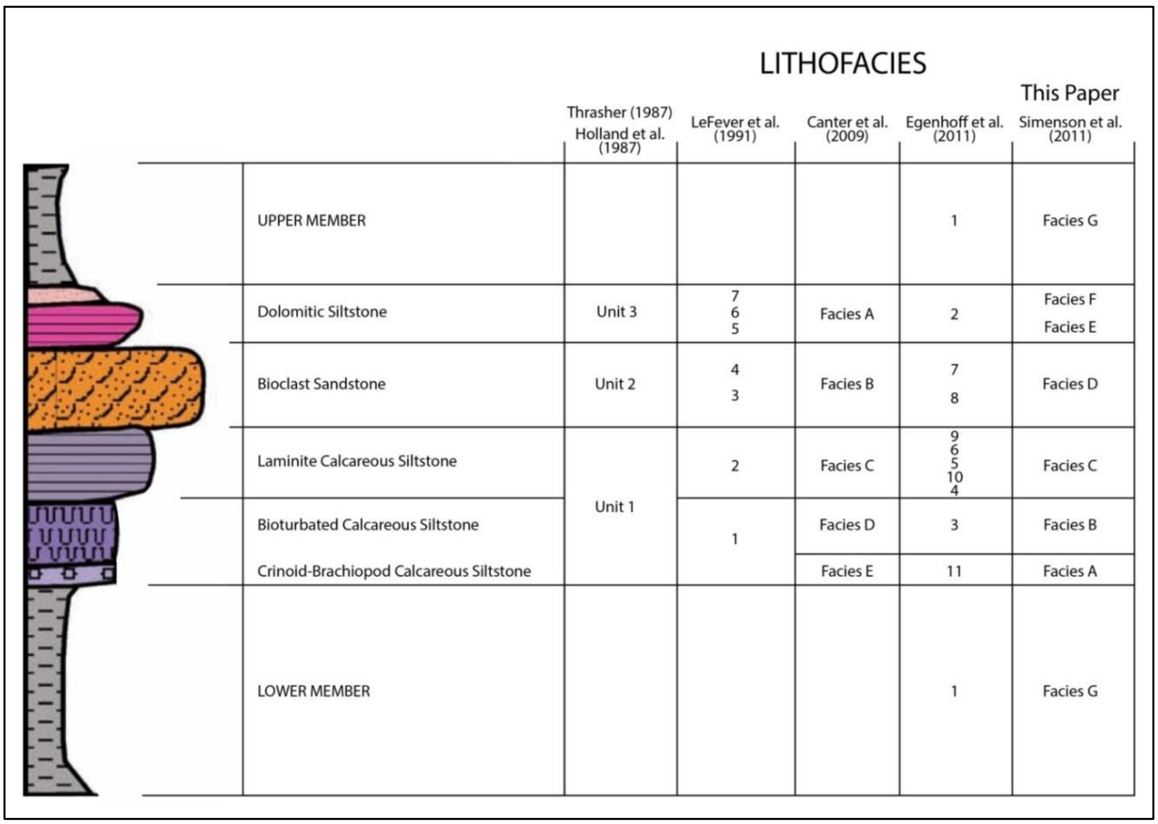

Figure 2.9. Composite lithofacies descriptions and correlations for the middle member of the Bakken Formation (The stratigraphic column is modified from Sonnenberg et al., 2011).

Canter et al. (2009), recognized five facies within the middle Bakken cores from the Sanish and Parshall Fields of Mountrail County, North Dakota. They named the facies Facies A to E from bottom to top.

Egenhoff et al. (2011) subdivided the Bakken Formation into 11 facies, ten of which characterize the middle Bakken, while the other forms the lower and upper Bakken shale members.

Simenson et al. (2011) identified six facies and designated them A to G ranging from bottom to top which differs from the division originally created by Canter et al which was oriented from top to bottom. (2009). In addition to this, Facies C was subdivided into facies C1 and C2 and Facies D was subdivided into facies D1 and D2 based on sedimentary structures. Facies E is subdivided into Facies E1 and E2 by considering bioturbation intensity and sedimentary features.

In this study, the names applied to the middle Bakken facies are consistent with that of Simenson et al. (2011) due to the fact that this is the most recent study written about Bakken facies naming. Six facies were described and the names were given alphabetically (A-G) from bottom to top.

2.2.2.1. Facies A. Muddy Lime Wackestone

Facies A consists of muddy lime wackestone that accommodates crinoids and brachiopod shell fragments. This thin bed is settled above the lower shale member and could correspond to the first carbonate influx into the system. It is composed of varying amounts of siltstone grains and carbonate and siliciclastic mudstone matrix. The facies is dark gray to tan in color depending on mud-silt content. Calcite and pyrite are the dominant cements, intergranular in porosity. The amount of pyrite increases closer to the lower Bakken contact. The thickness of individual units of this facies is from 1 to 5 ft.

The facies is also highly bioturbated and there are no relics of bedding preservation (Egenhoff et al., 2011; Simenson et al., 2011).

2.2.2.2. Facies B. Bioturbated, Argillaceous, Calcareous, Very-Fine-Grained Siltstone/Sandstone

This facies is composed of a light gray fine- to medium-grained siltstone with varying amounts of siliciclastic and carbonate mud. The facies is massive in size and has strong bioturbation which makes identification of many trace fossils difficult but *Helminthopsis/Sclarituba* burrow traces have been identified. On the other hand, Angulo and Buatois (2009) identified abundant occurrences of trace fossils *Nereites* and minor amounts of *Teichichnus*. Calcite cement and some pyrite cement are present in microfracture porosity. Beds of this facies range from 3 to 34 ft with an average of 20 ft (Egenhoff et al., 2011; Simenson et al., 2011).

2.2.2.3. Facies C. Planar to Undulose Laminated Shaly, Very-Fine-Grained Siltstone/Sandstone

Facies C consists of finely laminated shaly sandstone and siltstone where the lamination range anywhere from one millimeter to several centimeters. There are some wavy laminated parts which are possibly caused from microbial influence of the sediment, but the section is dominated by continuous planar laminations. The facies has intergranular and minimal amounts of intercrystaline porosity. In the upper portion of the facies there is a finely laminated to rippled, shaly, very fine-grained sandstone unit which reaches average 3 ft in thickness. The thickness of Facies C ranges from 2 to 15 ft with an average of 8 ft (Egenhoff et al., 2011; Simenson et al., 2011).

2.2.2.4. Facies D. Low Angle, Planar to Slightly Undulose, Cross-Laminated Sandstone with Thin Discontinuous Shale Laminations

Facies D is a light brown to light gray and massive sandstone, which consists of parallel to undulating laminated, low angle cross-laminated, well-sorted, very fine to medium grained, calcite-cemented, mostly quartz sand grains. Bioturbation is minor to absent in this facies. The thickness ranges from 0 to 22 ft with an average of 8 ft. Upper and lower contacts of the facies are generally sharp (Egenhoff et al., 2011; Simenson et al., 2011).

2.2.2.5. Facies E – F. Finely Inter-Laminated, Bioturbated, Dolomitic-Mudstone and Dolomitic Siltstone/ Sandstone – Bioturbated, Shaly, Dolomitic Siltstone

Interbedded dark gray, highly bioturbated siltstone, and light gray, very-fine grained thin parallel laminated sandstone forms Facies E. The sediments are affected by locally strong and moderate bioturbation. This unit is the most dolomitic zone of the middle Bakken and mainly consists of dolomite grains. The thickness of the interval ranges from 5 to 11 ft with an average of 8 ft. Facies F lies below the contact with the upper Bakken shale and consists of a bioturbated, shaly, dolomitic siltstone with the thickness from 0 to 3 ft, averaging 2 ft (Simenson et al., 2011).

2.2.2.6. Facies G. Organic-Rich Pyritic Brown/Black Mudstone

Facies G consists of dark gray, brownish-black to black, fissile, non-calcareous, carbonaceous and bituminous shale. There is pyrite precipitation throughout the laminae which also consists of silt and carbonate grains. Carbonate grains can be calcite or dolomite. This facies comprises both the lower and upper Bakken shales. Over and underlying lithologies of this facies can be sharp or gradational. Lags of pyritized bioclasts characterize the contact between the upper Bakken shale and the middle Bakken member. The black shales also show abundant calcite, pyrite, and quartz-filled cracks that are confined to distinct laminae or thin beds (Egenhoff et al., 2011; Simenson et al., 2011).

2.2.3. Depositional Environment

Deposition of the Three Forks Formation ended in Late Devonian with the deposition of shallow marine to terrestrial sediments during a marine regression to the northwest. During the Late Devonian to Early Mississippian time period, major uplift and erosion took place along the margins of the Williston Basin. Transgression of sea level supplied the deposition of the lower Bakken shale during the Late Devonian. Oxic conditions during the Three Forks deposition were replaced with an anoxic depositional environment during part of the Bakken time according to the nature of Bakken shale. During early Bakken time, some changes arose in either basin geometry, climate, or water circulation, which caused anoxic, likely tranquil conditions. An influx of coarser clastics into the basin ended these anoxic conditions in middle Bakken time. Fauna and bedding features of the middle Bakken demonstrate a normal shallow marine to near-shore marine depositional environment. Bedding features, oolitic carbonate grains, and trace fossils reveal shallow-marine conditions during part of middle Bakken deposition. Depositional environment returned to anoxic in the basin during the upper Bakken shale deposition. Normal, oxygenated water conditions prevailed during the Lodgepole carbonate sedimentation in the basin in Mississippian time (Webster, 1984).

2.2.3.1. Deposition of the Lower and Upper Bakken Members

Micro-laminated, fine-grained, organic-rich muds of the Lower and Upper Bakken deposited in a distal, deep water, marine setting took place throughout much of the Williston Basin (Figure 2.10). Suspended silt and clay-size siliciclastic sediment slowly accumulated on a tranquil basin floor remaining unaffected from any storm-wave generated surface water circulation. Based on conodont biostratigraphy, a sedimentation rate of approximately 1 to 3 m per million years took place for the Bakken mudstone members. The consistence of a fine grained texture of black mudstone expresses that the slow rate of sedimentation endured throughout the deposition of the lower and upper members.

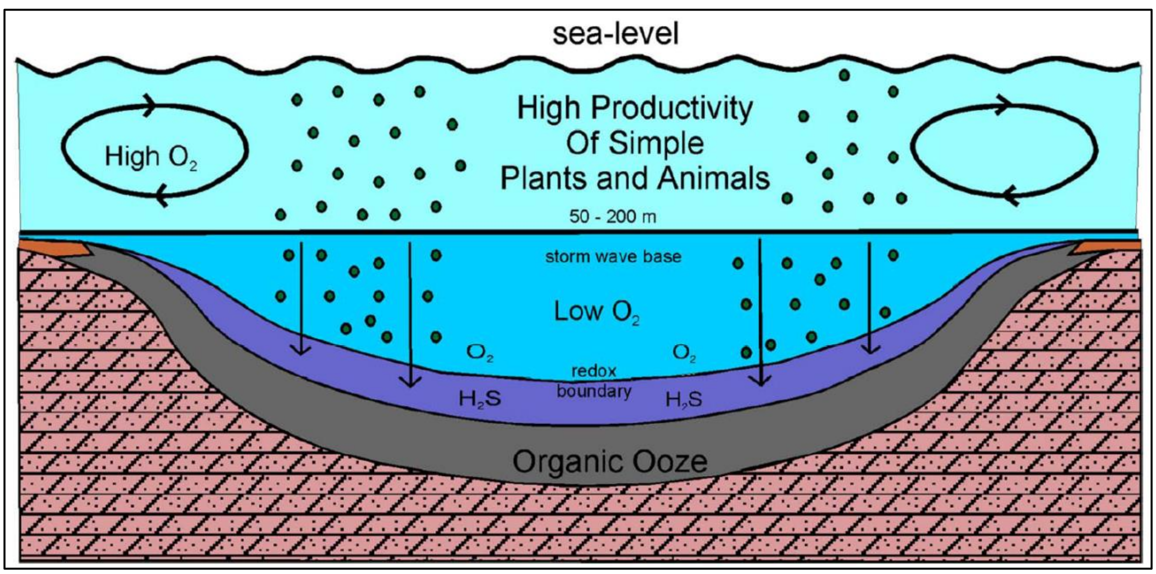

Figure 2.10. Depositional setting of the lower and upper Bakken members in the Williston Basin (Jin and Sonnenberg, 2012).

Numerous authigenic pyrite nodules, calcite/pyrite concretions, and calcite nodules reflect the conditions on the floor of the Williston Basin during the deposition of the black mudstone members. The formation of in situ pyrite took place in uncompacted sediments on the bottom of the basin under strongly reducing, moderately acidic to weakly alkaline, anoxic conditions with concentrations of dissolved Fe and hydrogen sulfide (H_2S) in pore water. Secondary calcite formation as well as the preservation of calcite shells demonstrate alkaline and reducing conditions in bottom waters. Anoxic conditions on the basin floor resulted from oxygen reduction in poorly circulating bottom waters caused by the decomposition of vast amount of organic matter in the bottom sediments. Complete depletion of dissolved oxygen followed by the depletion of dissolved sulfate in bottom waters generated the production of heightened, toxic, concentrations of H_2S (Smith and Bustin, 1996).

2.2.3.2. Deposition of the Middle Bakken Member

The middle Bakken member was deposited in a proximal coastal marine environment following a rapid sea-level drop (Smith and Bustin, 1995). Argillaceous, greenish-gray, highly fossiliferous, pyritic siltstones in the lower part of the member, reflect a shallow water marine environment which was moderately well oxygenated in the central part of the basin. Interbeds of highly bioturbated shale and sandstone higher in the section indicate lower shoreface deposition in the shoreline basinward (Pitman et al., 2001).

Facies A, which has the predominance of silt grains and carbonate as wells as siliciclastic mud, can be interpreted as deposited with low energy conditions overall. On the other hand, the range of grain sizes still demonstrates the varying energy conditions during deposition. Bioturbation also represents higher energy events, as wells as, the abundant benthic life which led to the ruin of all primary sedimentary structures, and reoriented the originally horizontally deposited shell fragments. In addition, fine-grained siltstone storm layers indicate the facies deposited close to the storm wave base in an upper offshore environment.

Facies B, which consists of fine-grained sediments and Helminthopsis/Sclarituba burrow traces, deposited under relatively low energy conditions. Although the strong bioturbation destroyed all sedimentary structures, the variation of siltstone and mud suggests deposition under varying energy regimes. The fluctuating energy conditions indicate that deposition occurred below the normal wave base but very likely above the storm wave base.

Facies C, which consists of shaly, very fine-grained siltsone/sandstone, deposited under varying conditions to high energy conditions. Deposition of laminated siltstones occurred in the shoreface to foreshore zone.

Sandstone deposition of Facies D indicates that deposition occurred above the normal wave base. Sediment structures represent upper shoreface to foreshore deposition.

Dolomitic mudstone and dolomitic siltstone/sandstone of Facies E formed under agitated to tranquil conditions, under the normal wave base, in terms of the varying sediments (Figure 2.11) (Egenhoff et al., 2011; Simenson et al., 2011).

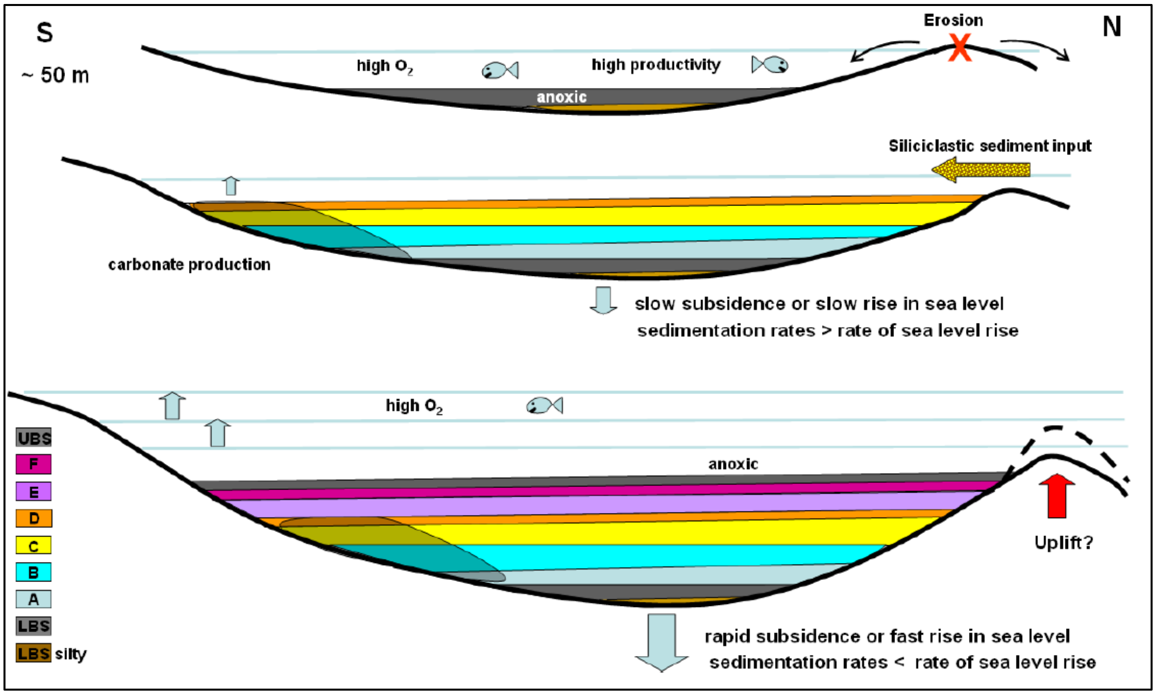

Figure 2.11. Depositional setting of the middle Bakken facies. UBS= Upper Bakken Shale, LBS= Lower Bakken Shale (Sonnenberg et al., 2011).

2.2.3. The Bakken Petroleum System

The Bakken Total Petroleum System (TPS) contains the Devonian Three Forks Formation, the Bakken Formation and the Lower Mississippian part of the Lodgepole Formation which is considered to include Bakken-sourced oil. The Devonian – Mississippian Bakken Formation is comprised of four members in upwards sequence: (1) the Pronghorn Member (Sanish Sand) (LeFever et al., 2011), (2) lower shale member, (3) middle member, and (4) upper shale member. Although the Pronghorn member is geologically and stratigraphically interpreted as a part of the Bakken Formation, it is associated with the Three Forks Formation due to its fluid communication with the Three Forks reservoirs. Therefore, Sanish Sand will be considered as a unit of the Three Forks Formation and not a part of the Bakken Formation in this study.

Five continuous assessment units (AUs) and one conventional AU were established in the Bakken Formation (Figure 2.12). Total undiscovered resources of these units are shown in Table 2.1.

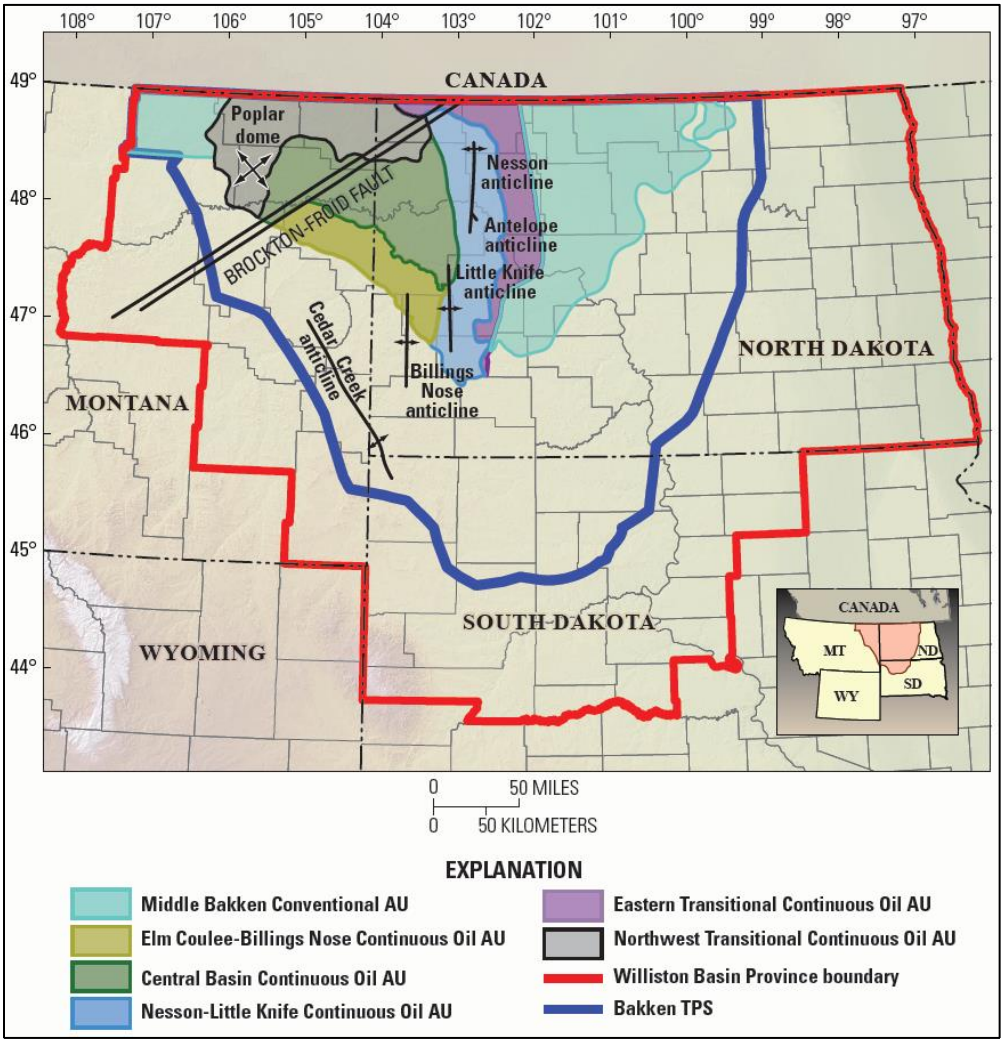

Figure 2.12. The location of Williston Basin province, the Bakken Total Petroleum System (TPS), and the Bakken Formation Assessment Units (AUs) (Gaswirth et al., 2013).

The Bakken Formation Assessment Units (AU)	Field type	Total Undiscovered Resources		
		Oil (MMBO)	Gas (BCFG)	NGL (MMBNGL)
		Mean	Mean	Mean
Bakken TPS				
Elm Coulee-Billings Nose Continuous Oil AU 50310161	*Oil*	283	283	22
Central Basin Continuous Oil AU 50310162	*Oil*	1,122	1,122	88
Nesson-Little Knife Continuous Oil AU 50310163	*Oil*	1,149	1,149	90
Eastern Transitional Continuous Oil AU 50310164	*Oil*	883	441	35
Northwest Transitional Continuous Oil AU 50310165	*Oil*	207	145	11
Total continuous resources		3,644	3,140	246
Middle Bakken Conventional AU 50310101	*Oil*	5	2	0
	Gas		0	0
Total conventional resources		5	2	0
Total undiscovered oil and gas resources		3,649	3,142	246

Table 2.1. Total Undiscovered Resources according to fully risked estimates (MMBO, million barrels of oil. BCFG, billion cubic feet of gas. MMBNGL, million barrels of natural gas liquids. F95, a 95 percent chance of at least the amount Gray shading, not applicable.) (modified from Gaswirth et al., 2013).

3. DATASET and WELL LOG INTERPRETATION

3.1. Dataset

In this study, well log data, core descriptions, mineralogical data, and production data were used for correlations and interpretations. The log and production data was acquired from the North Dakota Industrial Commission, Department of Mineral Resources, Oil and Gas Division (NDIC) website (www.dmr.nd.gov). Additional core data results were calculated based on a Colorado School of Mines thesis study that was prepared by Simenson (2010).

3.1.1. Well Log Data

In this study, 86 well logs, in the digital log ASCII Standard (.las) format, were chosen according to their Bakken information availability and plotted with Petra software. These wells are located in the northwest portion of North Dakota and include five counties: Williams, Mountrail, McKenzie, Dunn and Billings (Figure 3.1). Of the 86 wells, 72 had density porosity logs. Seventy-three wells had neutron porosity logs. Eighty-six wells had gamma ray logs. Seventy-six wells had photoelectric logs. Seventy-eight wells had resistivity logs and 35 wells had sonic logs which include both compressional and shear slowness. Compressional and shear slowness logs, which were both measured during drilling, were both obtained from the North Dakota Department of Mineral Resources. All measured logs, used in this study, were shown in Figure 3.2.

These 86 wells were used for well correlation, creating isopach and stratigraphy maps to analyze the Bakken distribution and the calculation of the petrophysical and elastic parameters. In addition to this, a detailed Bakken thickness map was created from the data of 2902 wells for which Bakken elevations were recorded and available in the state database.

During the facies top determination process, gamma ray, resistivity, neutron and density porosity, density, and photoelectric logs were used. During the correlation process, several structural and stratigraphic cross sections were created by using gamma ray and resistivity logs. In some of the cross sections, gamma ray logs, which are available in all 86 wells, were shown solely where resistivity logs were not available. During the calculation of petrophysical properties, gamma ray log was used first to calculate the shale volume. By using shale volume and density and neutron porosity logs, effective porosity was calculated. Effective porosity and density logs were used for water saturation calculation. During the calculation of elastic properties, density and compressional and shear slowness logs were used. In this process, compressional and shear slowness values were converted to velocity values which were required for elastic parameters' calculation. The calculation methods were explained more detailed in Chapter 4.

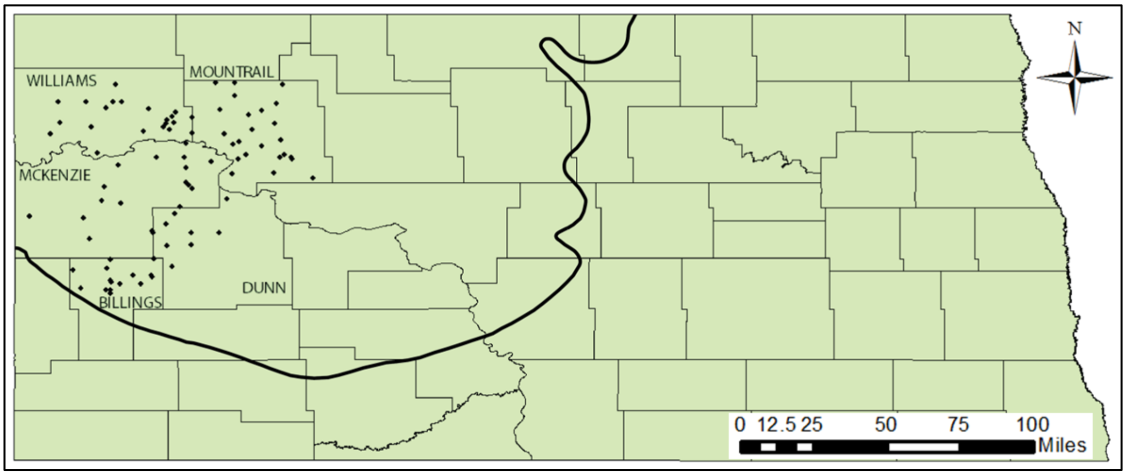

Figure 3.1. Study area and well locations. The 86 wells are located in the northwest part of North Dakota. The black line shows the Bakken limit in North Dakota.

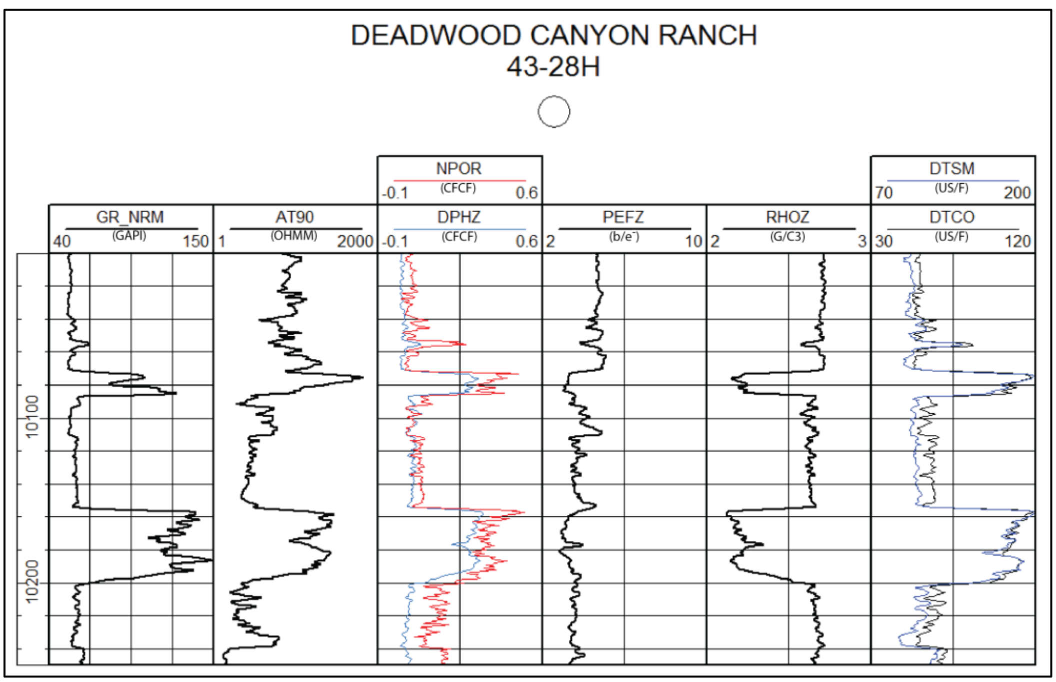

Figure 3.2. Measured log readings for the Deadwood Canyon Ranch 43-28H well (GR: Gamma ray log, AT90: Resistivity log, NPOR: Neutron porosity log, DPHZ: Density porosity log, PEFZ: Photoelectric log, RHOZ: Density log, DTSM: Shear slowness, DTCO: Compressional slowness).

3.1.2. Core Data

Core data results were acquired from the NDIC website. 14 core data results were used for analysis of petrophysical parameters, density, porosity and water saturation, and 5 core mineralogy results were used for the calculation of elastic parameters. The mineralogy results for the Deadwood Canyon Ranch 43-28H well were acquired from the Simenson, 2010 study since the NDIC website excluded this information from the data file of this particular well. These core data results were compared with the results of log data calculations to check the accuracy of the study. Available core data information is showed in Table 3.1 and core locations is showed in Figure 3.3.

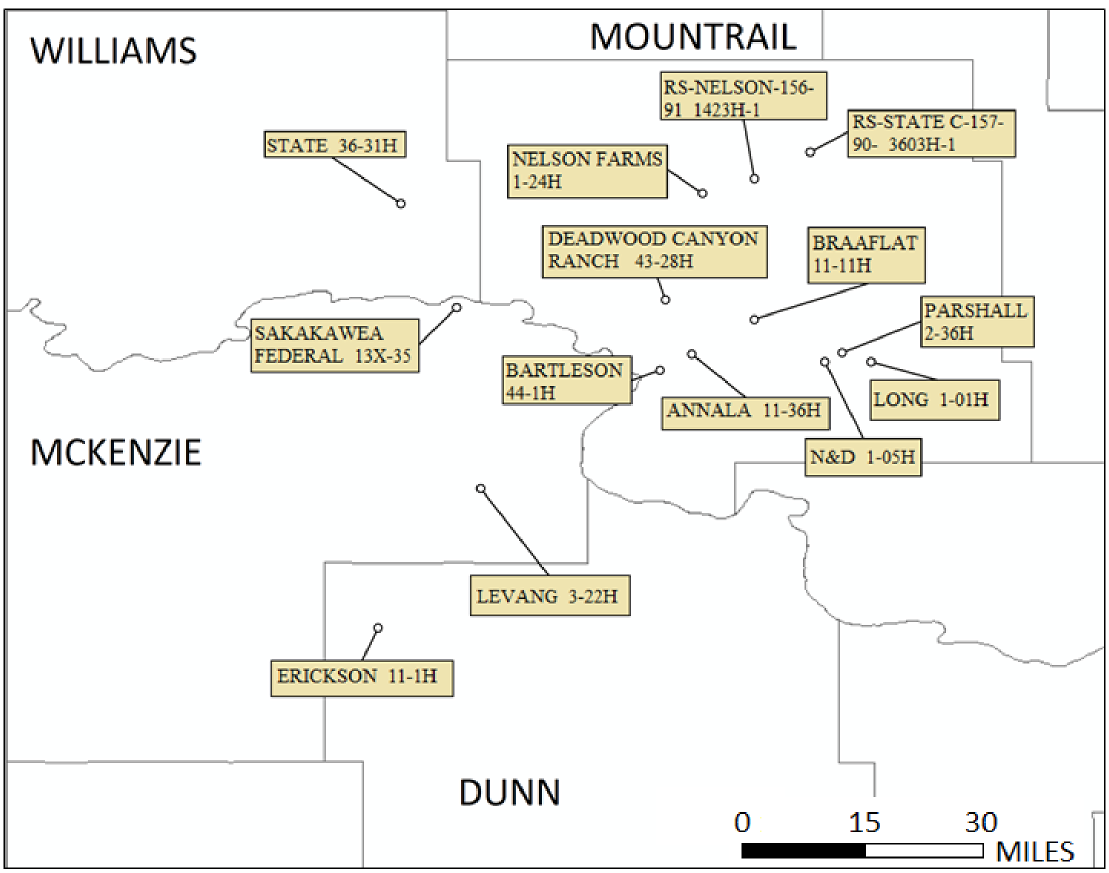

Figure 3.3. Locations of wells from which core data are available.

Current Well Name	Field Name	County Name	Operator	Latitude	Longitude
STATE 36-31H	BEAVER LODGE	WILLIAMS	HESS BAKKEN INVESTMENTS II, LLC	48.296477	-102.963717
LEVANG 3-22H	BLUE BUTTES	MCKENZIE	QEP ENERGY COMPANY	47.803068	-102.826092
SAKAKAWEA FEDERAL 13X-35	CHARLSON	MCKENZIE	XTO ENERGY INC.	48.115130	-102.868751
ERICKSON 11-1H	LITTLE KNIFE	DUNN	HESS BAKKEN INVESTMENTS II, LLC	47.560383	-103.004287
PARSHALL 2-36H	PARSHALL	MOUNTRAIL	EOG RESOURCES, INC.	48.036865	-102.199690
N&D 1-05H	PARSHALL	MOUNTRAIL	EOG RESOURCES, INC.	48.021856	-102.229529
LONG 1-01H	PARSHALL	MOUNTRAIL	EOG RESOURCES, INC.	48.022058	-102.148158
NELSON FARMS 1-24H	ROSS	MOUNTRAIL	HESS BAKKEN INVESTMENTS II, LLC	48.313559	-102.440163
RS-NELSON-156-91 1423H-1	ROSS	MOUNTRAIL	HESS BAKKEN INVESTMENTS II, LLC	48.339908	-102.351351
RS-STATE C-157-90-3603H-1	ROSS	MOUNTRAIL	HESS BAKKEN INVESTMENTS II, LLC	48.386315	-102.253201
BARTLESON 44-1H	SANISH	MOUNTRAIL	WHITING OIL AND GAS CORPORATION	48.007887	-102.514722
ANNALA 11-36H	SANISH	MOUNTRAIL	FIDELITY EXPLORATION & PRODUCTION COMPANY	48.036260	-102.458873
DEADWOOD CANYON RANCH 43-28H	SANISH	MOUNTRAIL	FIDELITY EXPLORATION & PRODUCTION COMPANY	48.129139	-102.504910
BRAAFLAT 11-11H	SANISH	MOUNTRAIL	WHITING OIL AND GAS CORPORATION	48.094893	-102.350748

Table 3.1. Information of available cores

3.1.3. Production Data

Monthly oil production data can be accessed from the NDIC website. Of the 86 wells used in this study, 49 are producing from the Bakken Formation. From these 49 wells, several cumulative oil production maps were plotted and compared with the middle Bakken isopach map to test the relationship between thickness and production. In addition, some charts were created for comparison of the production and calculated elastic parameters to check a relationship between them. The maps and charts are shown in the Results section.

3.2. Well Log Interpretation

In this study, 13 vertical wells, 61 horizontal wells and 12 directional wells were used for facies determination, correlation and interpretation of depositional environment. Figure 3.4 shows the horizontal and directional drilling pathways for two different wells.

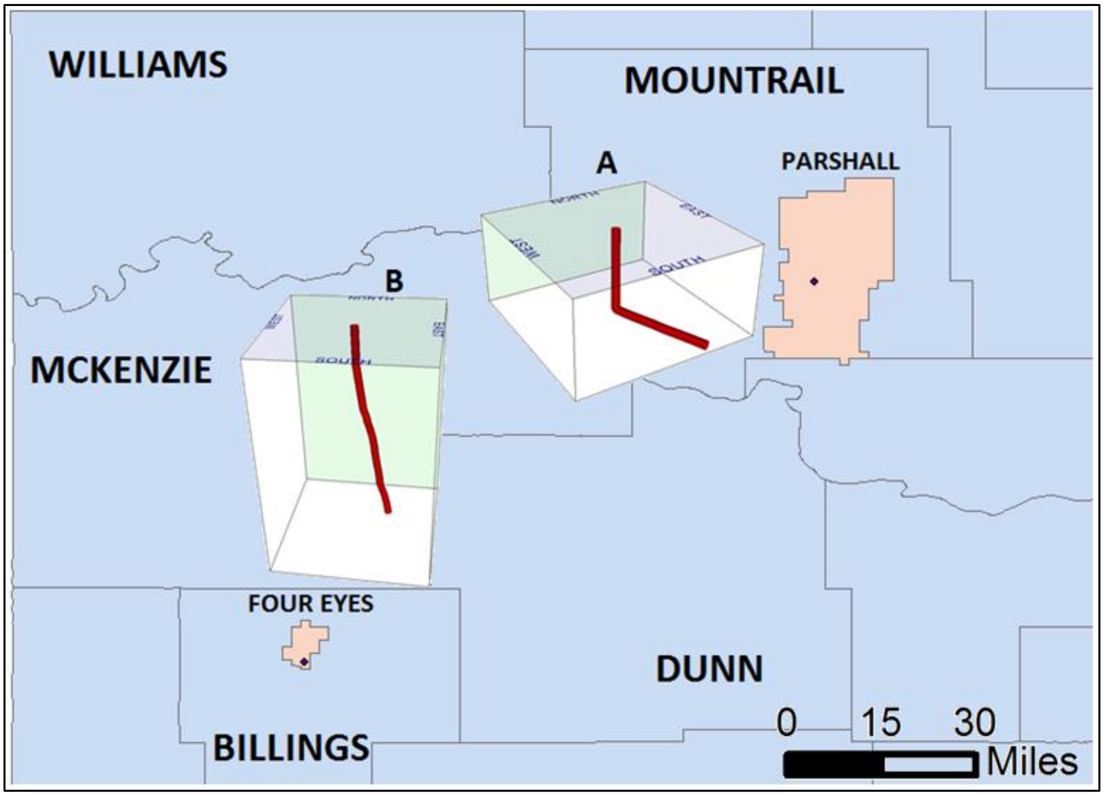

Figure 3.4. Horizontal and directional well profiles. A) Horizontal drilling for the well Parshall N&D 1-05H. B) Directional drilling for the well Four Eyes KORDON 11-32.

3.2.1. Well Log Descriptions

Gamma-ray logs are used to measure the formations' natural radioactivity and can be utilized for lithology identification and zone correlation. The gamma-ray tool is sensitive to radioactive elements such as uranium, thorium and potassium (Rider and Kennedy, 2011). Shale-free sandstones and carbonates give low gamma-ray readings due to their low concentrations of radioactive elements. The gamma-ray log response increases with the increase of shale content because of the concentration of radioactive material in shale. However, clean sandstones, which have low shale content, can give a high gamma ray response with the presence of potassium feldspars, micas, glauconite, or uranium-rich waters (Asquith and Gibson, 1982). Thus, while high gamma ray values are a good indicator of shale, interpretations must be based on other logs as well.

Resistivity logs are electric logs that measure the ability of electricity to be transmitted through the unit (Rider and Kennedy, 2011). They can be used for different evaluations such as determining hydrocarbon versus water-bearing zones, indicating permeable zones, and estimating porosity. The most important use of resistivity logs is to determine hydrocarbon versus water-bearing zones. Since rock matrix or grains are non-conductive, the current transmitting ability of a rock depends on the function of water in pores. Hydrocarbons are also non-conductive; therefore, with the increase of hydrocarbon saturation in pores, the rock's resistivity also increases (Asquith and Gibson, 1982).

The formation-density log is a porosity log and measures a formation's electron density. It is used by geologists for different purposes such as identifying evaporate minerals, detecting gas-bearing zones, determining hydrocarbon density, and evaluating shaly sand reservoirs and complex lithologies.

A neutron log is also a porosity log that measures the hydrogen-ion concentration in a formation. In clean formations such as a shale-free formation, where water or oil fill the pore space, the neutron log measures liquid-filled porosity. When the pores are filled with gas rather than oil or water, neutron porosity will be lowered due to less concentration of hydrogen in gas compared to oil or water.

A sonic log provides the acoustic characteristic of the formation which measures the formation's slowness or interval transit time. (Rider and Kennedy, 2011). Interval transit time, meaning the reciprocal of the velocity of a compressional sound wave in feet per second, is dependent upon both lithology and porosity (Asquith and Krygowski, 2004).

A photoelectric log is a supplementary measurement in the latest generation of density logging tools, and continuously records the effective photoelectric absorption cross-section index of a formation. The measurement strongly depends on the atomic number of the constituents of the formation (Rider and Kennedy, 2011). It is mildly affected by pore volume or fluid/gas content, however, it is an excellent indicator of mineralogy (Doveton, 1994).

All digital logs were loaded into Petra software. After entering all data information, including well name, well number, operator name, and location into the appropriate section, each facies top of the Bakken Formation was picked for all 86 wells. Facies thickness values were determined with defined tops. Then, several isopach maps were created for the lower Bakken, middle Bakken, and upper Bakken as well as each middle Bakken facies.

3.2.2. Determination of the Facies Tops

Each Bakken facies top was picked according to its log responses. During this process, several logs were used such as the gamma ray log (GR_NRM), resistivity log (AT90), neutron porosity log (NPOR), density porosity log (DPHZ), photoelectric log (PEFZ), and the density log (RHOZ) (Figure 3.5).

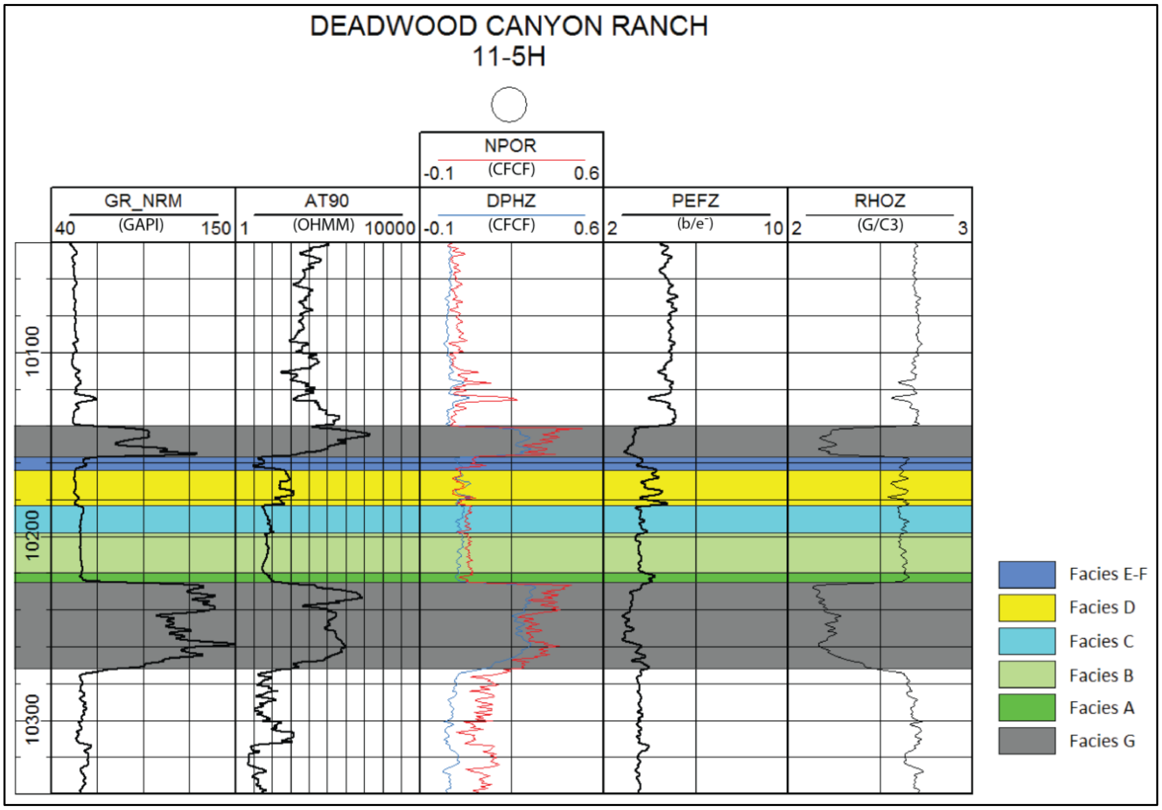

Figure 3.5. Facies top determination for the DEADWOOD CANYON RANCH 11-5H well.

The Bakken Formation can be easily recognized in wire-line logs. Upper and lower members (Facies G) can be picked easily due to their high gamma ray content. Facies A has a cleaner gamma ray and higher photoelectric log response than the underlying Facies G. Facies B has a slightly increasing resistivity and lower photoelectric log response than the underlying Facies A. Moreover, at the top, neutron and density porosity intersection is an indicator for defining the top of Facies B, as well as, the base of Facies C. In Facies C, density and neutron porosity logs converge unlike in Facies B. The gamma ray response in Facies D has the cleanest response in the Bakken Formation and has a higher photoelectric log reading than overlying and underlying facies. Facies E-F has higher gamma ray and lower resistivity responses than the underlying Facies D. In the cases where Facies D is absent, Facies E-F can be recognized by observing a larger separation in the density – neutron porosity separation curves.

4. PETROPHYSICAL AND ELASTIC PROPERTIES OF THE BAKKEN FORMATION

The analysis of petrophysical and elastic parameters has an importance for assessment of oil presence and determination of drilling pathway. Since the shale members' abnormally high gamma ray and resistivity values gave unrealistic results, in the study, the calculation of elastic and petrophysical parameters was undertaken for the middle Bakken member. Core results, which include water saturation, density, porosity and mineralogy, were taken from the well log reports which were published in the NDIC website. The log and core data calculation results were compared with each other to check their consistency. Different calculation methods were applied to decide the best way to calculate actual results. For well-log data calculations, 25 wells were used for petrophysical calculations and 10 wells were used for elastic parameters calculation. Five core data results were used for comparison of the petrophysical properties and five mineralogy results were used for calculation of elastic properties.

4.1. Calculations of Petrophysical Parameters from Well Logs

4.1.1. Shale Volume Calculation

Since shale is usually more radioactive than sand or carbonate, gamma ray logs are used to calculate the volume of shale. The volume of shale is explained as a decimal fraction or percentage called V_{sh}. The gamma ray index is the first step to determine the volume of shale from a gamma ray log:

$$I_{GR} = \frac{GR_{log} - GR_{min}}{GR_{max} - GR_{min}}$$

Where: I_{GR} = gamma ray index

GR_{log} = gamma ray reading of formation

GR_{min} = minimum gamma ray (clean sand or carbonate)

GR_{max} = maximum gamma ray (shale)

There is a relationship between gamma ray responses and shale volume. These responses can be nonlinear empirical responses as well as a linear response. The nonlinear responses depend on the geographic area or formation age as well as other available information chosen to fit local information. All nonlinear relationships are more optimistic than the linear response. The linear response is used for the first order estimation of shale volume, where $V_{shale} = I_{GR}$.

The nonlinear responses are used to increase optimism for the shale volume (Asquith and Krygowski, 2004). For this study, two different shale volume calculation methods were applied:

Steiber (1970), $$V_{sh} = \frac{I_{GR}}{3 - 2 * I_{GR}}$$

Clavier (1971), $$V_{sh} = 1.7 - [3.38 - (I_{GR} - 0.7)^2]^{\frac{1}{2}}$$

Where: I_{GR} = gamma ray index

V_{sh} = Shale volume

4.1.2. Porosity Calculation

Shale correction in the density and neutron porosity logs give a very good approximation for porosity (Crain's Petrophysical Handbook). Therefore, the shale correction process was applied for all the density and neutron logs.

$$PHIdc = PHID - (V_{sh} * PHIDSH)$$

Where: PHIdc = Porosity from density log corrected for shale (fractional)

PHID = Porosity from uncorrected density log (fractional)

V_{sh} = Shale volume

PHIDSH = Density porosity log reading in 100% shale (fractional)

$$PHInc = PHIN - (V_{sh} * PHINSH)$$

Where: PHInc = Porosity from neutron log corrected for shale (fractional)

PHIN = Porosity from uncorrected neutron log (fractional)

V_{sh} = Shale volume

PHINSH = Neutron porosity log reading in 100% shale (fractional)

PHIdc and PHInc parameters will be shown as $Ø_D$ and $Ø_N$ during the study.

The combination of neutron and density porosity logs is applied for effective porosity calculation, in addition to the determination of lithology and gas-bearing zones (Asquith and Gibson, 1982). Effective porosity was calculated by integrating density and neutron porosity log values into a formula:

$$\emptyset_{N-D} = \sqrt{\frac{\emptyset_N{}^2 + \emptyset_D{}^2}{2}}$$

Where: $\emptyset_{N\text{-}D}$ = neutron – density porosity

$\emptyset_N$ = neutron porosity

$\emptyset_D$ = density porosity

4.1.3. Water Saturation Calculation

Water saturation denotes the occupying formation water in the pore volume of a rock. Water saturation is usually calculated because of its direct calculation equations such as Archie’s equation even though hydrocarbon saturation is the quantity of interest. Hydrocarbon saturation (S_h) can be determined by the difference between unity and water saturation (S_w):

$$S_h = 1 - S_w$$

Different water saturation methods such as Archie’s equation and the Simandoux model were applied to test their applicability for the Bakken Formation.

Archie’s (1942) water saturation formula is applied to a reservoir’s uninvaded zone (Asquith and Krygowski, 2004).

$$S_w = \left(\frac{a * R_w}{\emptyset^m * R_t}\right)^{\frac{1}{n}}$$

Where: S_w = Water saturation

R_w = Formation water resistivity

R_t = True formation resistivity

$\emptyset$ = Porosity

a = Tortuosity exponent

m = Cementation exponent

n = Saturation exponent

Porosity values were used from the neutron – density porosity combination. R_w is determined to be 0.02 ohm-m and R_t is taken from a deep resistivity curve. The tortuosity exponent (a) and the saturation exponent (n) values are taken from a previous study (Simenson, 2010), while the cementation factor (m) value is determined according to whether the water saturation of core and log data curve match. The cementation exponent values vary for each middle Bakken facies (Table 4.1).

Facies	a	m	n
Facies E-F	1	1.65	1.74
Facies D	1	1.45	1.74
Facies C	1	1.50	1.74
Facies B	1	1.65	1.74
Facies A	1	1.80	1.74

Table 4.1. Parameters determined to calculate water saturation for Archie's equation

4.2. Calculation of the Elastic Parameters from Well Logs

The Bakken Formation has a high degree of anisotropy, which means physical properties (velocity, fractures, and permeability) change according to directions. The elastic parameters (Poisson's ratio, Young's modulus, and brittleness index) are important in terms of determining fracture conditions of the rock.

4.2.1. Poisson's Ratio Calculation

Poisson's ratio is defined as the ratio between transverse strain (e_t) and longitudinal strain (e_l) in the elastic loading direction. Different materials respond to stress in different ways, therefore, materials with different Poisson's ratios behave differently under different mechanical conditions (Greaves et al., 2011).

Required parameters for Poisson's ratio calculation are compressional and shear wave velocities. Velocities were calculated from compressional and shear slowness values which are both available in .las files:

$$V_p = \frac{1}{DTCO}$$

Where: V_p = P-wave (compressional) velocity

DTCO = Compressional slowness

$$V_s = \frac{1}{DTSM}$$

Where: V_s = S-wave (shear) velocity

DTSM = Shear slowness

From the conversion of slowness values, compressional and shear wave velocities were used for Poisson's ratio calculation:

$$\nu = \frac{\left(V_p/V_s\right)^2 - 2}{2 * \left(V_p/V_s\right)^2 - 2}$$

Where: ν = Poisson's ratio

V_p = P-wave (compressional) velocity

V_s = S-wave (shear) velocity

4.2.2. Young's Modulus Calculation

Young's modulus is defined as the ratio of extensional stress to extensional strain (Mavko et al., 2003). In the study, Young's modulus (E) is calculated by using Poisson's ratio, P-wave velocity, and density parameters.

$$E = \frac{{V_p}^2 \, \rho \, (1+\nu)\,(1-2\nu)}{1-\nu}$$

Where: E = Young's modulus

V_p = P-wave velocity

ρ = Density

ν = Poisson's ratio

4.2.3. Brittleness Index Calculation

Brittleness is the measurement of stored energy before failure and is the function of rock strength, lithology, texture, effective stress, temperature, fluid type, diagenesis, and TOC. The identification of brittle regions is important to optimally stimulate an unconventional reservoir hydraulically, based on knowledge of the geology, petrophysics, mineralogy, and rock mechanics of the study area. The brittleness index is the most commonly used parameter for the quantification of rock brittleness (Perez, 2013). Brittleness values are calculated from Poisson's ratio and Young's modulus:

$$\nu_{brittleness} = \frac{\nu - \nu_{max}}{\nu_{min} - \nu_{max}}$$

Where: ν = Poisson's ratio

ν_{min} = Minimum values of Poisson's ratio logged in the formation

ν_{max} = Maximum values of Poisson's ratio logged in the formation

$$E_{brittleness} = \frac{E - E_{min}}{E_{max} - E_{min}}$$

Where: E = Young's modulus

E_{min} = Minimum Young's modulus measured in the formation

E_{max} = Maximum Young's modulus measured in the formation

The Brittleness index is determined from the average of Poisson's Ratio and Young's Modulus brittleness:

$$Brittleness\ Average = \frac{(\nu_{brittleness} + E_{brittleness})}{2}$$

4.3. Calculations from Core Data

In terms of petrophysical parameters, the core data already has the porosity and water saturation results. The brittleness was calculated by using the mineral percentages from different equations such as Jarvie (2007) and Wang (2009):

$$\mathrm{BI}_{Jarvie(2007)} = \frac{\mathrm{Qz}}{\mathrm{Qz} + \mathrm{Ca} + \mathrm{Cly}}$$

$$\mathrm{BI}_{Wang(2009)} = \frac{\mathrm{Qz} + \mathrm{Dol}}{\mathrm{Qz} + \mathrm{Dol} + \mathrm{Ca} + \mathrm{Cly} + \mathrm{TOC}}$$

Where: Qz = Quartz

Ca = Calcite

Cly = Clay

Dol = Dolomite

TOC = Total organic carbon

Since there is not an available TOC result from the core data for the Wang's brittleness calculation, it is estimated as 5% (Flannery, 2006).

Besides the given formulas for brittleness calculation, during this study, some brittleness calculation methods were created by using mineralogy and the minerals' actual Poisson's ratio and Young's modulus values to examine their applicability. The calculation methods were applied for the Deadwood Canyon Ranch 11-5H well. During the calculation process, the mineralogy parameters were applied in both percentages (Table 4.2) and friction mode (Table 4.3).

MINERALS / Depth (ft)	10160	10168	10173	10177	10185.67	10213.33
Quartz	38	45	53	38	26	39
K-Feldspar	4	4	4	3	2	5
Plagioclase	8	3	7	4	3	8
Calcite	3	32	9	29	60	16
Ankerite/Fe-Dolomite	3	1	2	3	2	0
Dolomite	30	12	19	17	3	15
Pyrite	1	0	0	0	1	2
Clay	12	3	6	5	4	14

Table 4.2. The mineralogy values for the Deadwood Canyon Ranch 11-5H well as shown in percentages.

MINERALS / Depth (ft)	10160	10168	10173	10177	10185.67	10213.33
Quartz	0.38	0.45	0.53	0.38	0.26	0.39
K-Feldspar	0.04	0.04	0.04	0.03	0.02	0.05
Plagioclase	0.08	0.03	0.07	0.04	0.03	0.08
Calcite	0.03	0.32	0.09	0.29	0.6	0.16
Ankerite/Fe-Dolomite	0.03	0.01	0.02	0.03	0.02	0
Dolomite	0.3	0.12	0.19	0.17	0.03	0.15
Pyrite	0.01	0	0	0	0.01	0.02
Clay	0.12	0.03	0.06	0.05	0.04	0.14

Table 4.3. The mineralogy values for the Deadwood Canyon Ranch 11-5H well shown in friction mode.

The first calculation method from Poisson's ratio and Young's modulus was applied in friction mode. In the formulas below, f indicates the friction mode of minerals:

$$\frac{1}{\nu_{BI}} = \frac{f_{qz}}{\nu_{qz}} + \frac{f_{ca}}{\nu_{ca}} + \frac{f_{dol}}{\nu_{dol}} + \frac{f_{clay}}{\nu_{clay}}$$

$$\frac{1}{E_{BI}} = \frac{f_{qz}}{E_{qz}} + \frac{f_{ca}}{E_{ca}} + \frac{f_{dol}}{E_{dol}} + \frac{f_{clay}}{E_{clay}}$$

$$Brittleness\ Average = \frac{(\nu_{BI} + E_{BI})}{2}$$

The second calculation method from Poisson's ratio and Young's modulus was applied in friction mode:

$$\nu_{BI} = f_{qz} * \nu_{qz} + f_{ca} * \nu_{ca} + f_{dol} * \nu_{dol} + f_{clay} * \nu_{clay}$$

$$\mathrm{E}_{BI} = f_{qz} * \mathrm{E}_{qz} + f_{ca} * \mathrm{E}_{ca} + f_{dol} * \mathrm{E}_{dol} + f_{clay} * \mathrm{E}_{clay}$$

$$Brittleness\ Average = \frac{(\nu_{BI} + E_{BI})}{2}$$

The third calculation method was examined by using the minerals' percentages and their actual Poisson's ratio and Young's modulus values:

$$\nu_{\mathrm{BI}} = \frac{\mathrm{Qz\%} * \nu_{\mathrm{qz}} + \mathrm{Dol\%} * \nu_{\mathrm{Dol}} + \mathrm{Ca\%} * \nu_{\mathrm{Ca}} + \mathrm{Clay\%} * \nu_{\mathrm{Clay}}}{\nu_{\mathrm{qz}} + \nu_{\mathrm{Dol}} + \nu_{\mathrm{Ca}} + \nu_{\mathrm{Clay}}}$$

$$\mathrm{E}_{\mathrm{BI}} = \frac{\mathrm{Qz\%} * \mathrm{E}_{\mathrm{qz}} + \mathrm{Dol\%} * \mathrm{E}_{\mathrm{Dol}} + \mathrm{Ca\%} * \mathrm{E}_{\mathrm{Ca}} + \mathrm{Clay\%} * \mathrm{E}_{\mathrm{Clay}}}{\mathrm{E}_{\mathrm{qz}} + \mathrm{E}_{\mathrm{Dol}} + \mathrm{E}_{\mathrm{Ca}} + \mathrm{E}_{\mathrm{Clay}}}$$

$$Brittleness\ Average = \frac{(\nu_{BI} + E_{BI})}{2}$$

The Poison's ratio and Young's modulus values, applied in the formula, are shown in the Table 4.4:

Minerals	Poisson's ratio	Young's modulus	References
Quartz	0.08	13.69	Carmichael, 1982
Calcite	0.32	11.57	Crain's petrophysical handbook (2)
Dolomite	0.30	16.68	Crain's petrophysical handbook (2)
Clay	0.26	11.27	Modified from Wang et al., 2001

Table 4.4. Poisson's ratio and Young's modulus values of the minerals

Another formula was created for the calculation of compressional slowness by using mineralogy and minerals' actual compressional slowness values. During this process, the aim was to examine if these calculated slowness values would show a consistency with log data slowness readings. The following formula was applied for the calculation:

$$\mathrm{Calculated_{DT}} = \mathrm{Qz\%} * \mathrm{DT_{qz}} + \mathrm{Cal\%} * \mathrm{DT_{cal}} + \mathrm{Dol\%} * \mathrm{DT_{dol}} + \mathrm{Clay\%} * \mathrm{DT_{clay}}$$

The actual compressional velocity values were obtained from different studies. The compressional slowness values were calculated from the velocity values as explained in Chapter 4.2.1. These values were shown in Table 4.5:

Minerals	Vp (m/s)	DT (µs/f)	References
Quartz	6050	50.38	Carmichael, 1982
Calcite	6530	46.68	Carmichael, 1982
Dolomite	7345	41.50	Crain's petrophysical handbook (2)
Clay	5993	50.86	Wang et al., 2001

Table 4.5. V_p (compressional velocity) values of minerals. Second column shows the calculated compressional slowness values.

4.4. Comparison of Calculations

In this part, several compared petrophysical and elastic parameters, from log and core data calculation, are shown. Calculations have been made for the middle Bakken member. The first petrophysical and elastic calculations were applied for the Bartleson 44-1H well which is located in the Sanish Field, Mountrail County.

There is an average 0.1 g/cc density difference between the core and log data. The different log data readings may be caused by borehole conditions, environmental effects or measurement errors. This difference was neglected during the calculations (Figure 4.1).

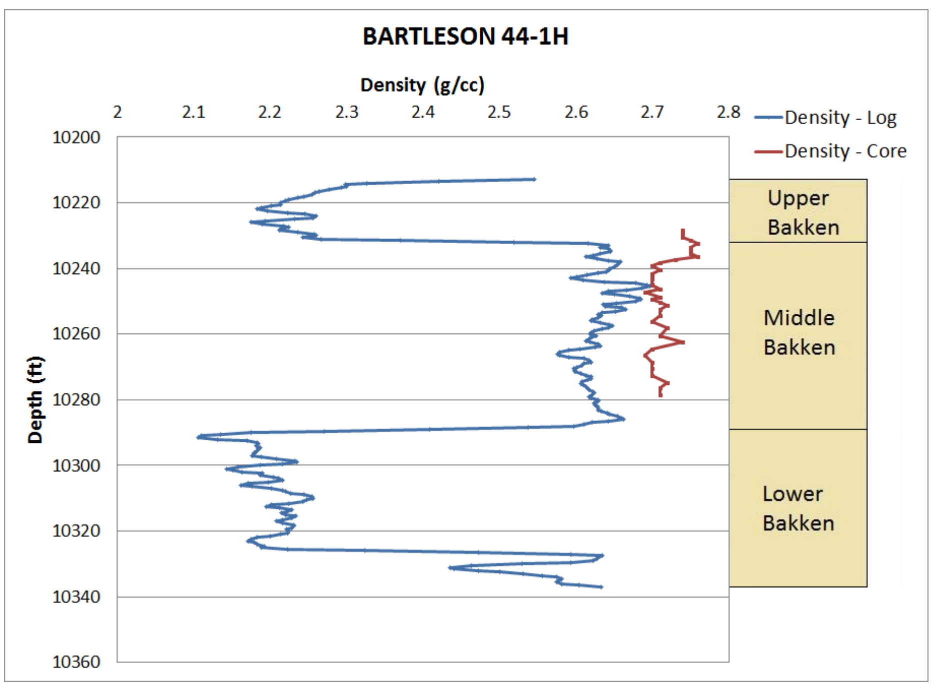

Figure 4.1. Comparison between core data and log data density for the Bartleson 44-1H well.

Calculated log data effective porosity results from Clavier and Stieber's methods and core data porosity results were compared (Figure 4.2). During rest of the study, porosity results calculated from Stieber method were used since Clavier and Stieber porosity results show consistency with each other. Although the core porosity shows fluctuated picks, it shows a harmonious trend with the log data calculation.

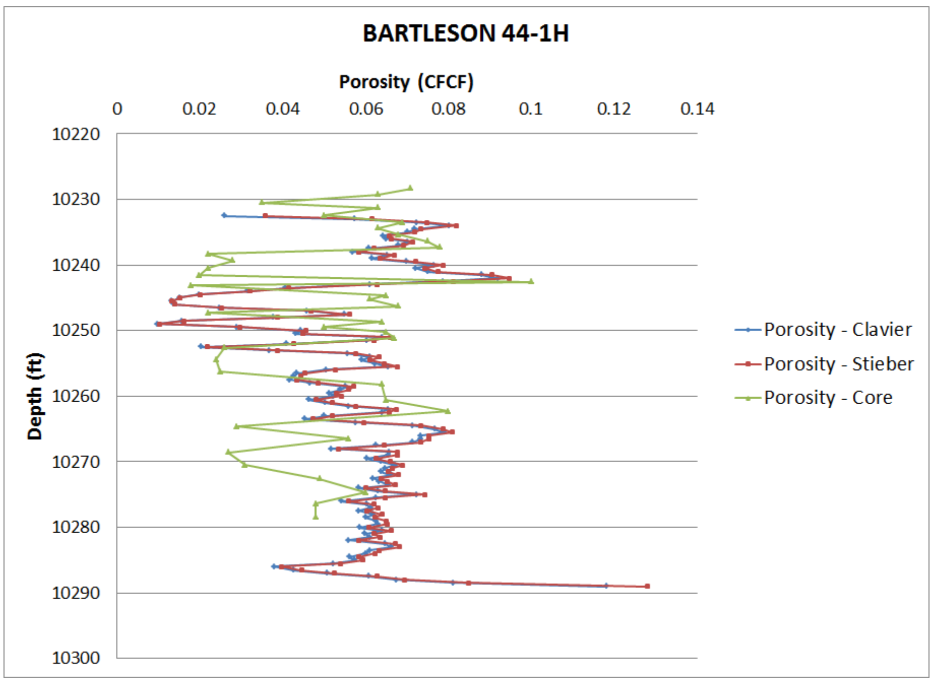

Figure 4.2. Comparison between core data and calculated porosity results for the Bartleson 44-1H well.

Two kinds of water saturation calculation were applied from Simandoux and Archie's equations. The water resistivity value used during Archie's equation calculation was 0.02 ohm-m, however 0.01 ohm-m was used during the Simandoux model water saturation calculation since the first R_w value caused bad results. The results were compared with the core data water saturation results. The core data and Archie's equation water saturation results show consistency. On the other hand, the Simandoux model estimates higher water saturation values (Figure 4.3).

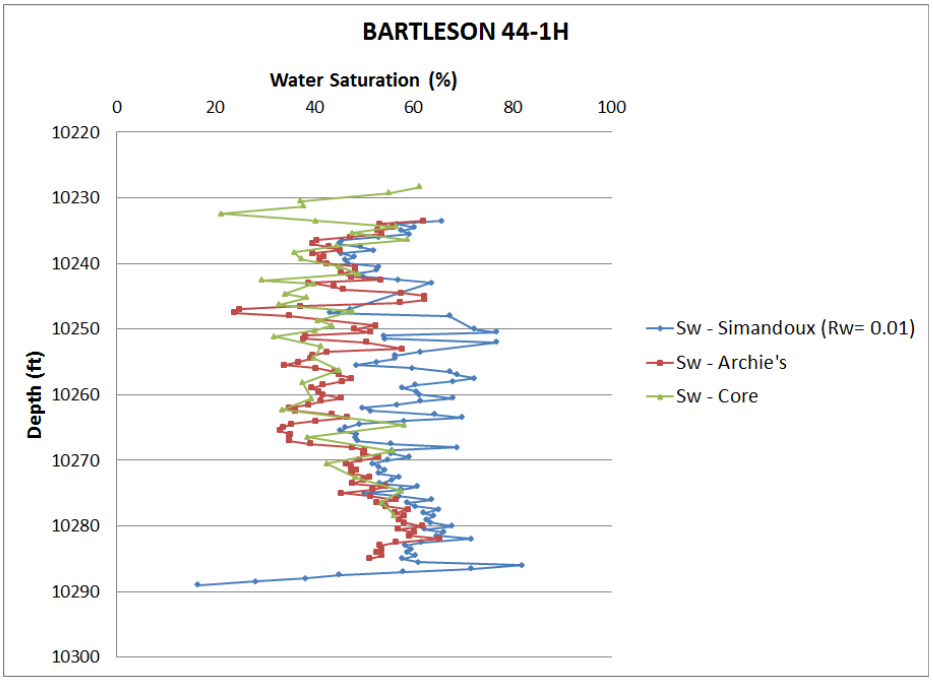

Figure 4.3. Comparison between core data and calculated log data water saturation for the Bartleson 44-1H well.

Another petrophysical calculation was applied for the Braaflat 11-11H well which is located in Sanish Field, Mountrail County. Calculations were only applied for the middle Bakken member. Although the core data and log data results show different values in the upper and lower parts of the middle Bakken, they have the same trend (Figure 4.4).

Core data water saturation results show fluctuated picks. However, they have a harmonious trend with the calculated log data water saturation results (Figure 4.5).

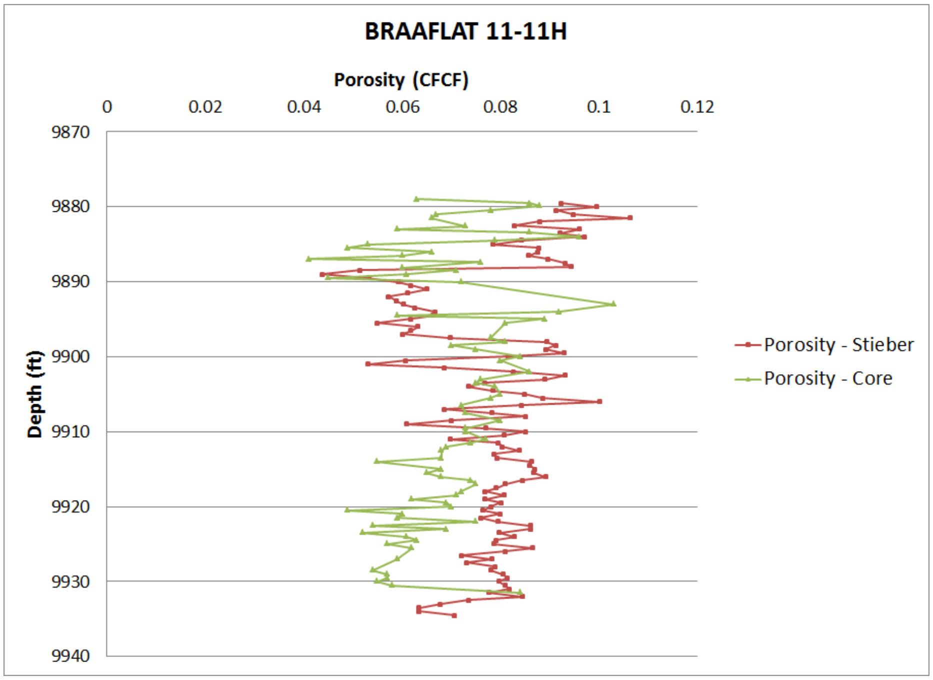

Figure 4.4. Comparison between core porosity and shale corrected log data porosity for the Braaflat 11-11H well.

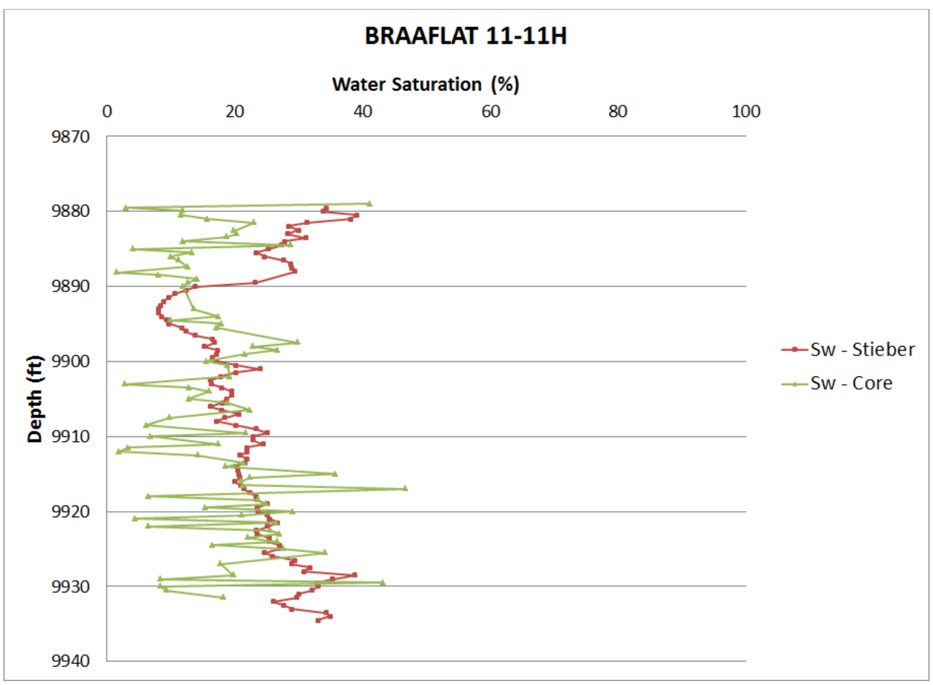

Figure 4.5. Comparison between core data and calculated log data water saturation for the Braaflat 11-11H well.

The Deadwood Canyon Ranch 11-5H well which is located in Sanish Field, Mountrail County was used for the elastic property calculations. The brittleness was calculated from Wang and Jarvie equations, log data, combination of actual Poisson's ratio and Young's modulus values and actual compressional slowness values.

Figure 4.6 shows the comparison of brittleness calculations from actual Poisson's ratio and Young's modulus values with the log data calculation. According to the figure, calculated brittleness values from the mineralogy and actual Poisson's ratio and Young's modulus show conflicting results from the log data brittleness values.

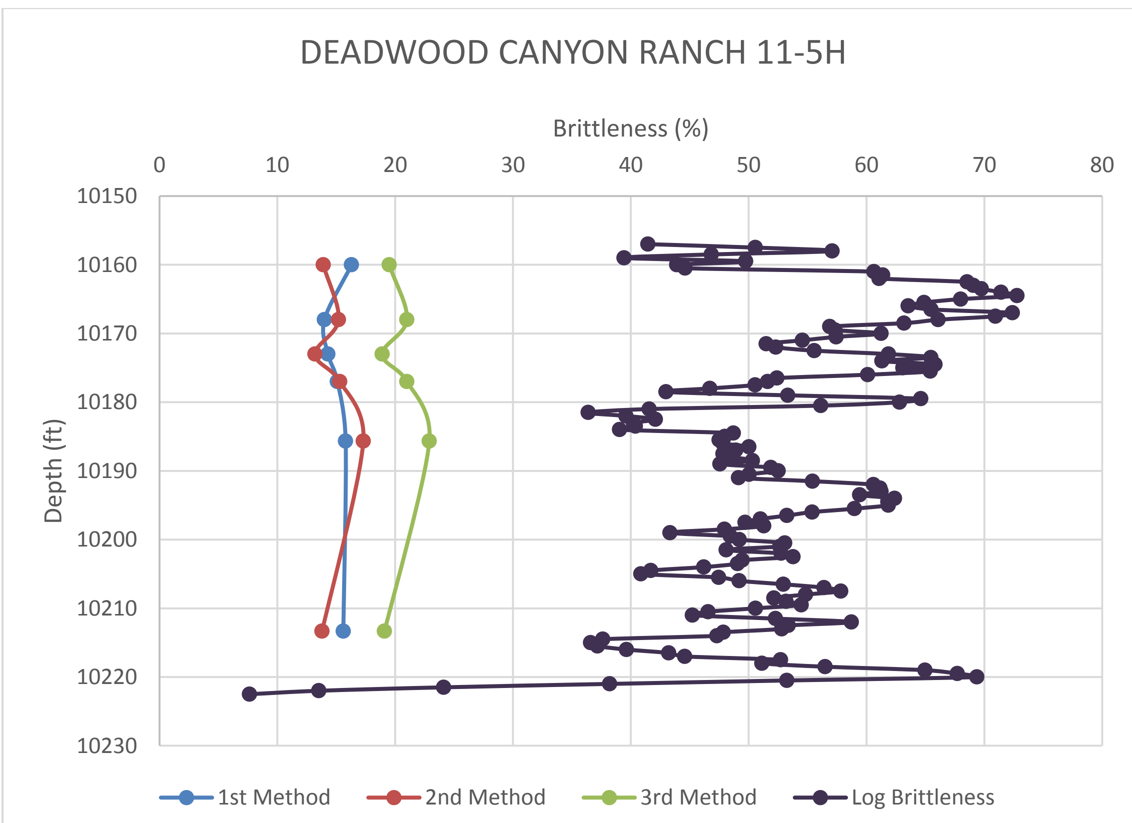

Figure 4.6. Comparison of brittleness values between created methods and log data calculation.

Figure 4.7 shows a comparison of brittleness values from Wang and Jarvie equations, log data calculations and a created formula which is the 3rd method previously discussed by using mineralogy and minerals' actual Poisson's ratio and Young's modulus values. The core data has limited brittleness values. The brittleness results calculated from both the Wang equation and the Jarvie equation were found to be almost the same. Although there is almost a 20% difference between the log data and the core data brittleness in the middle part, they show the same trend. The brittleness calculation from the created formula (3rd method) gave inconsistent results from the other calculations.

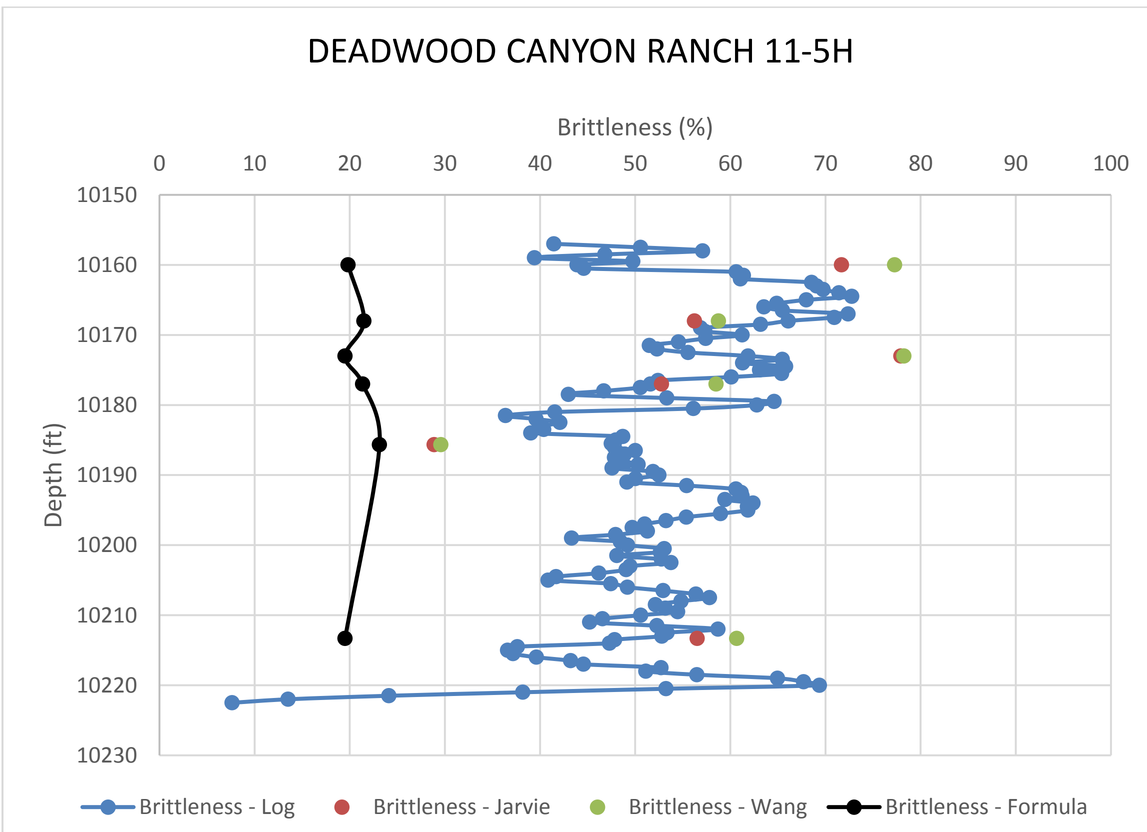

Figure 4.7. Compared brittleness values applied for the Deadwood Canyon Ranch 11-5H well.

Compressional slowness was calculated by using mineralogy and minerals' actual compressional slowness values. The calculation results were compared with log data readings in Table 4.6. The calculated slowness values show minimum 14% difference from slowness readings from the log.

DEPTH (ft)	DT log reading (µs/f)	Calculated DT (µs/f)	Difference
10160	64.3636	39.098	25.2656
10168	59	44.1144	14.8856
10173	63	41.8392	21.1608
10177	57	42.2796	14.7204
10185.5	63.8182	44.3862	19.432
10213	63.4545	40.4624	22.9921

Table 4.6. Comparison between calculated slowness and measured slowness from the log.

5. RESULTS

5.1. Cross Sections

Five structural cross sections and six stratigraphic cross sections were plotted, which cover the northwest part of North Dakota, to examine the Bakken thickness change and depositional trends. During correlation, the gamma ray and resistivity logs were shown in figures. Some wells, which do not have a resistivity log, were just shown with the gamma ray log.

5.1.1. Structural Cross Sections

Five structural cross sections, oriented west-east and south-north, were constructed to determine the Bakken thickness change over the whole study area (Figure

5.1). Cross sections 1-1’, 2-2’, and 3-3’ are oriented in a west-east direction (Figure 5.2, 5.3, and 5.4). Cross sections 4-4’ and 5-5’ have a south-north orientation (Figure 5.5 and 5.6).

In Figure 5.2, the Bakken reaches 143 ft in thickness in the Nesson State 42X-36 well. In the west and east part of the cross section, the thickness values are 71 and 73 ft. According to Figure 5.3, the Bakken has a maximum thickness of 124 ft in the Bartleson 44-1H well. Its thickness reaches 88 ft and 83 ft in the east and west parts, respectively, in the cross section. Figure 5.4 shows that the Bakken has a 40 ft thickness in the west, while in the east it reaches up to 73 ft. In Figure 5.5, the deepest part, which is in the Charlotte 1-22H well, has a 91 ft. thickness. In the southern part, where the middle and lower Bakken members are absent, the Bakken has a thickness of 4 ft. According to Figure 5.6, the Deadwood Canyon Ranch 43-28H well has the maximum thickness of 129 ft. In the south and north parts of the cross section, the thickness values are 73 ft and 66 ft.

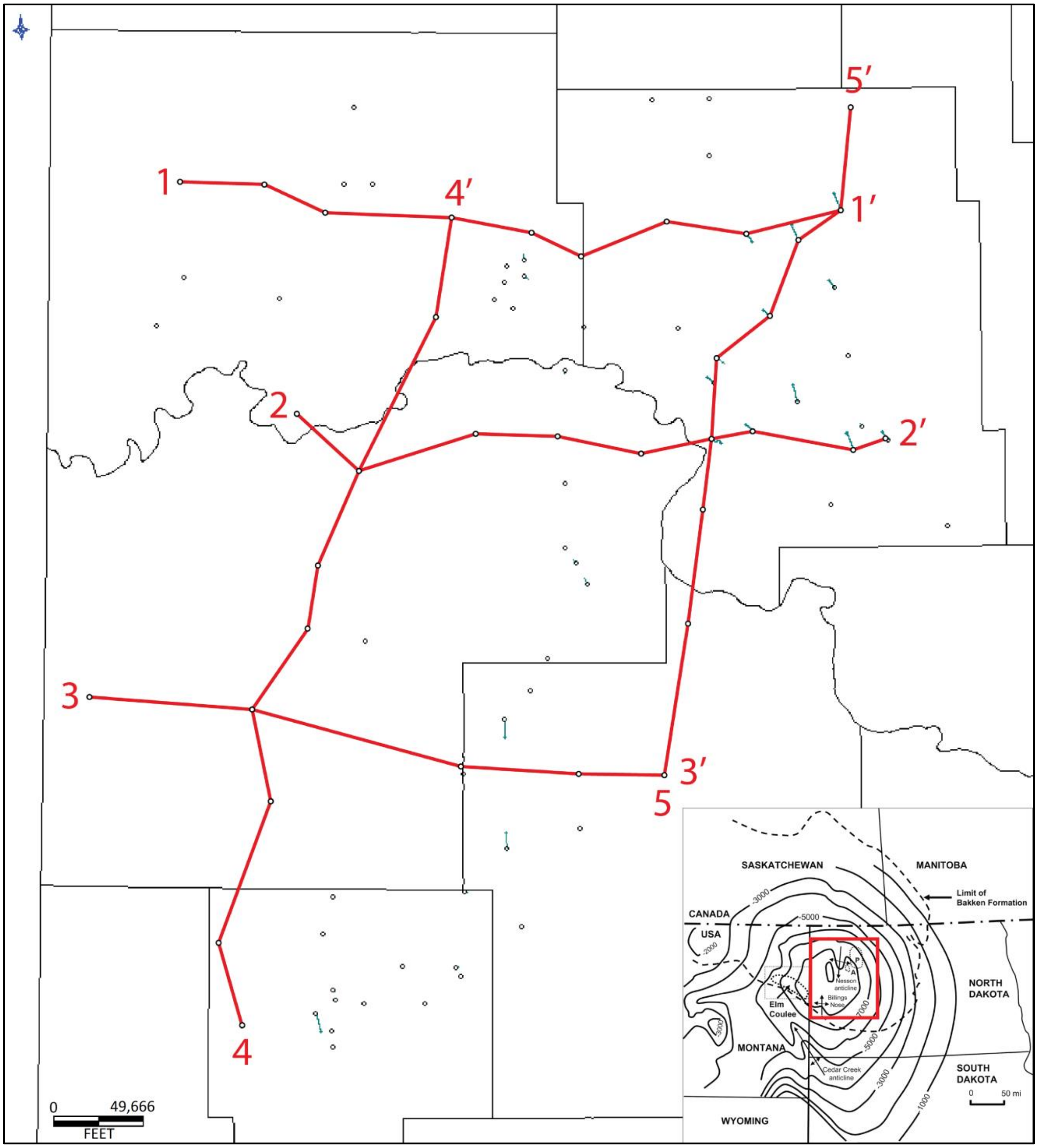

Figure 5.1. The locations of five structural cross sections. Section lines shown in red. The red frame in the bottom right shows the study area.

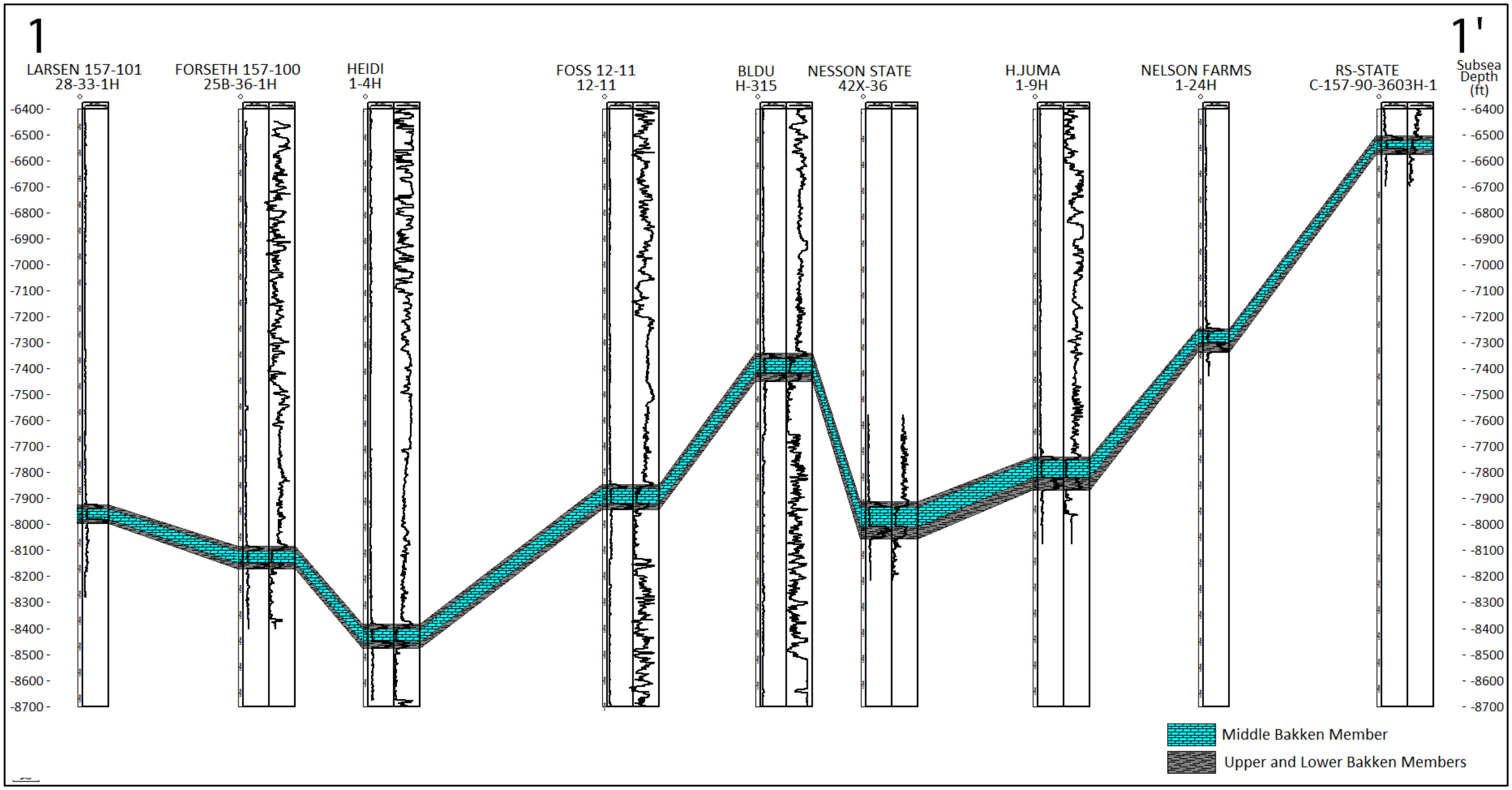

Figure 5.2. West-east oriented structural cross section 1-1'. The Bakken thins at the edges. Location of the cross section is shown in Figure 5.1. Gamma-ray is represented on the left, and resistivity on the right where two logs are presented. Where one log is present, only gamma ray is represented.

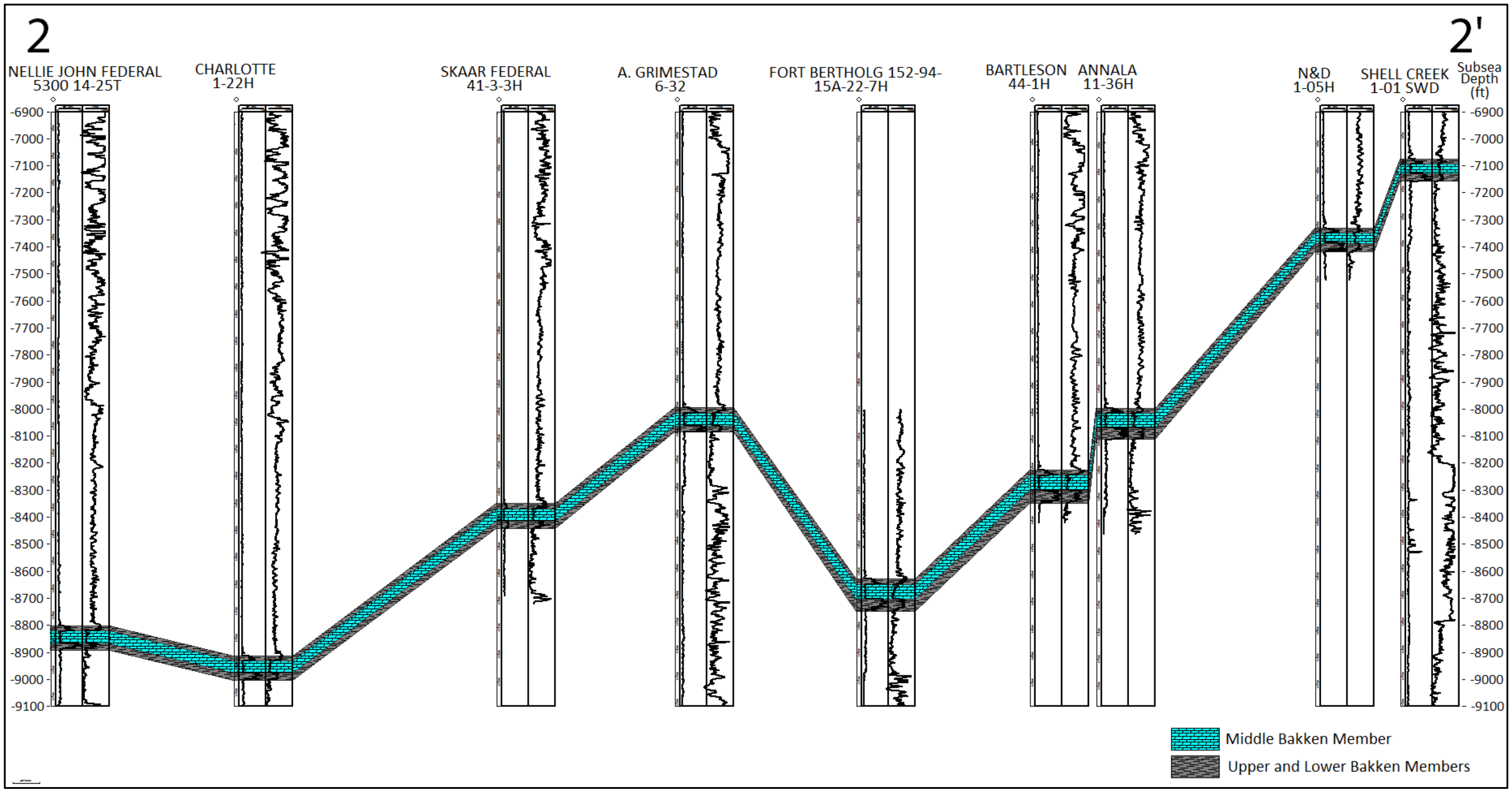

Figure 5.3. East-west oriented structural cross section 2-2'. Location of the cross section is shown in Figure 5.1. Gamma-ray is represented on the left, and resistivity on the right where two logs are presented.

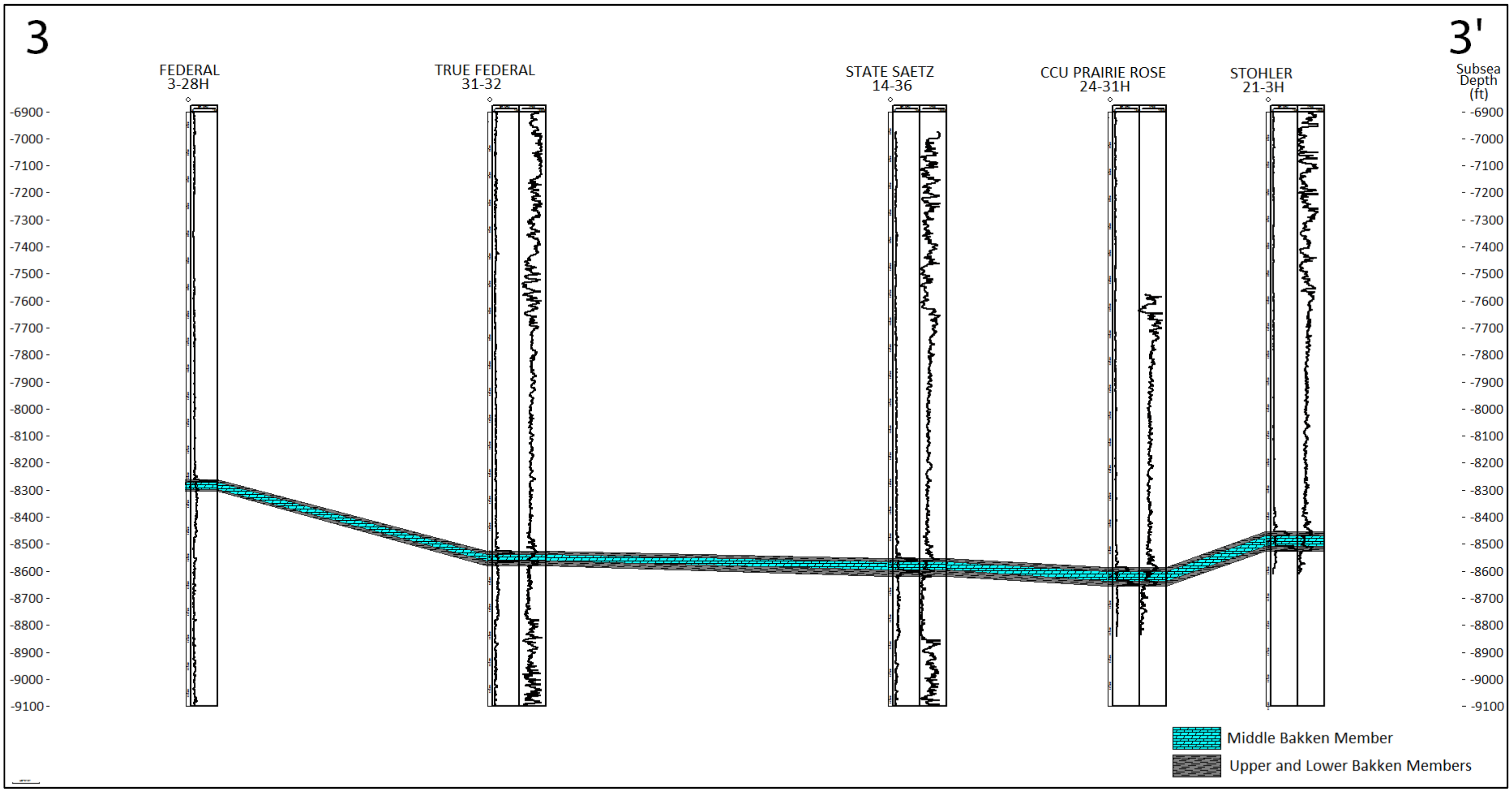

Figure 5.4. West-east oriented structural cross section 3-3'. There is no major thickness change. Location of the cross section is shown in Figure 5.1. Gamma-ray is represented on the left, and resistivity on the right where two logs are presented. Where one log is present, only gamma ray is represented.

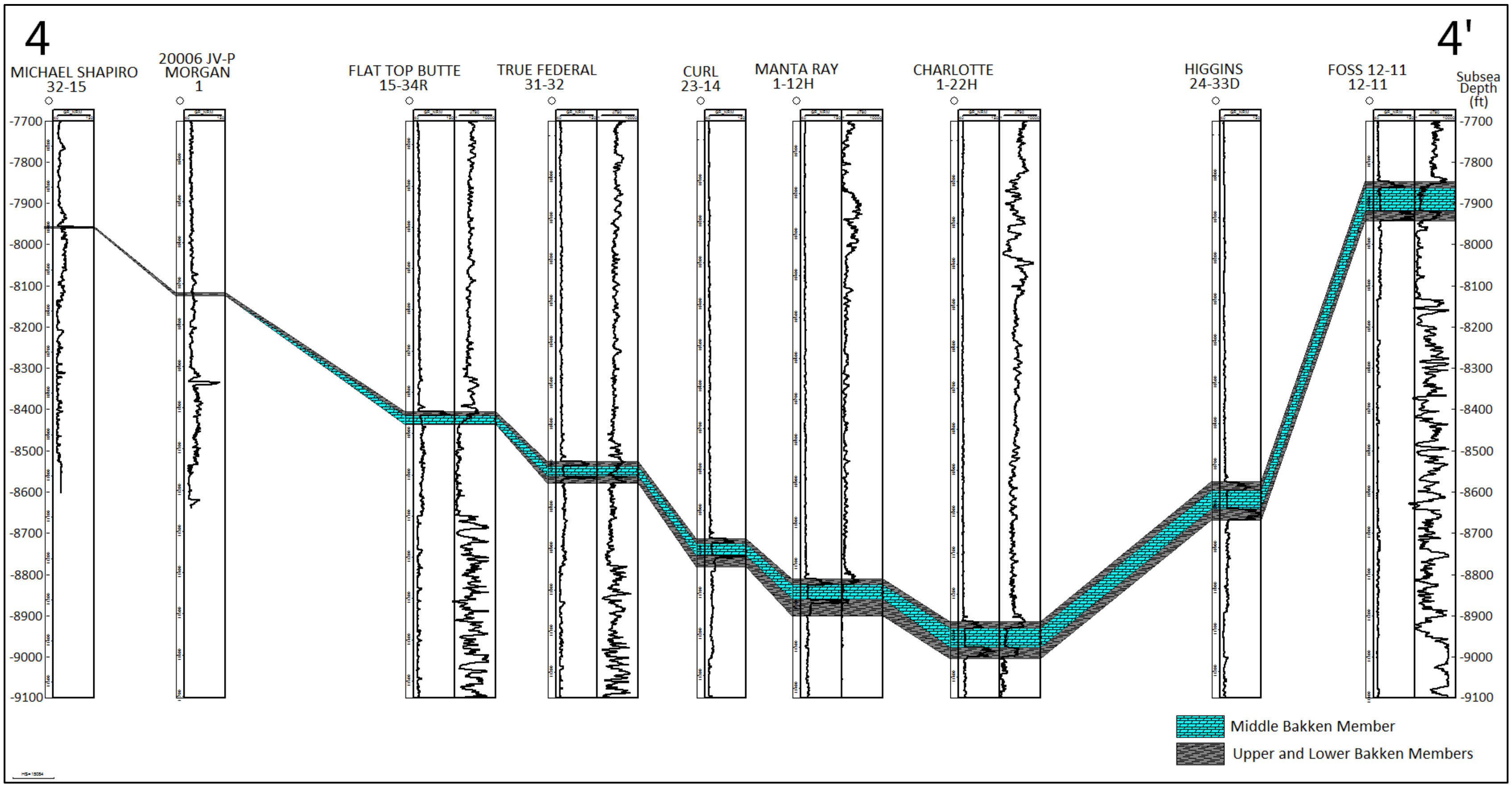

Figure 5.5. South-north oriented structural cross section 4-4'. The middle Bakken is absent in the southern part. Location of the cross section is shown in Figure 5.1. Gamma-ray is represented on the left, and resistivity on the right where two logs are presented. Where one log is present, only gamma ray is represented.

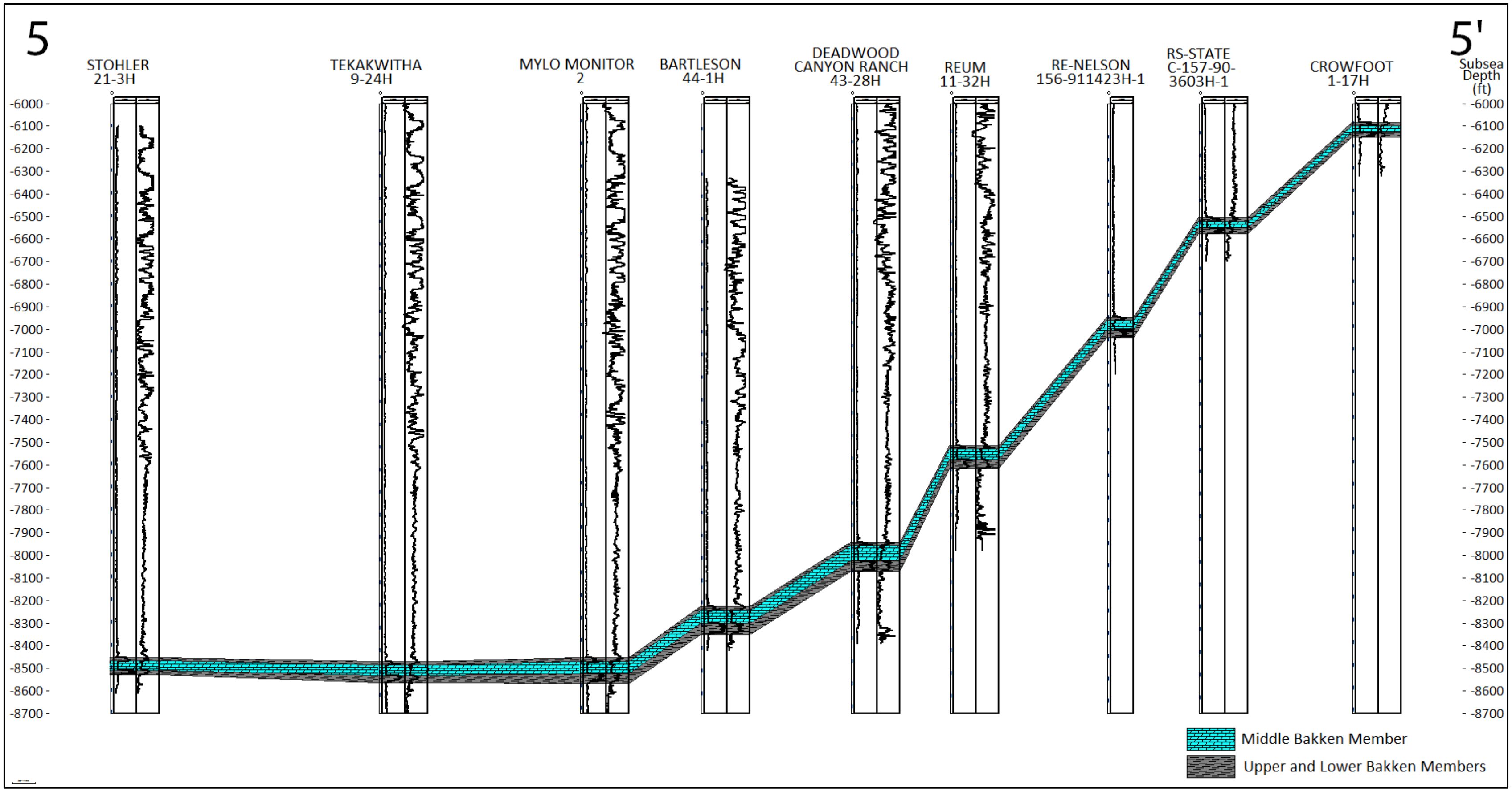

Figure 5.6. South-north oriented structural cross section 5-5'. In the southern part, the Bakken depth remains the same while in the north, it becomes shallower and thins. Location of the cross section is shown in Figure 5.1. Gamma-ray is represented on the left, and resistivity on the right where two logs are presented. Where one log is present, only gamma ray is represented.

5.1.2. Stratigraphic Cross Sections

Six east-west and south-north oriented stratigraphic cross sections were constructed (Figure 5.7). The correlated cross sections show thickness and facies' variations in the Bakken facies. Cross sections A-A', B-B', and C-C' are oriented in a west-east direction (Figure 5.8, 5.9, and 5.10). Cross sections D-D', E-E' and F-F' have a south-north orientation (Figure 5.11, 5.12, and 5.13).

The top of the upper Bakken member was used as a datum in the stratigraphic cross sections. Facies D is absent in some parts which was explained in the figures. There is very thin Facies A deposition and it is absent in some parts. Facies B, Facies C and Facies E-F are almost continuously deposited in the study area.

There is an onlap relation between Bakken members and the underlying Three Forks Formation. The Bakken uncomformably overlies the Three Forks Formation which means erosion occurred before the deposition of the Bakken Formation.

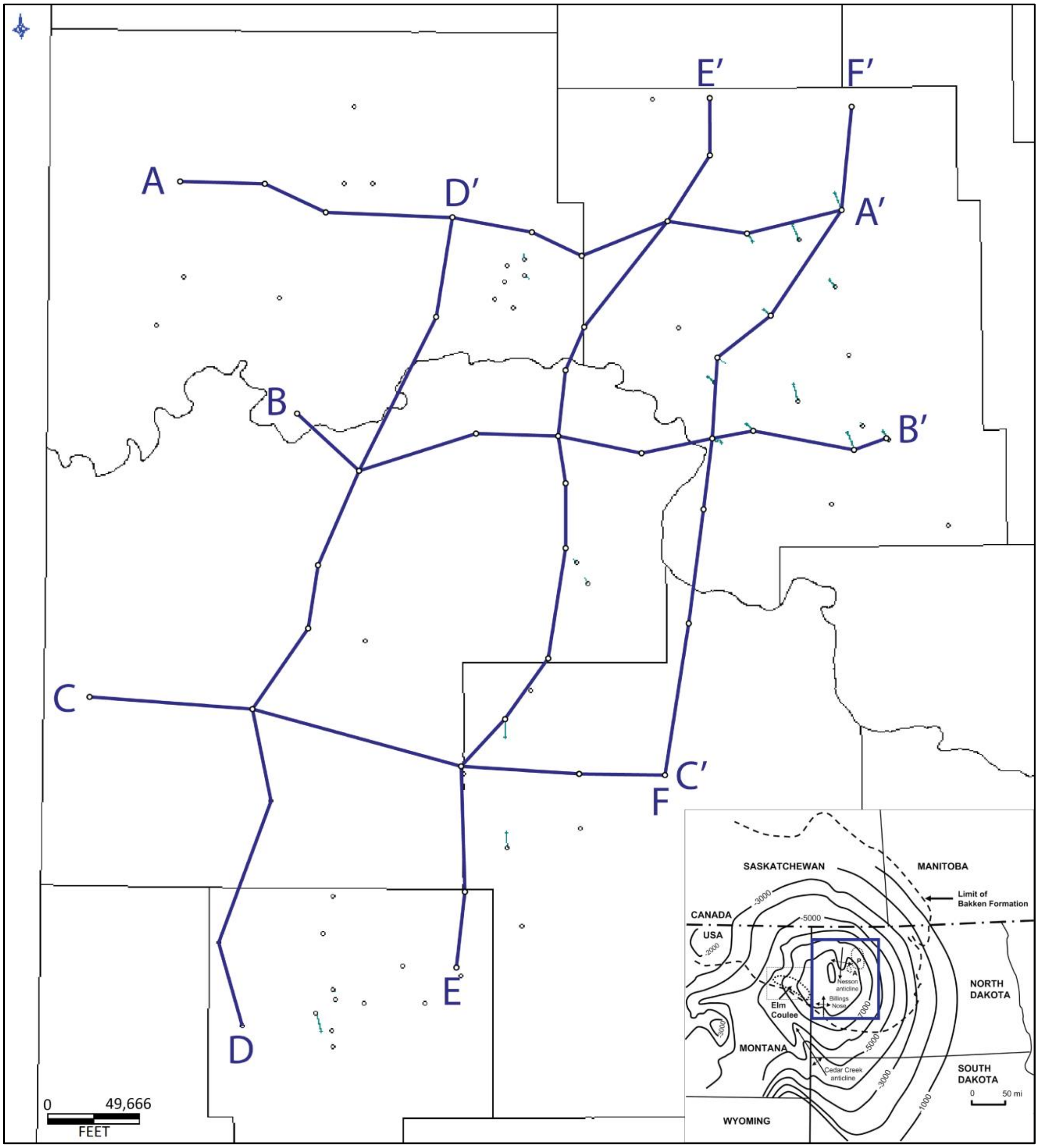

Figure 5.7. The locations of six stratigraphic cross sections. Section lines shown in blue. The blue frame in the bottom right shows the study area.

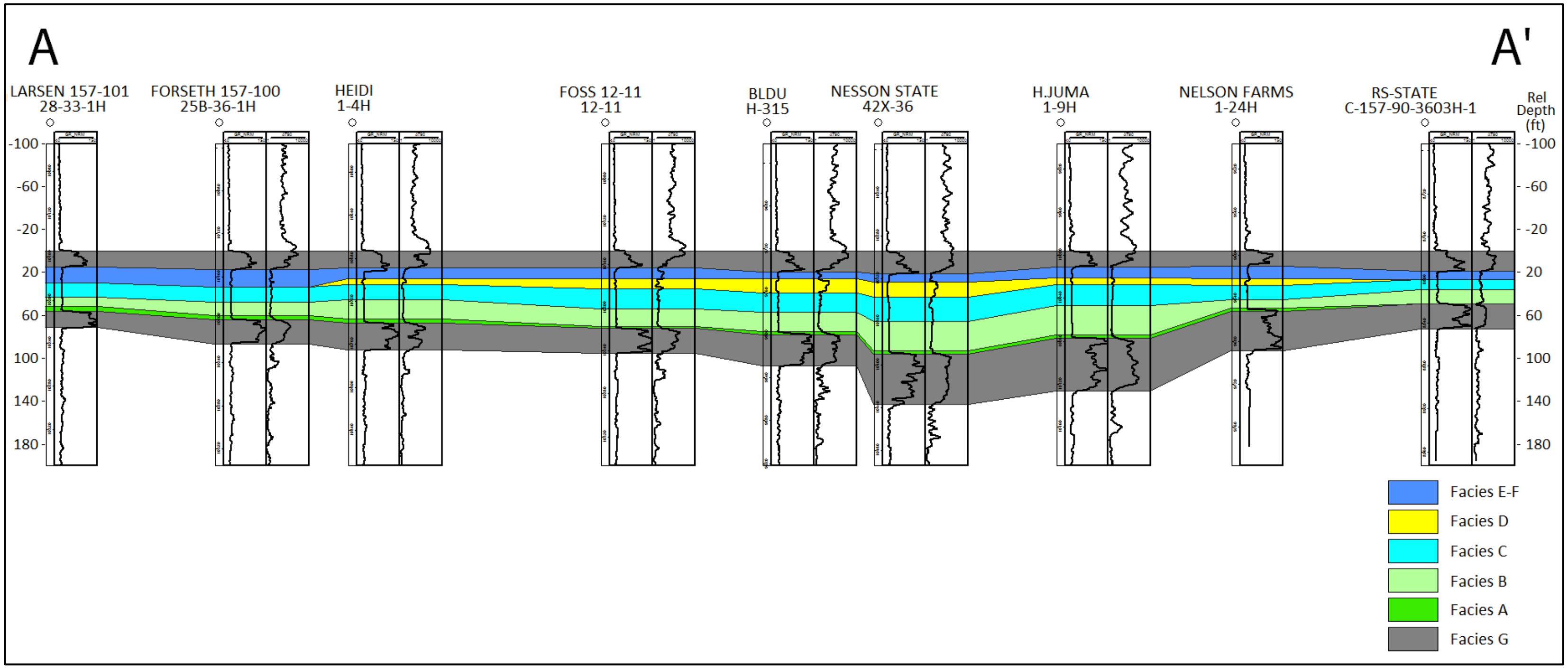

Figure 5.8. East-west oriented stratigraphic cross section A-A'. The middle Bakken thickens toward the middle. Facies D can be seen in most wells and thickens toward the center. In the east, Facies E thickens where Facies D is absent. Location of the cross section is shown in Figure 5.7. Gamma-ray is represented on the left, and resistivity on the right where two logs are presented. Where one log is present, only gamma ray is represented.

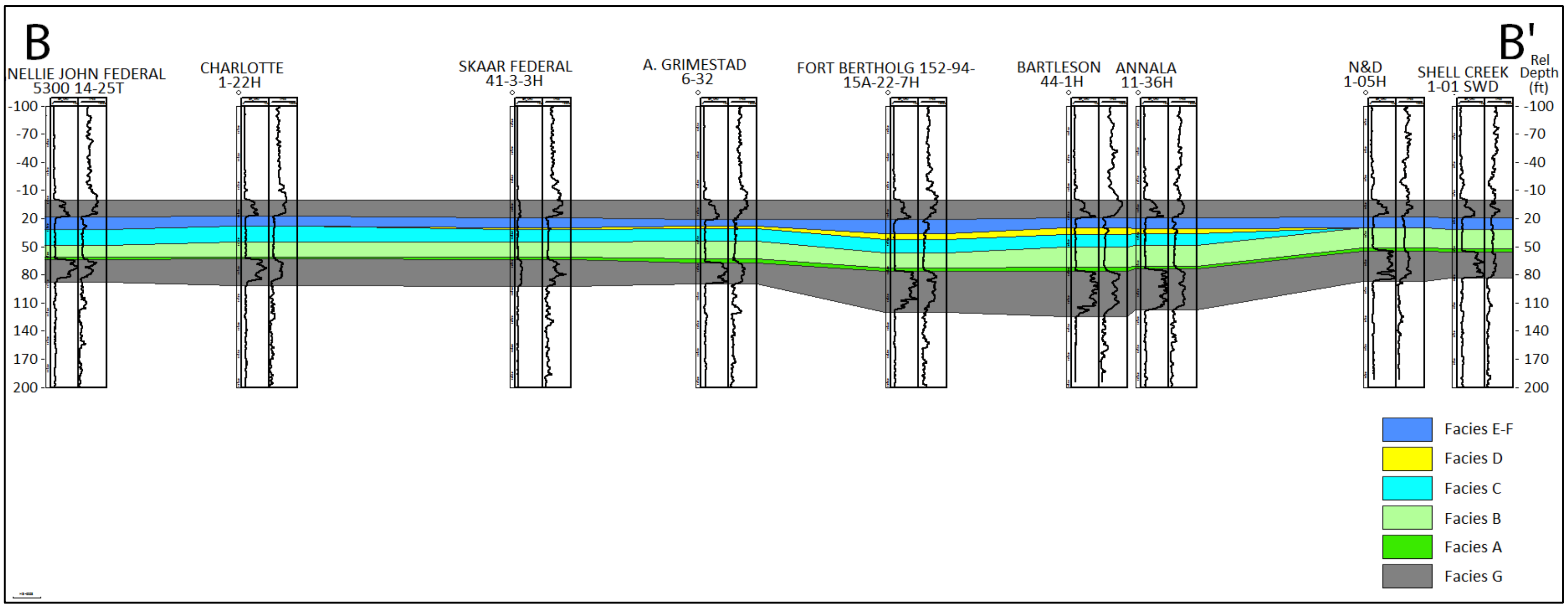

Figure 5.9. East-west oriented stratigraphic cross section B-B'. The middle Bakken slightly thickens in the center. Facies D thins and becomes absent through the west. In the westerly part, neither Facies D nor Facies C is present. Location of the cross section is shown in Figure 5.7. Gamma-ray is represented on the left, and resistivity on the right where two logs are presented.

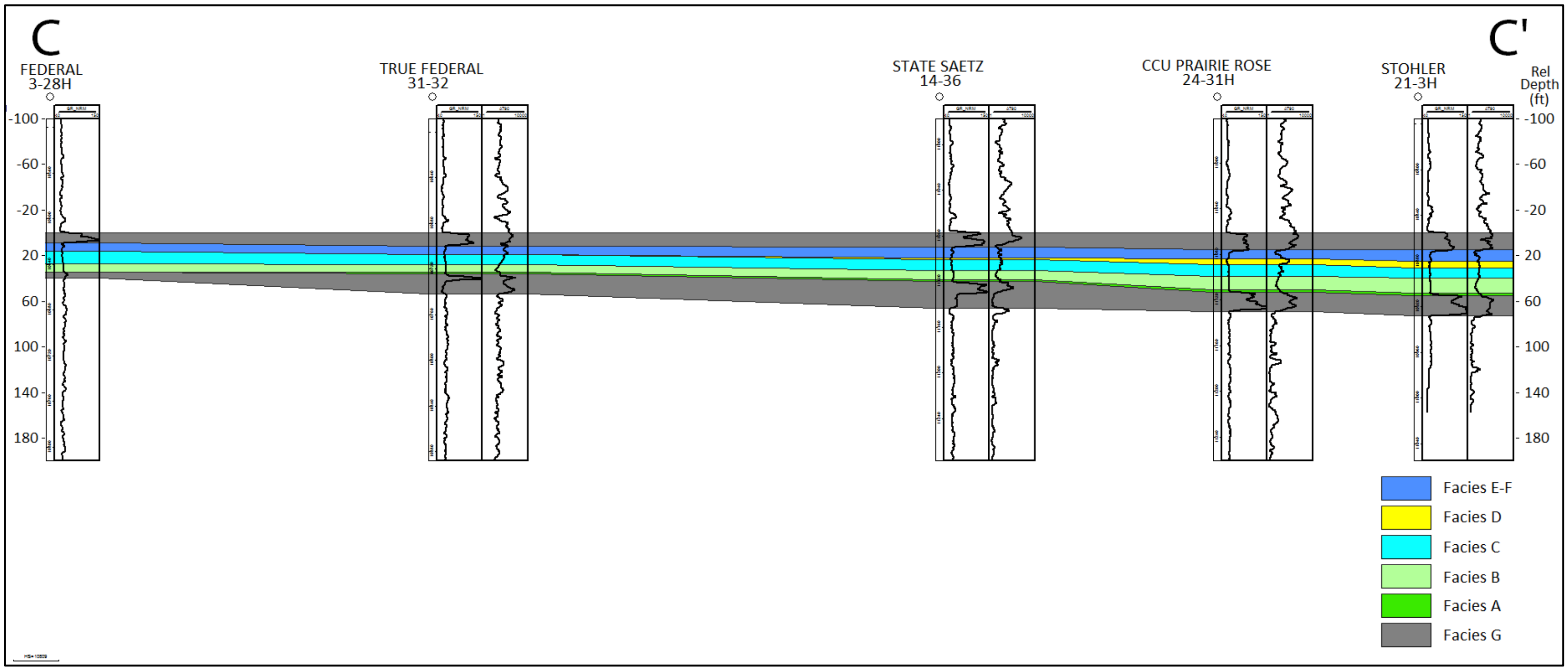

Figure 5.10. East-west oriented stratigraphic cross section C-C'. The cross section corresponds to the southern part of the study area. There is no major thickness change in the middle Bakken to the east. The middle Bakken thickens and Facies D is present towards the east. Location of the cross section is shown in Figure 5.7. Gamma-ray is represented on the left, and resistivity on the right where two logs are presented. Where one log is present, only gamma ray is represented.

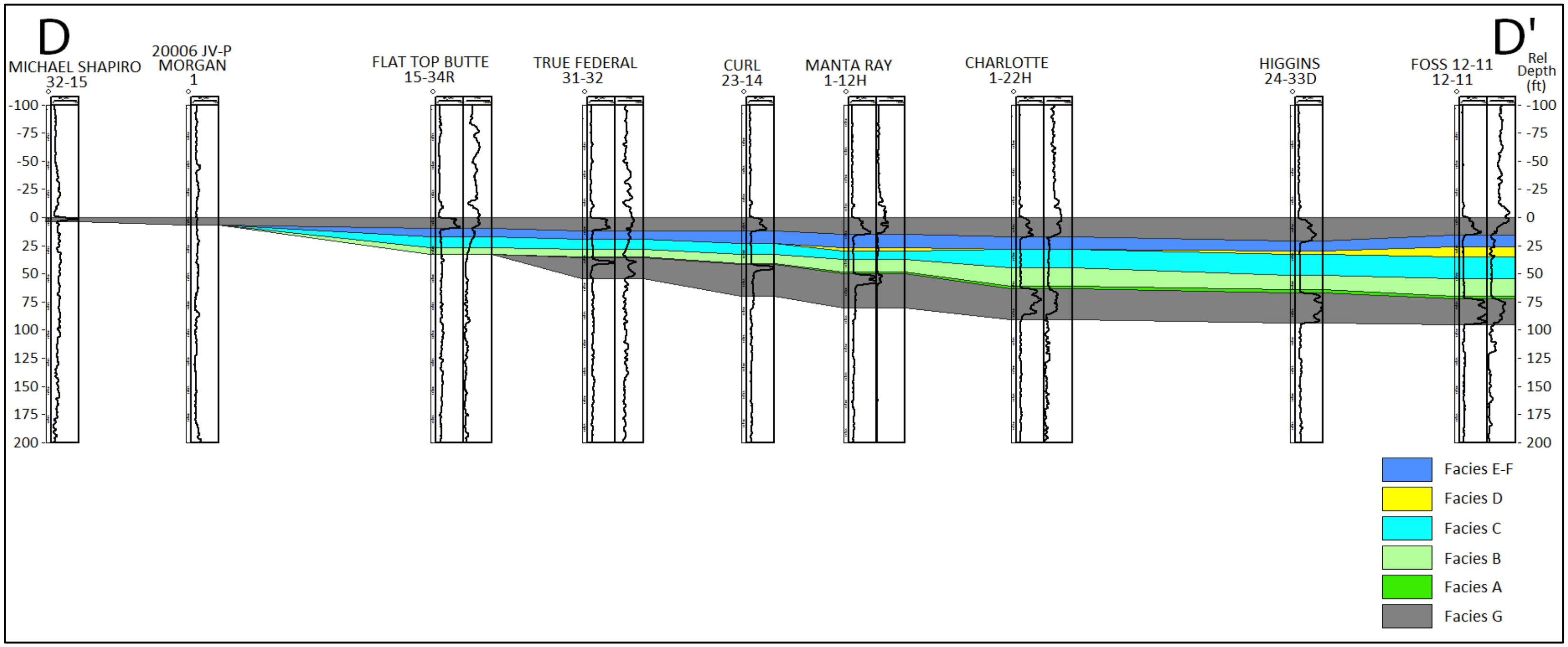

Figure 5.11. South-north oriented stratigraphic cross section D-D'. All Bakken facies thin through the south where the middle Bakken facies and lower Bakken becomes absent. There is Facies D deposition in the Manta Ray 1-12H well. Facies D is present in the northern part and thickens. Location of the cross section is shown in Figure 5.7. Gamma-ray is represented on the left, and resistivity on the right where two logs are presented. Where one log is present, only gamma ray is represented.

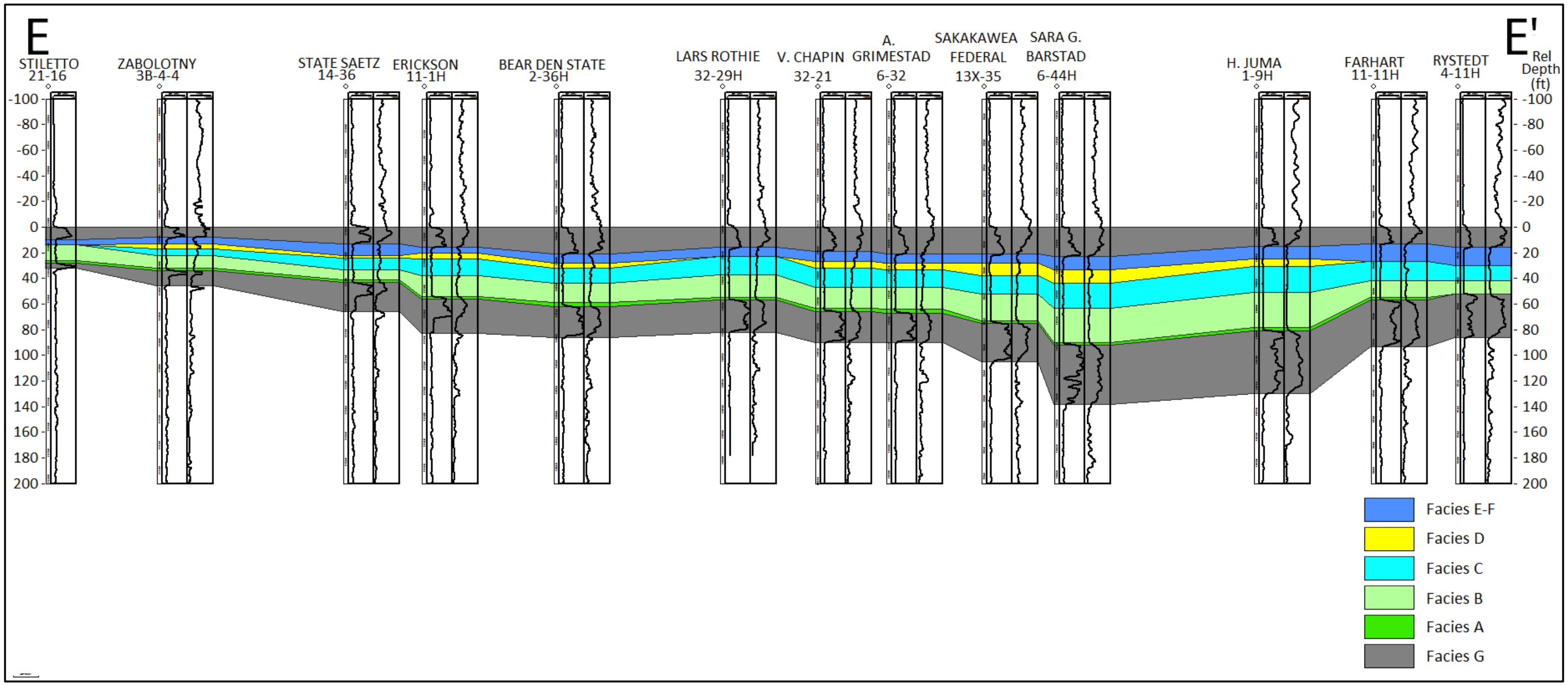

Figure 5.12. South-north oriented stratigraphic cross section E-E'. The cross section includes 13 wells and corresponds to the middle part of the study area. In most wells, there is Facies D assemblage and which is absent in the north. The middle Bakken Facies thins towards the south. Location of the cross section is shown in Figure 5.7. Gamma-ray is represented on the left, and resistivity on the right where two logs are presented. Where one log is present, only gamma ray is represented.

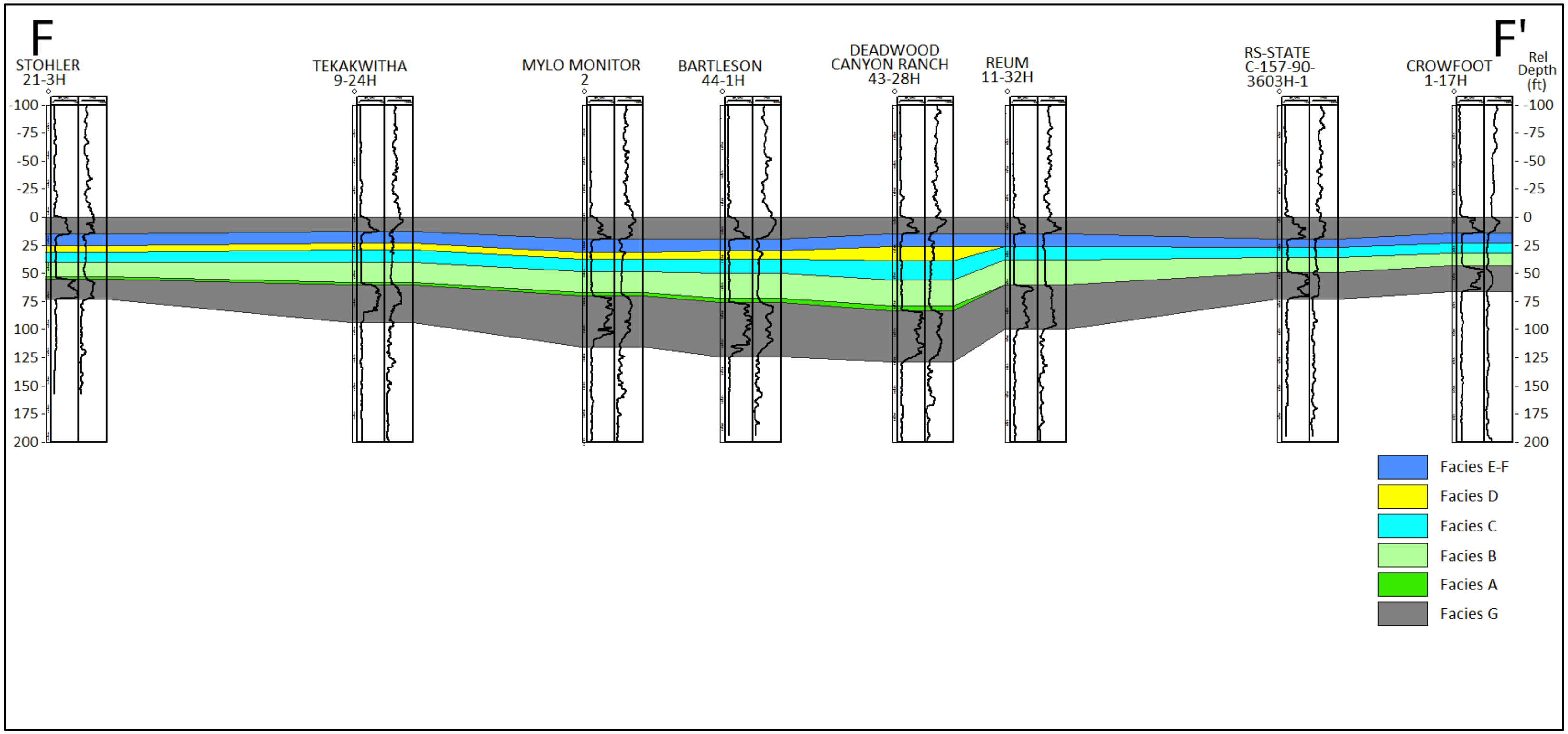

Figure 5.13. South-north oriented stratigraphic cross section F-F'. There is Facies D deposition to the Reum 11-32H well from the southern part. North of this well Facies D and Facies A become absent and the remaining middle Bakken facies thin toward the north. Location of the cross section is shown in Figure 5.7. Gamma-ray is represented on the left, and resistivity on the right where two logs are presented.

5.2. Isopach Maps

A detailed isopach map was plotted for the total Bakken by using 2914 wells (Figure 5.14). The top and base values of the Bakken Formation were provided in the NDIC website. In addition, seven more isopach maps were constructed to check thickness change in upper and lower members and middle Bakken facies by using 86 wells. An isopach map of Facies A was not plotted since its thickness varies from zero to six feet.

The thickness of the Bakken Formation reaches maximum value in the western region of Mountrail County, which corresponds to the center of the Williston basin. From this region, the Bakken thins in every direction. This trend can be seen for each Bakken member.

The lower Bakken member reaches 50 feet in thickness in the center of the basin (Figure 3.19). Contour intervals converge between Williams and Mountrail counties due to the Nesson Anticline. The middle Bakken member reaches 75 feet in thickness in the central part and becomes absent through the margins (Figure 3.20). The thickness of Facies B reaches up to 27 feet in the center, and gradually decreases and becomes zero towards the edges. There is a little thickening in the central part of the McKenzie County (Figure 3.21). Facies C reaches its maximum value of 19 feet on the edge of the Williams and Mountrail counties (Figure 3.22). Facies D is not continuously deposited in the formation and its maximum thickness reaches 75 feet. It is almost entirely absent in the eastern region of Mountrail County (Figure 3.23). Facies E-F shows thickness variations and slightly thins in the center of the study area. It reaches 21 feet in thickness in the northern part and its continuity cannot be seen due to the lack of wells in that area (Figure

3.24). The upper Bakken member is the most extensive layer in the Bakken Formation. It can be seen in all wells where other members are absent. Its maximum thickness is measured 25 feet in the center (Figure 3.25).

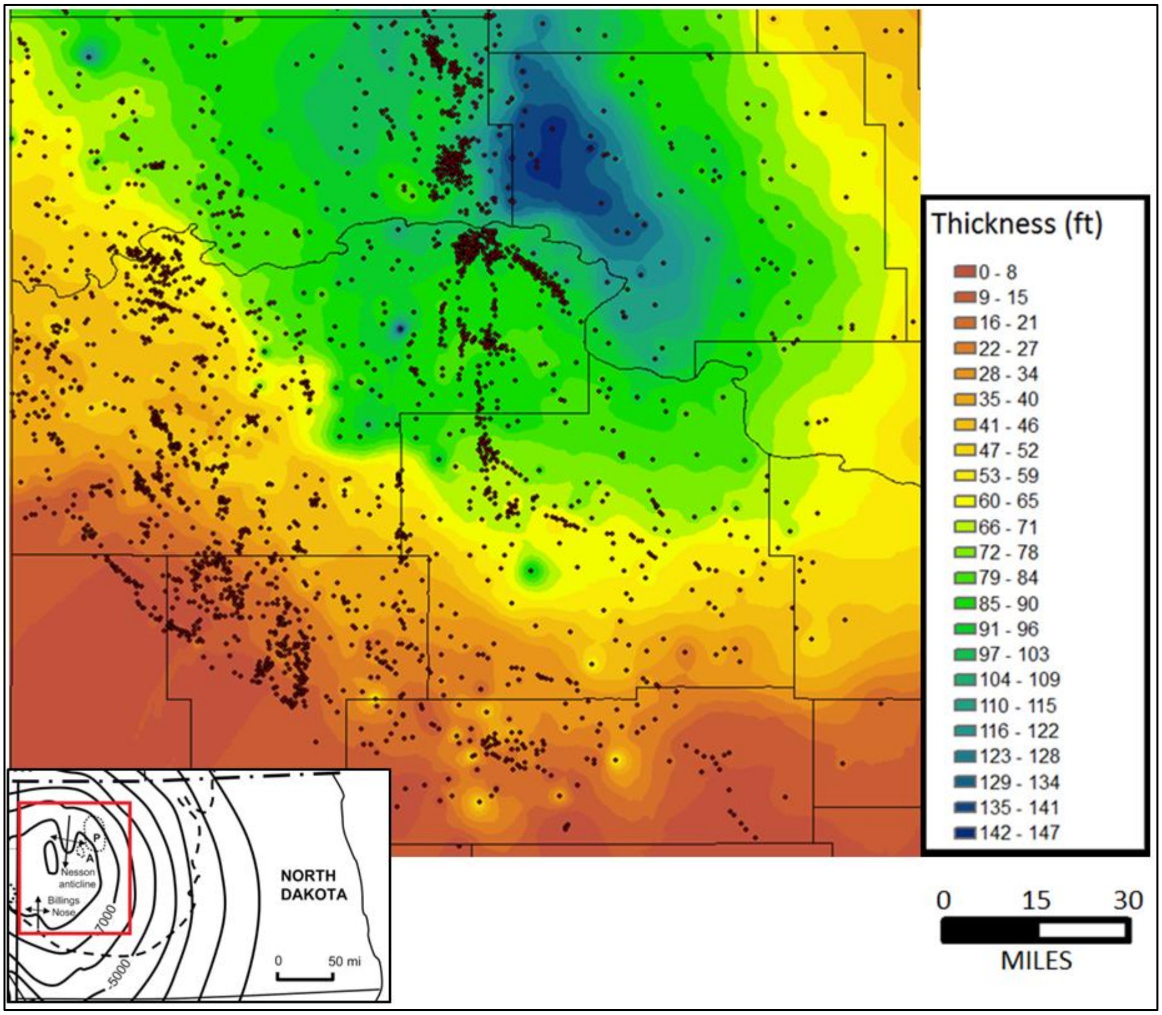

Figure 5.14. Isopach map of the total Bakken Formation. The thickness of the Bakken Formation ranges from 1 to 154 feet. The red frame in the bottom left shows the map location.

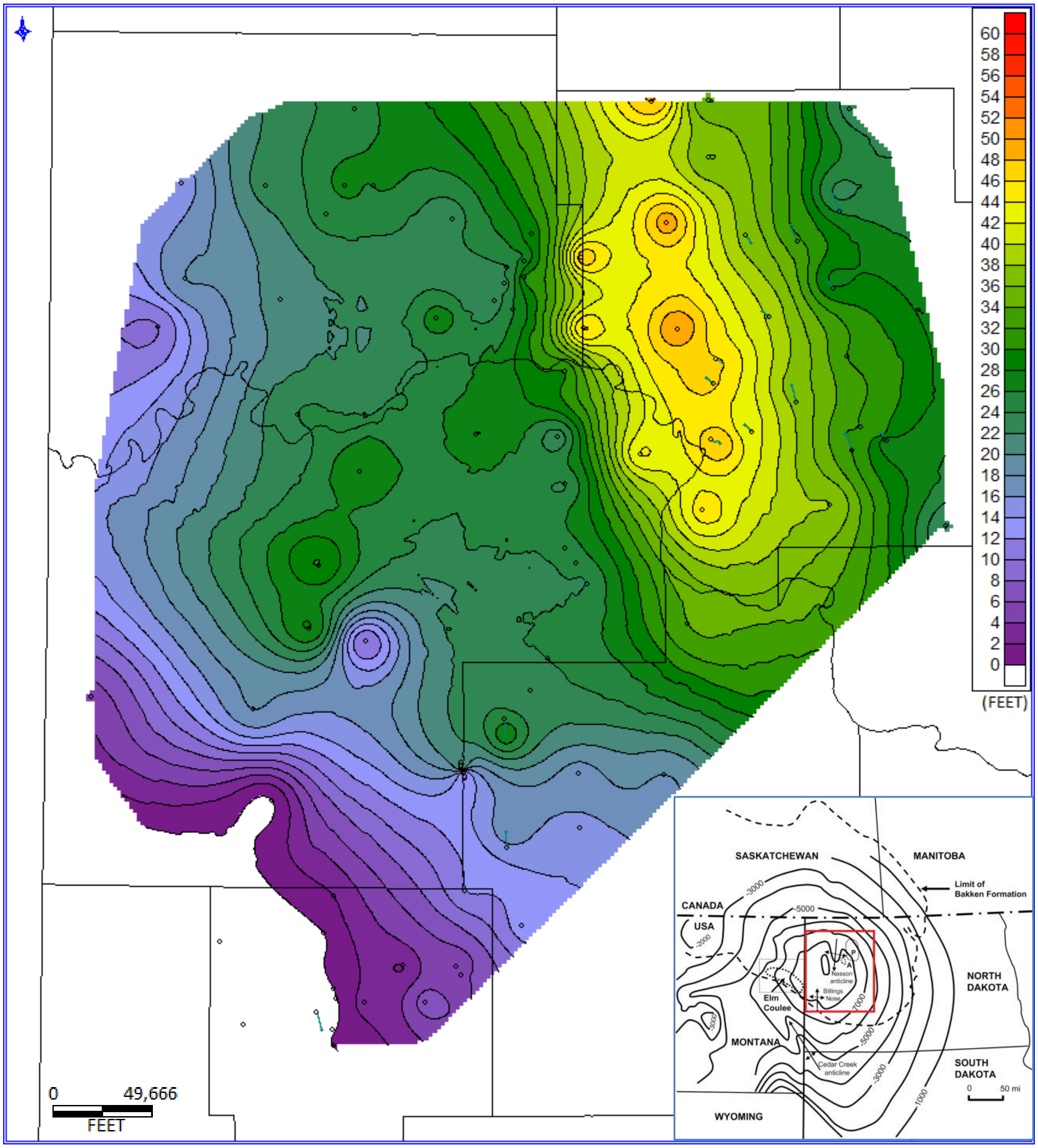

Figure 5.15. Isopach map of the lower Bakken member. Contour interval is 2 feet. The maximum thickness of the lower Bakken member is measured 50 feet. The red frame in the bottom right shows the map location.

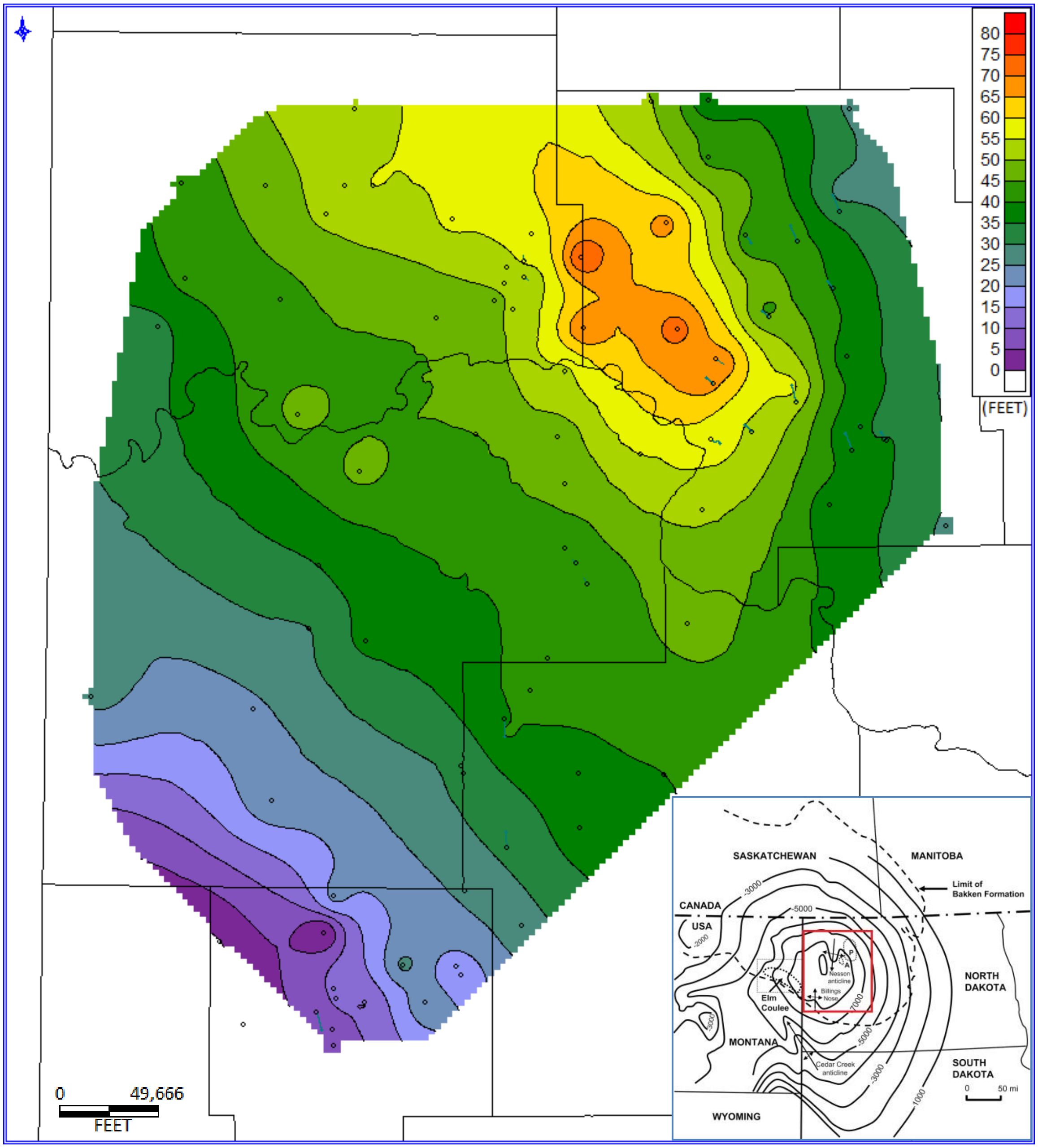

Figure 5.16. Isopach map of the middle Bakken member. Contour interval is 5 feet. The maximum thickness of the middle Bakken member is measured 75 feet. The red frame in the bottom right shows the map location.

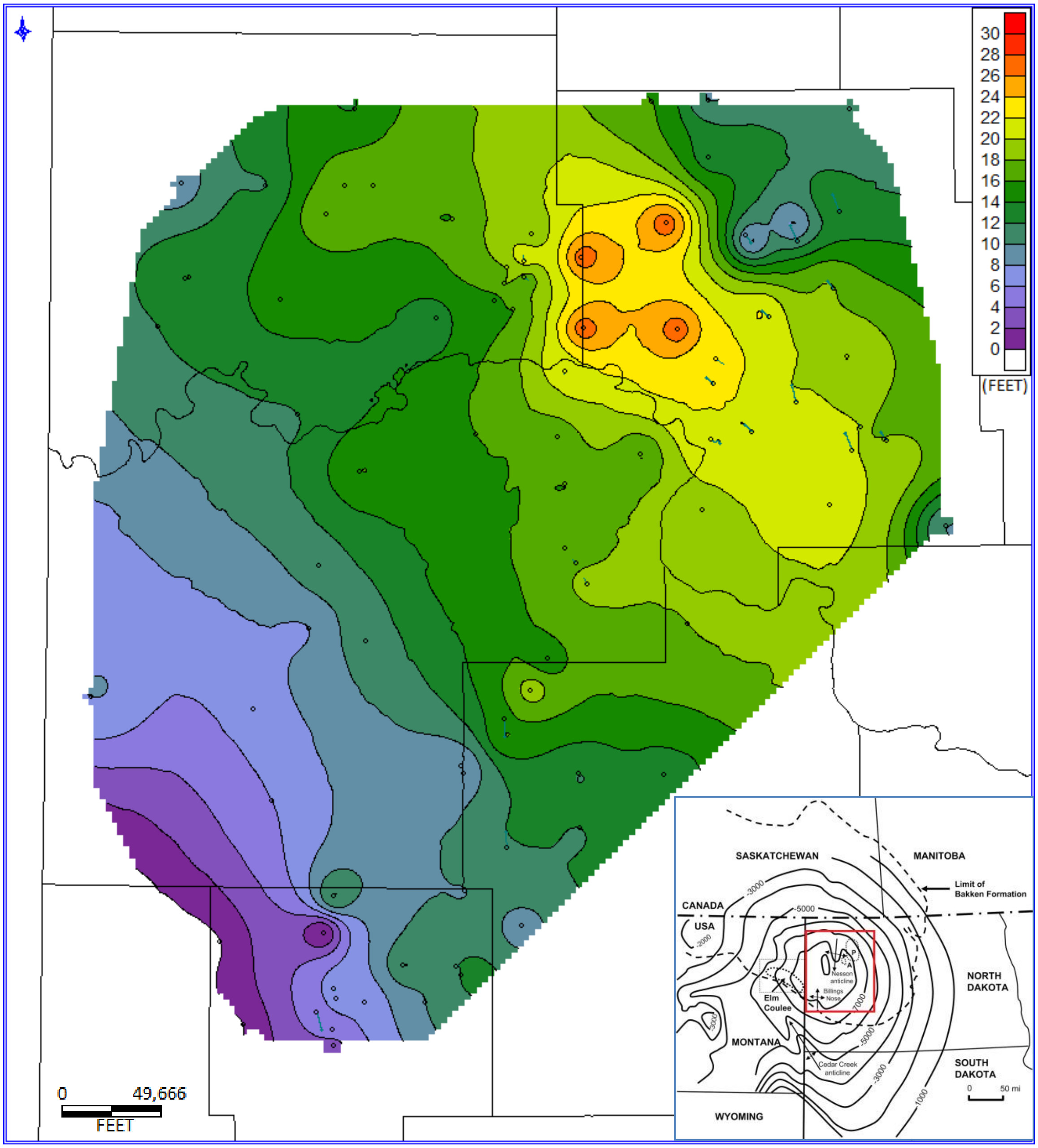

Figure 5.17. Isopach map of Facies B. Contour interval is 2 feet. The maximum thickness of Facies B is measured 27 feet. The red frame in the bottom right shows the map location.

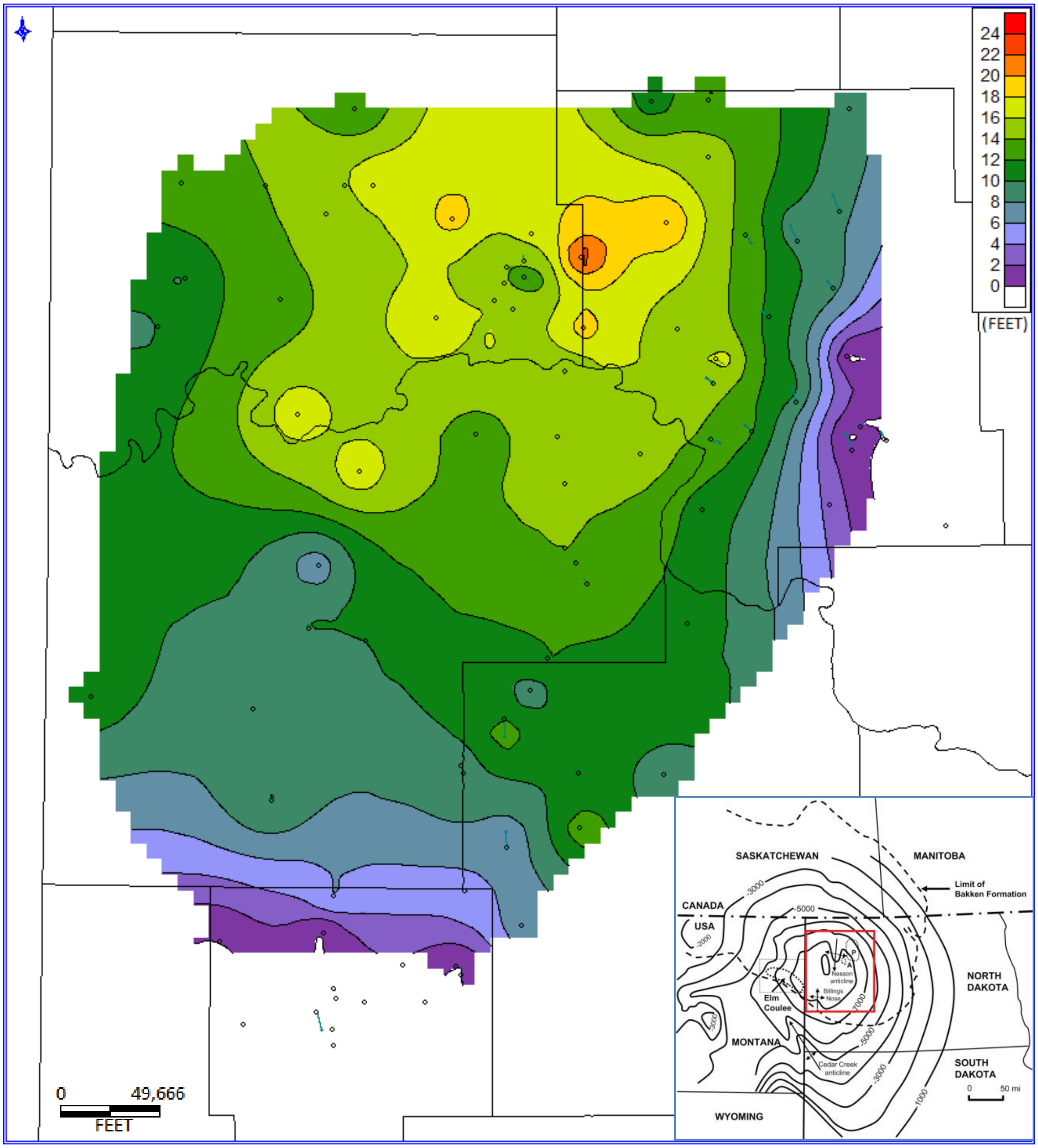

Figure 5.18. Isopach map of Facies C. Contour interval is 2 feet. The maximum thickness of Facies C is measured 23 feet. The red frame in the bottom right shows the map location.

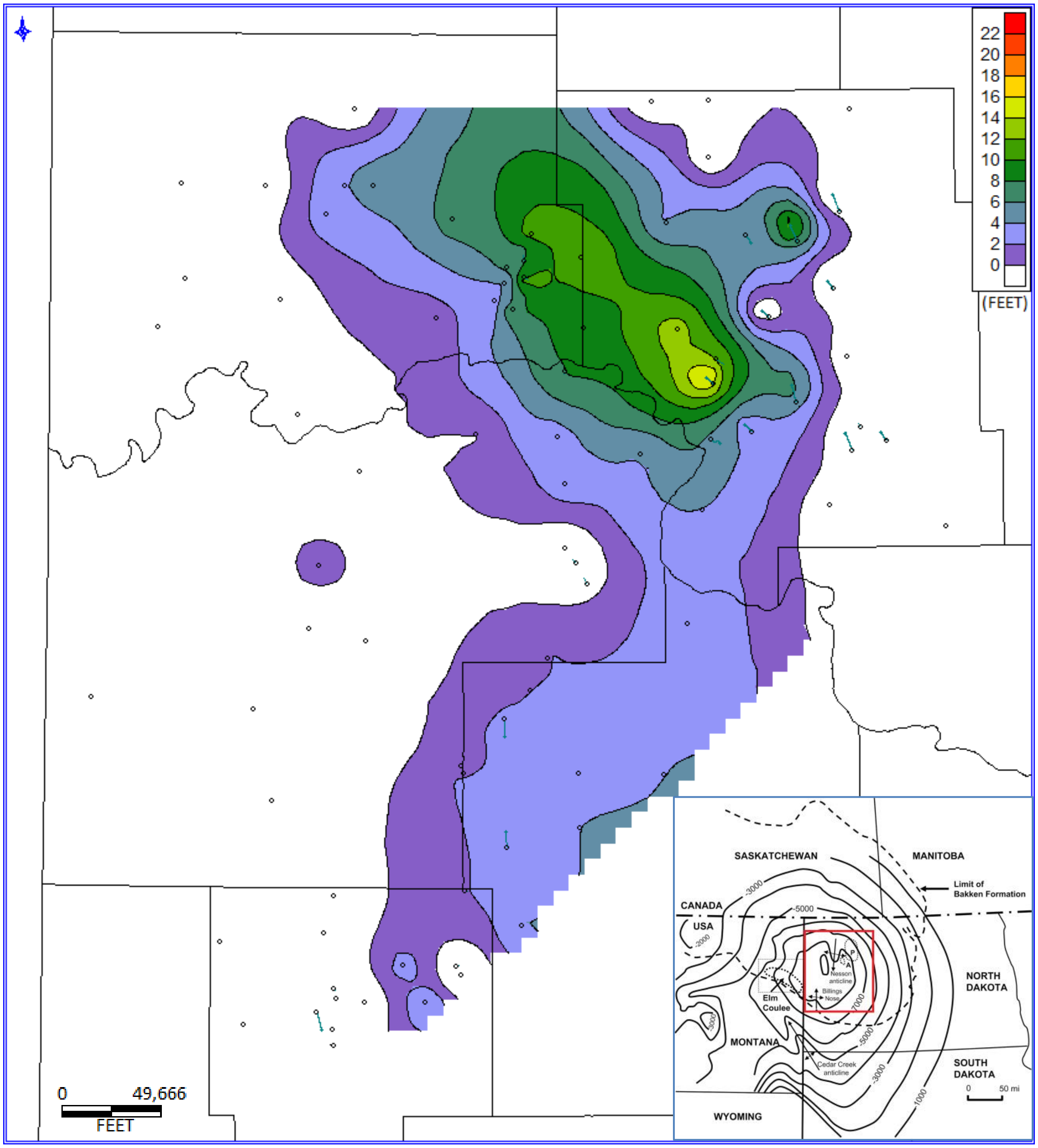

Figure 5.19. Isopach map of Facies D. Contour interval is 2 feet. The maximum thickness of Facies D is measured 19 feet. The red frame in the bottom right shows the map location.

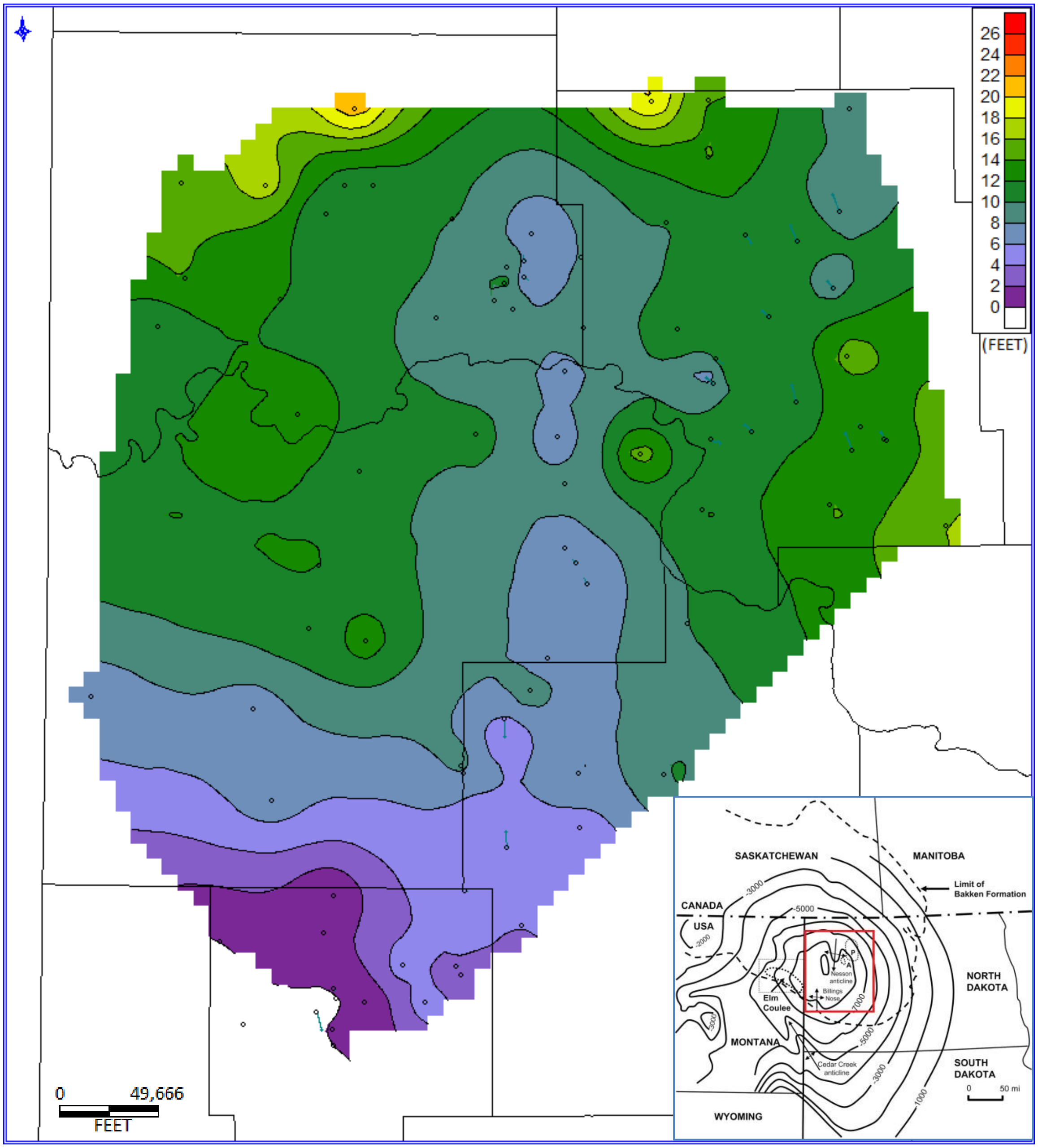

Figure 5.20. Isopach map of Facies E-F. Contour interval is 2 feet. The maximum thickness of Facies E-F is measured 21 feet. The red frame in the bottom right shows the map location.

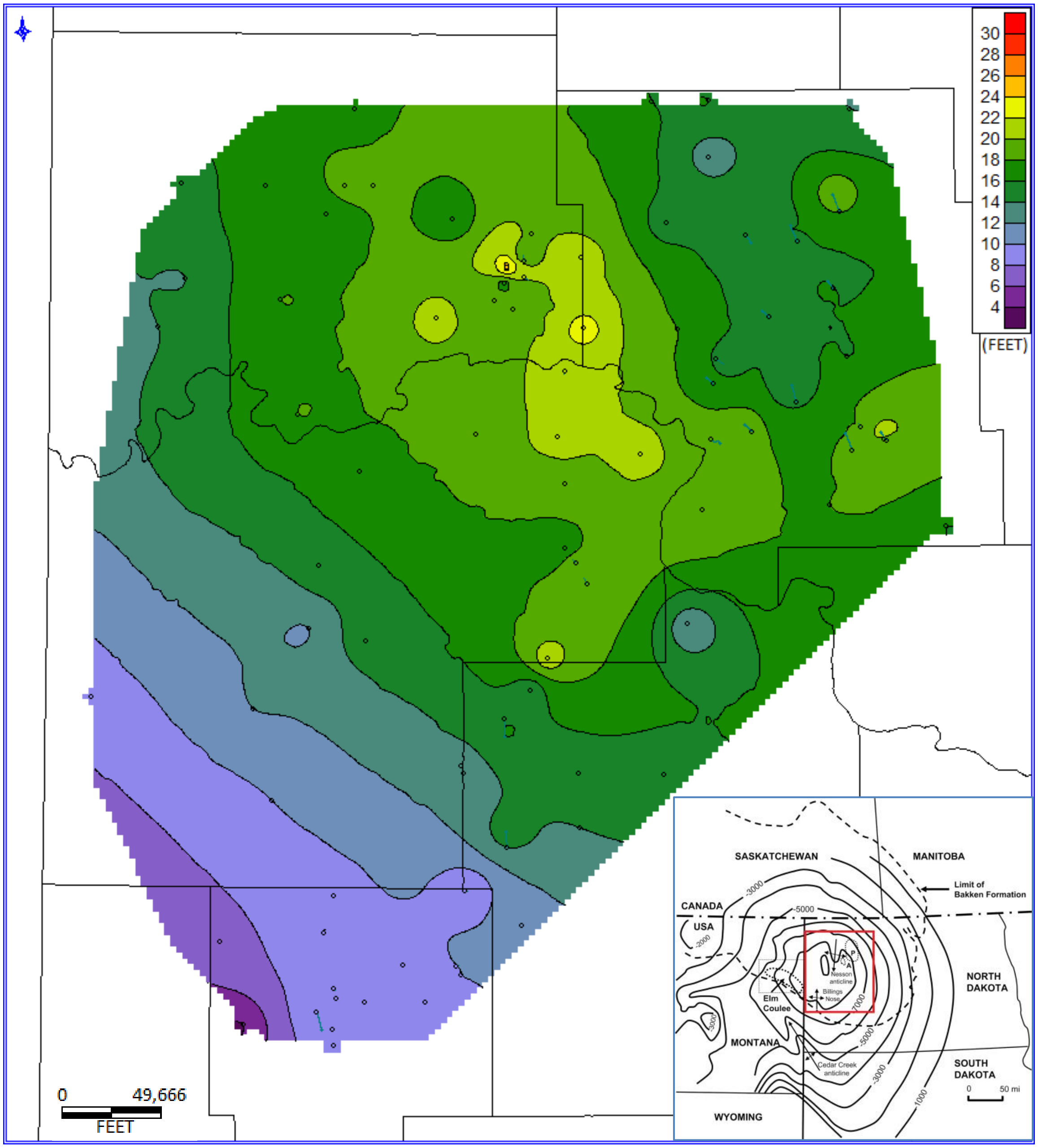

Figure 5.21. Isopach map of the upper Bakken member. Contour interval is 2 feet. The maximum thickness of the Upper Bakken member is measured 25 feet. The red frame in the bottom right shows the map location.

5.3. Depositional Environment Interpretation

For the upper and lower shales it has been interpreted that they deposited in an offshore marine environment (Webster, 1984; Pitman et al., 2001). Both of these shales were deposited in a stratified hydrologic regime identified by the lack of benthic fauna, presence of pyrite, and high organic matter. It has been interpreted that the middle member was deposited in a shallow water marine environment (Smith and Bustin, 1996). The middle Bakken member has been divided into lithofacies A-F in this study and these provide the framework for a sequence stratigraphic interpretation of the Bakken stratigraphic system.

The Bakken Formation consists of two depositional sequences. The first sequence begins with the tectonically enhanced unconformity at the top of the Three Forks Formation which also corresponds to a transgressive surface where the sea level rise took place (Figure 5.22). This unconformity is overlain by a transgressive system tract that is composed of the lower part of the lower Bakken shale. The top of high-density values mid-way through the lower Bakken shale is interpreted as a maximum flooding surface. Resistivity, photoelectric, gamma ray and porosity log readings increase above this surface. The transgressive tract is overlain by a highstand system tract which contains the upper portion of the lower Bakken shale and Facies A, B and C of the middle Bakken member. The shift from higher to lower density within the shale suggests a higher preservation of organic matter as the basin deepens during transgression. Facies A which consists of skeletal wackestone deposited in the offshore marine environment. Nereites fossils within Facies B indicate that it was deposited under low energy conditions while siltstone and mud sediment deposits indicate varying energy conditions. Facies B is interpreted as being deposited in an outer ramp environment. The deposition of Facies C occurred in a lower shoreface to middle shoreface setting since laminated sandstone and muddy siltstone indicates it was affected by tidal influences. Gradational contacts between Facies A and Facies B, and Facies B and Facies C indicate that they belong to the same system. In general, it can be interpreted that a highstand system tract is characterized by shallowing upwards from deep water sediments to a proximal outer ramp environment (Figure 5.23). The first Bakken sequence ends with an erosional sequence boundary at the base of Facies D which is representative of a drop in sea-level. Cross-bedding, coarser texture, quartz sandstones or ooid grainstones indicate that Facies D was deposited in a high energy, shoaling facies. Variable thickness and aerial extent of this facies represent down-ramp shoreline deposits. Facies D is the lowstand system tract of the second Bakken sequence. The top of Facies D is marked by a transgressive surface which indicates a rise in sea-level. Facies E-F deposition occurred in a deeper environment which is represented by a deepening upward transgressive system tract. The maximum flooding surface occurs within the upper Bakken shale where there is another shift to a lower density value. The highstand system tract of this sequence includes the upper portion of the Bakken shale and the lower part of the overlying Lodgepole Formation.

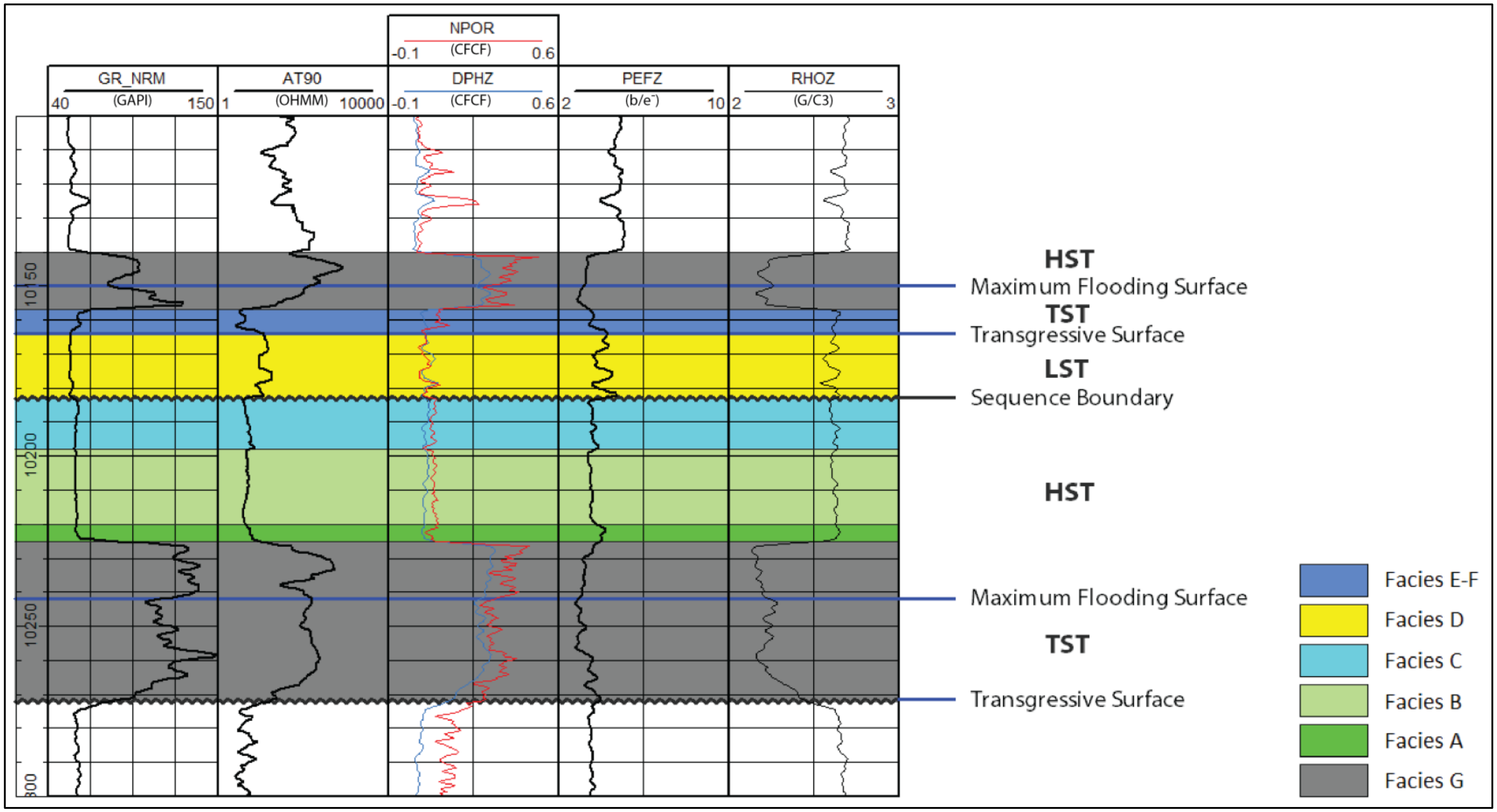

Figure 5.22. Depositional surfaces and system tracts of the Bakken Formation for the Deadwood Canyon Ranch 11-5H well located in Sanish Field, Mountrail County. HST= Highstand System Tract, TST= Transgressive System Tract, LST= Lowstand System Tract.

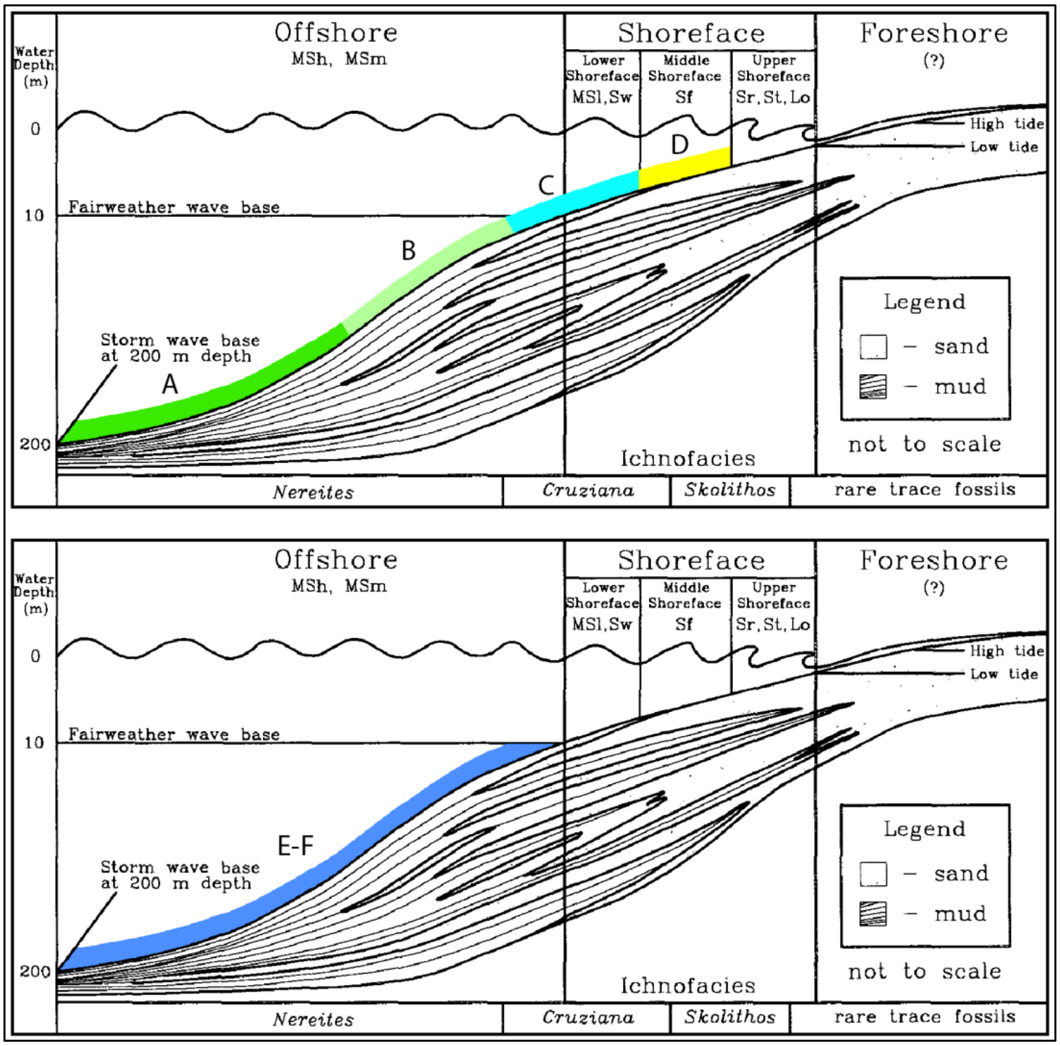

Figure 5.23. Depositional environment interpretation of the middle Bakken facies. Deposition of Facies A, B and C takes place from offshore marine to a lower shoreface environment. Facies D was deposited in a middle shoreface environment. Facies E-F was deposited under fair weather wave base with a rise in sea level (Modified from Smith and Bustin, 1996; Simenson, 2010).

5.4. Production Maps

Unconventional wells, which have an initial rush of production, tend to decline quickly. In its second year of production, a typical horizontal oil well generally produces

55 percent of what it produced the first year. Therefore, more wells need to be drilled to produce oil from unconventional shale formations in order to continue to produce at a rate comparable to a first-year production rate of a traditional well. Figure 5.24 shows an example of the typical decline in production in an unconventional well. Three kinds of production maps were plotted, which show the production for the month of April 2014 (the last month where data was available via NDIC website) (Figure 5.25), the first eight months of production (Figure 5.26), and the total production of oil (Figure 5.27). These maps were constructed on top of the isopach map of the middle Bakken member. Thus, production distribution rates over the study area and relations with the Bakken thickness can be determined from these maps. The relationship between production amounts and Bakken thickness are discussed in the Discussion chapter.

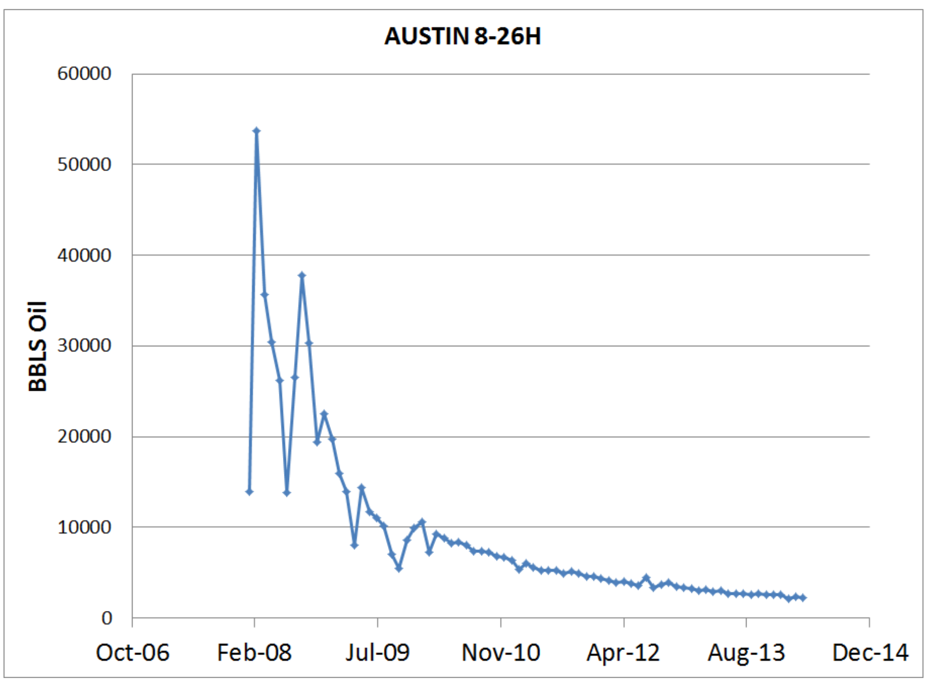

Figure 5.24. A typical Bakken well production decline curve. Monthly oil production of Austin 8-26H well located in Parshall Field, Mountrail County from February 2008 to April 2014.

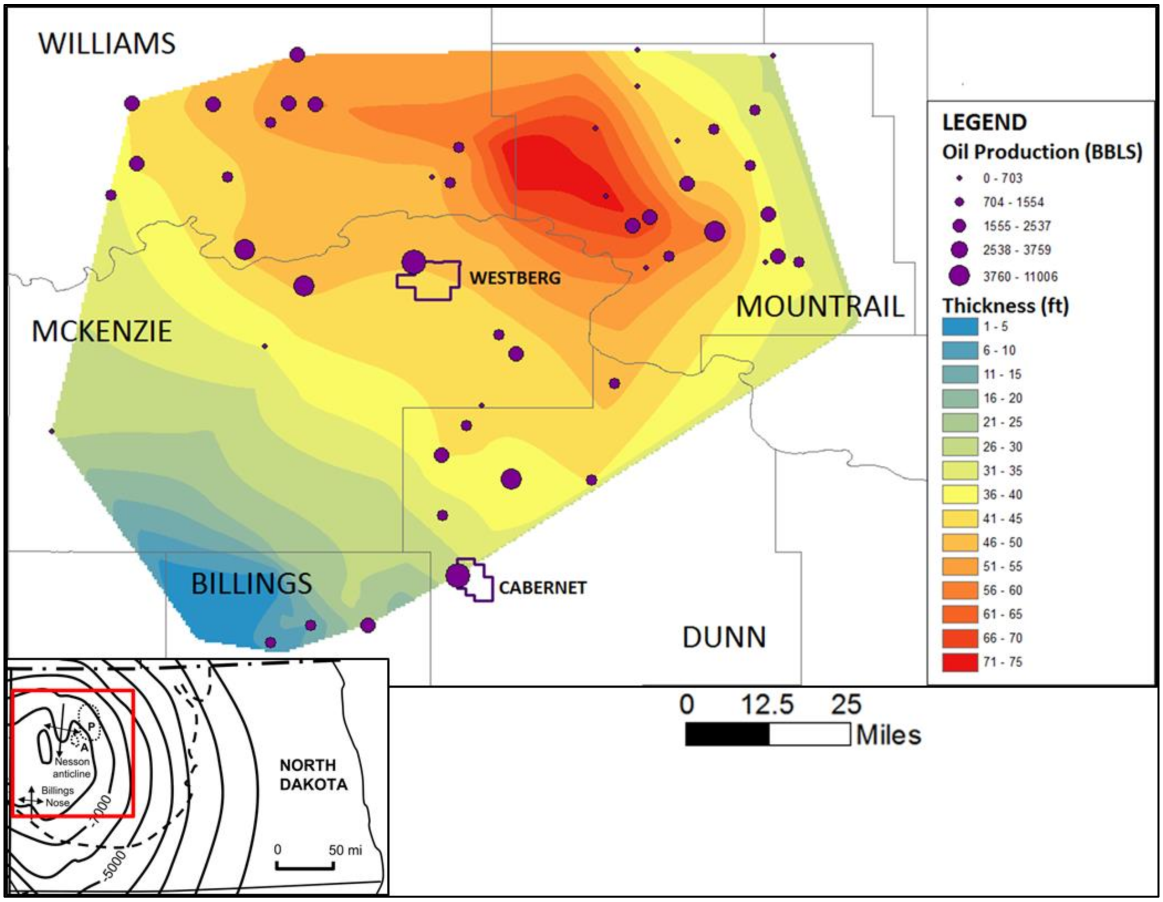

Figure 5.25. The April 2014 oil production values of 49 wells on top of the isopach map of the middle Bakken member. According to the last month's trend, the wells in the Westberg and Cabernet fields have higher production rates than the other wells. The well EVELYN KARY 2-22-15H-144-97, in Westberg Field, started to produce from the Bakken Formation in June of 2013. The well SKAAR FEDERAL 41-3-3H, in Cabernet Field, started to produce from the Bakken Formation in August, 2013. The red frame in the bottom left shows the map location.

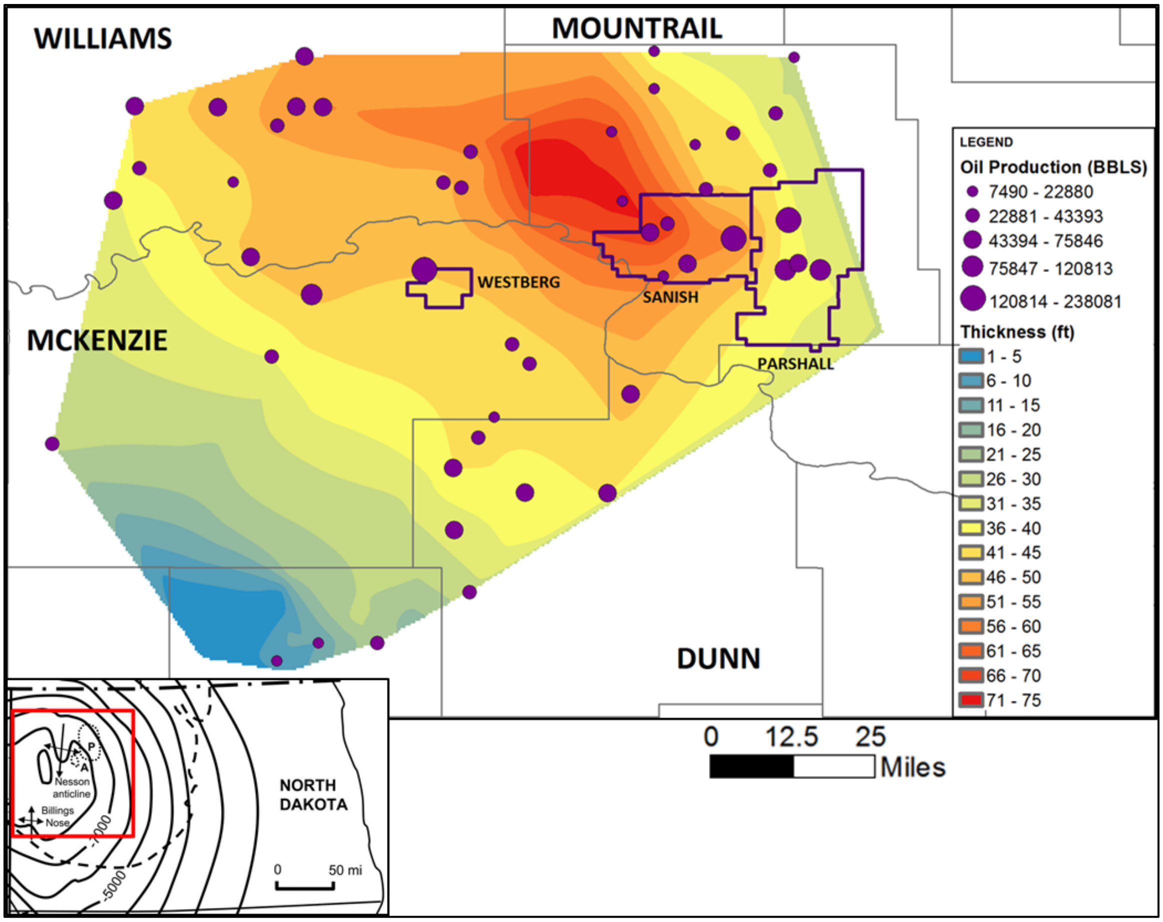

Figure 5.26. The first eight months of oil production values of 49 wells on top of the isopach map of the middle Bakken member. The wells in Sanish, Parshall, and Westberg fields have higher production rates compared to all other wells. The red frame in the bottom left shows the map location.

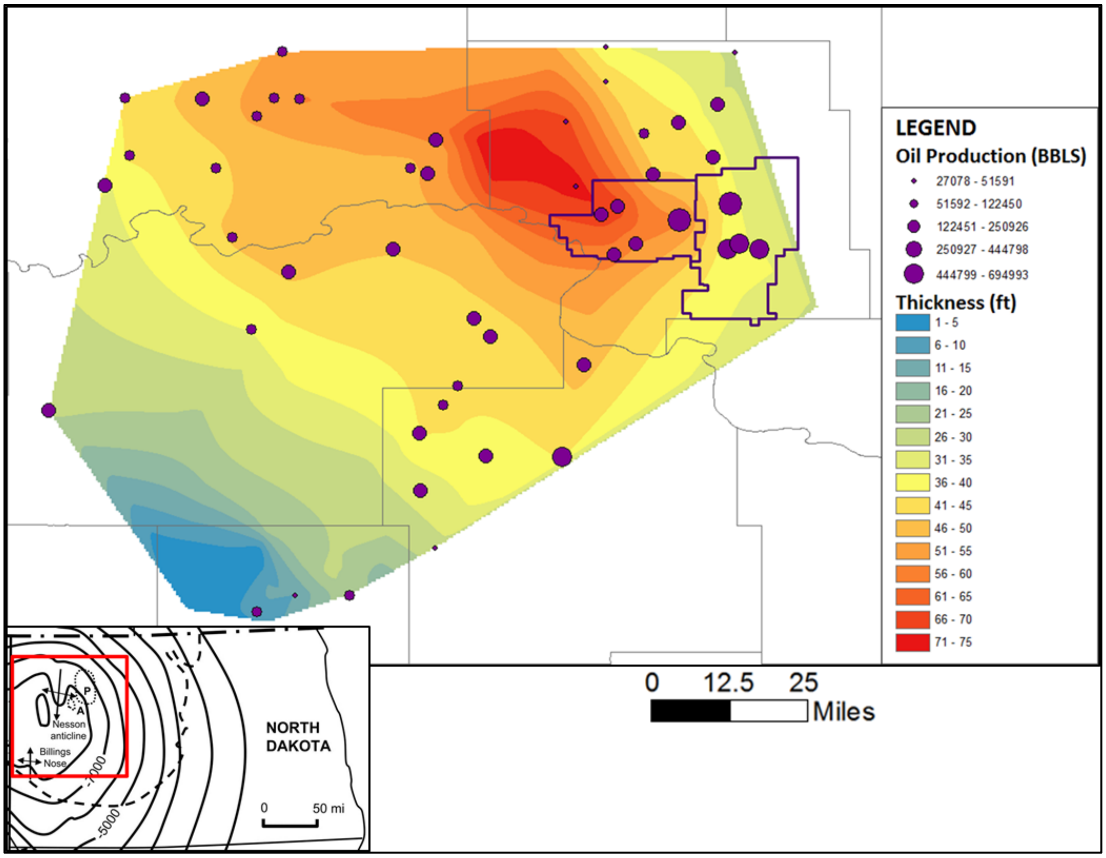

Figure 5.27. The total oil production values of 49 wells on top of the isopach map of the middle Bakken member. In the study area, most productive wells are located in Sanish and Parshall fields in Mountrail County. The red frame in the bottom left shows the map location.

5.5. Comparison of Log Data with Petrophysical and Elastic Parameters

Log data parameters such as gamma ray and resistivity, as well as, log data calculations including effective porosity, water saturation, and brittleness values were compared within the same chart to examine their effects on productivity. This process was applied for the following three wells: Nelson Farms 1-24H located in Ross Field, Mountrail County (Figure 5.5), Deadwood Canyon Ranch 43-28H located in Sanish Field, Mountrail County (Figure 5.6), and V. Chapin 32-21 located in Hawkeye Field, McKenzie County (Figure 5.7). These charts are discussed in the Discussion chapter.

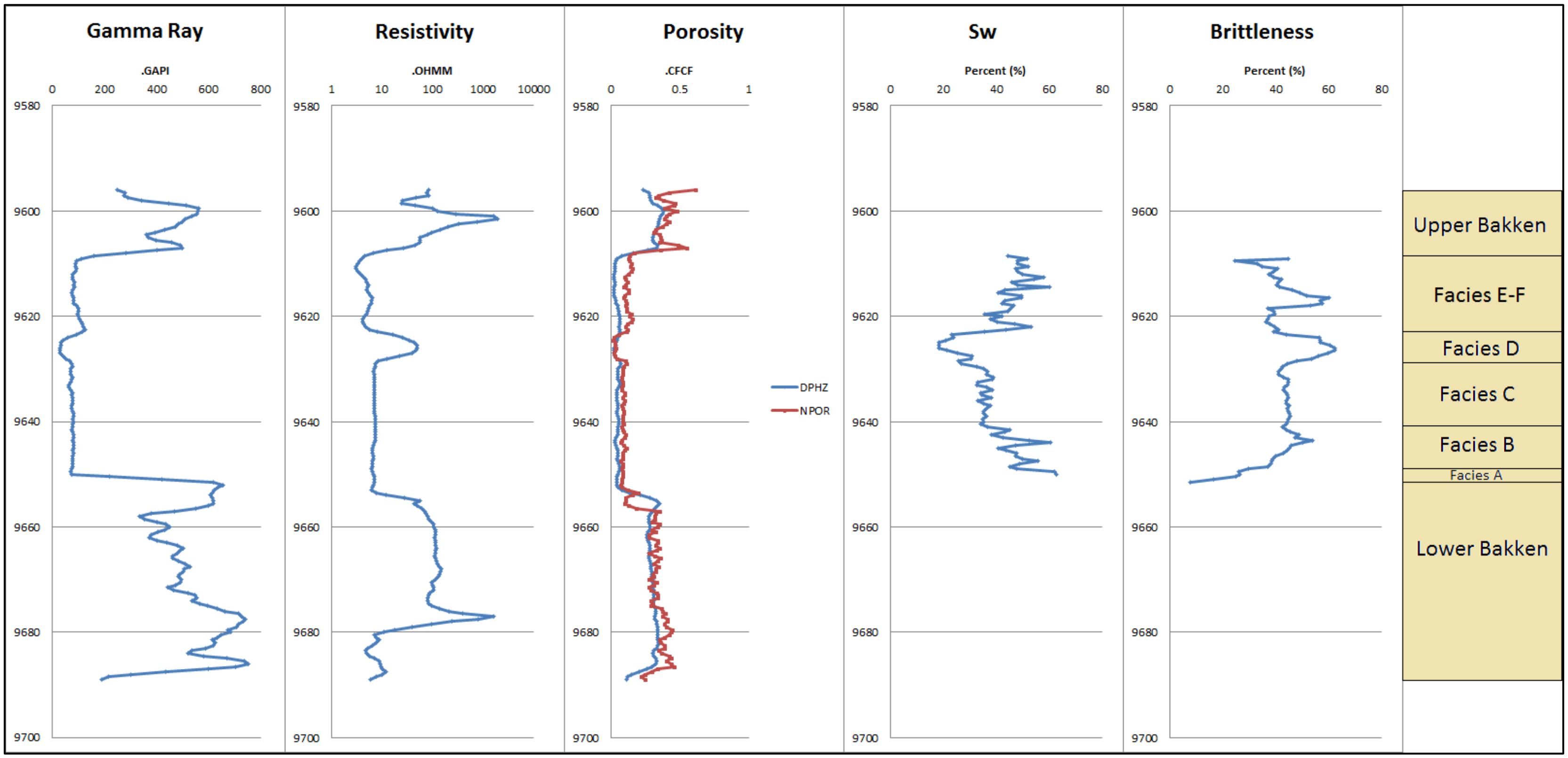

Figure 5.28. Petrophysical and elastic parameters of the Nelson Farms 1-24H well.

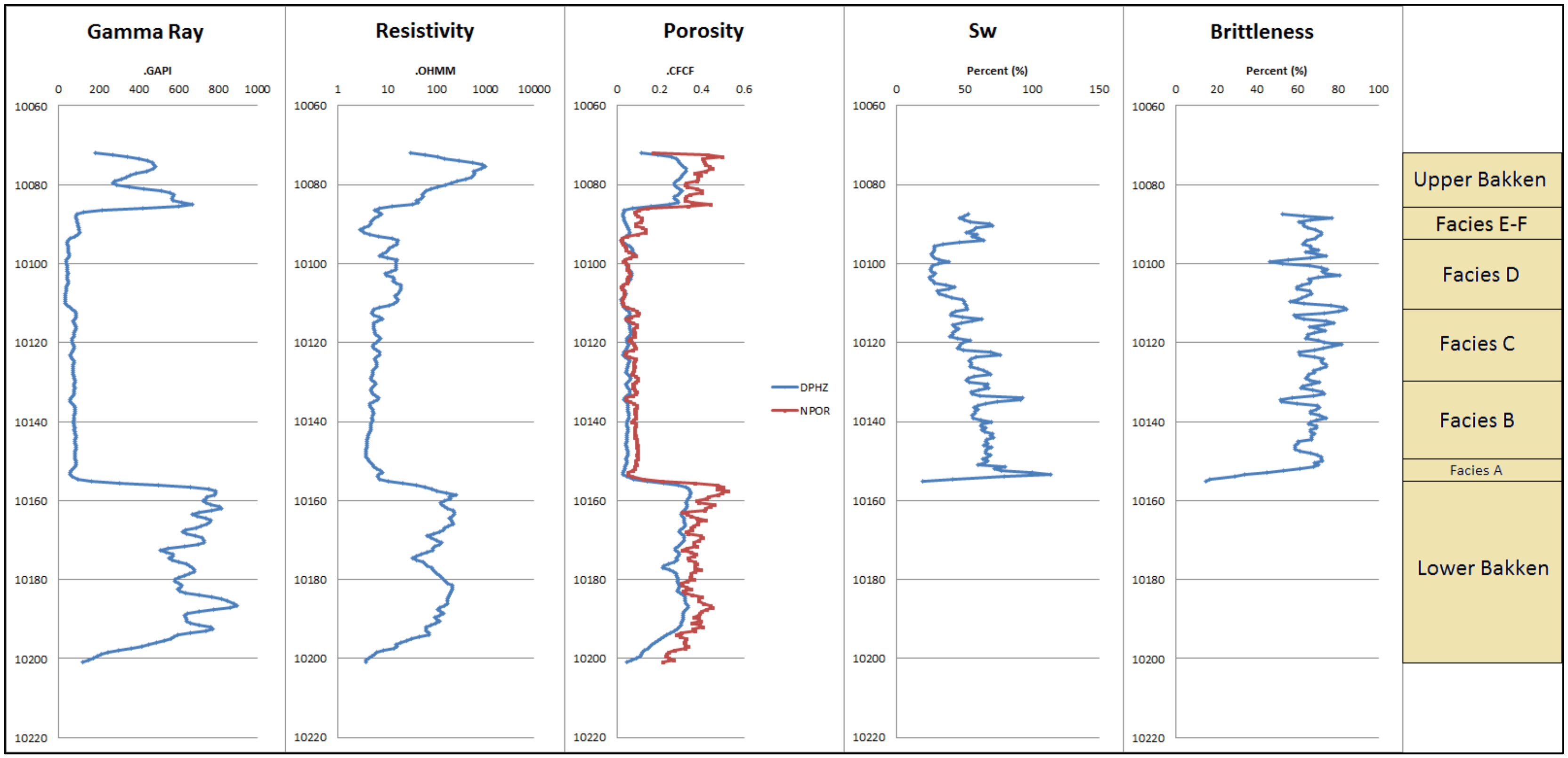

Figure 5.29. Petrophysical and elastic parameters of the Deadwood Canyon Ranch 43-28H well.

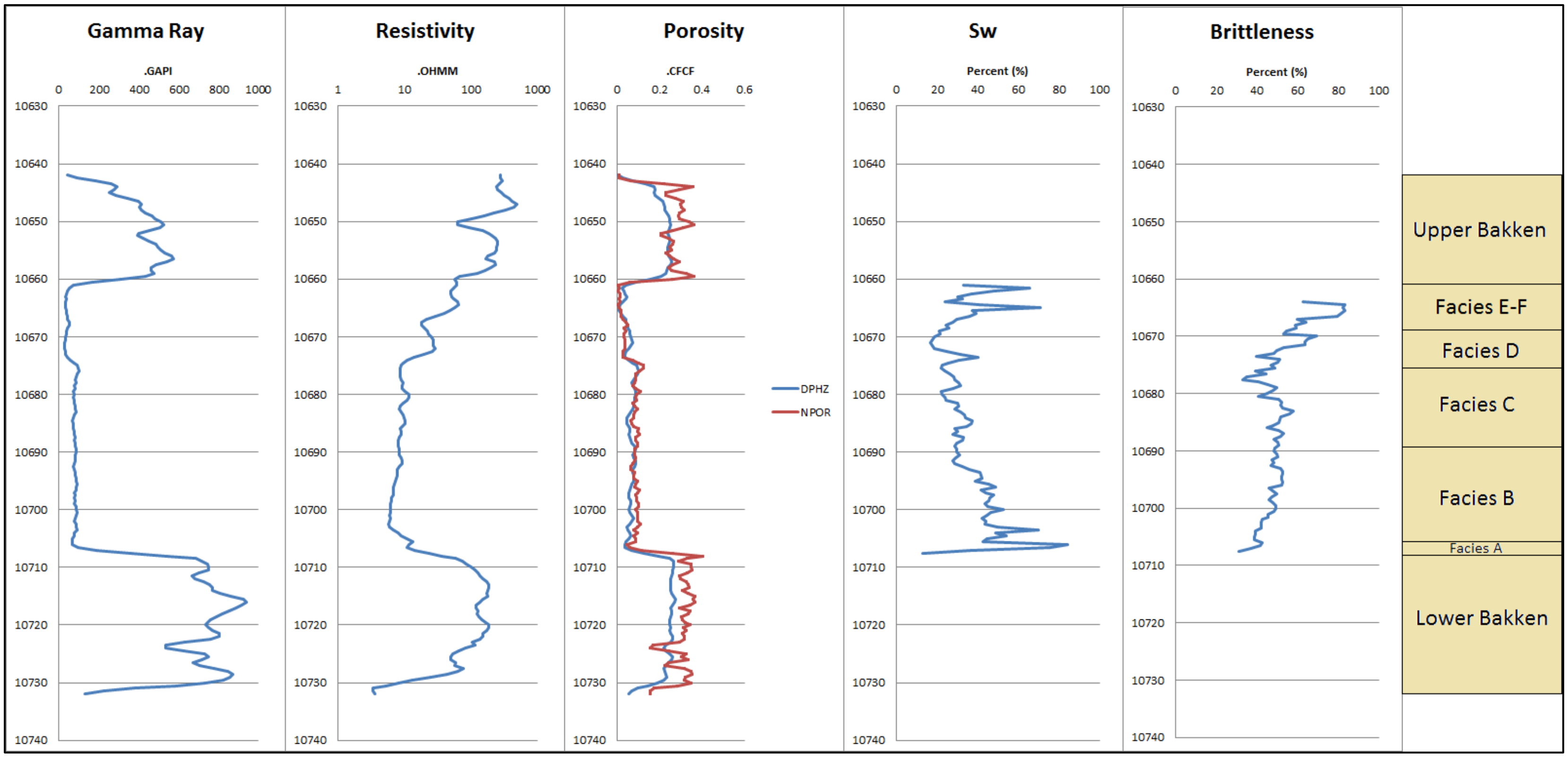

Figure 5.30. Petrophysical and elastic parameters of the V. Chapin 32-21 well.

5.6. Comparison of Production and Thickness

Several charts were created to test the relationship between thickness and production in the Bakken Formation. In Figure 5.31, the middle Bakken thickness and the first 8 months production values were compared. Moreover, each facies thickness was also compared with the first 8 months production values to examine facies thickness changes in productive wells. The comparison of thickness and production values of Facies B through D where shown in Figure 5.32, 5.33, 5.34 and 5.35. The green box in each figure below represents an anomaly of production.

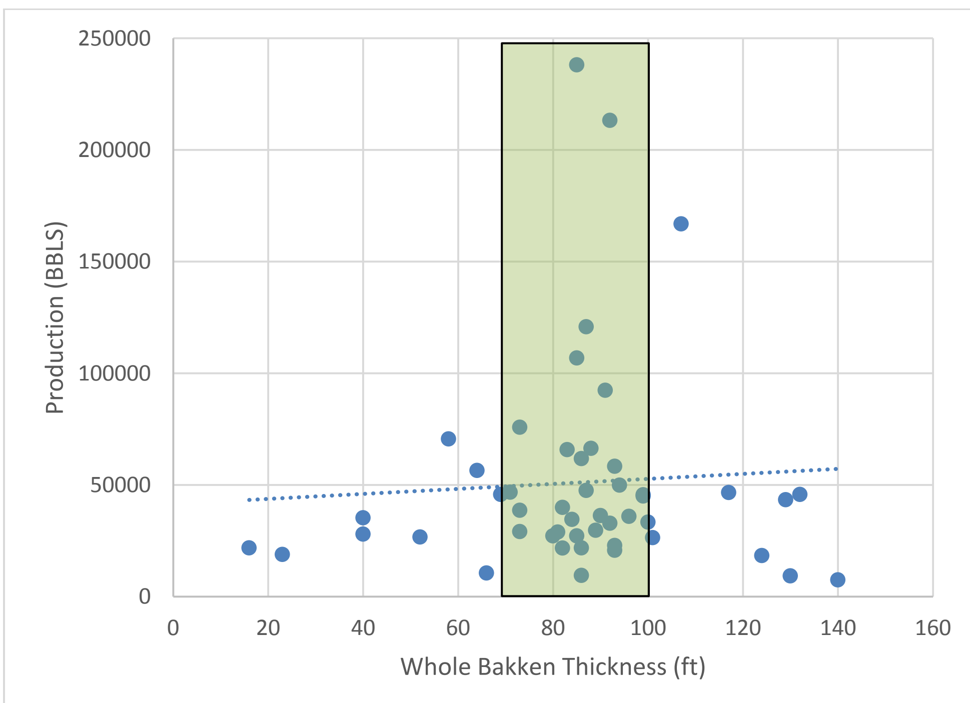

Figure 5.31. Comparison of the whole Bakken thickness with the first 8 months production.

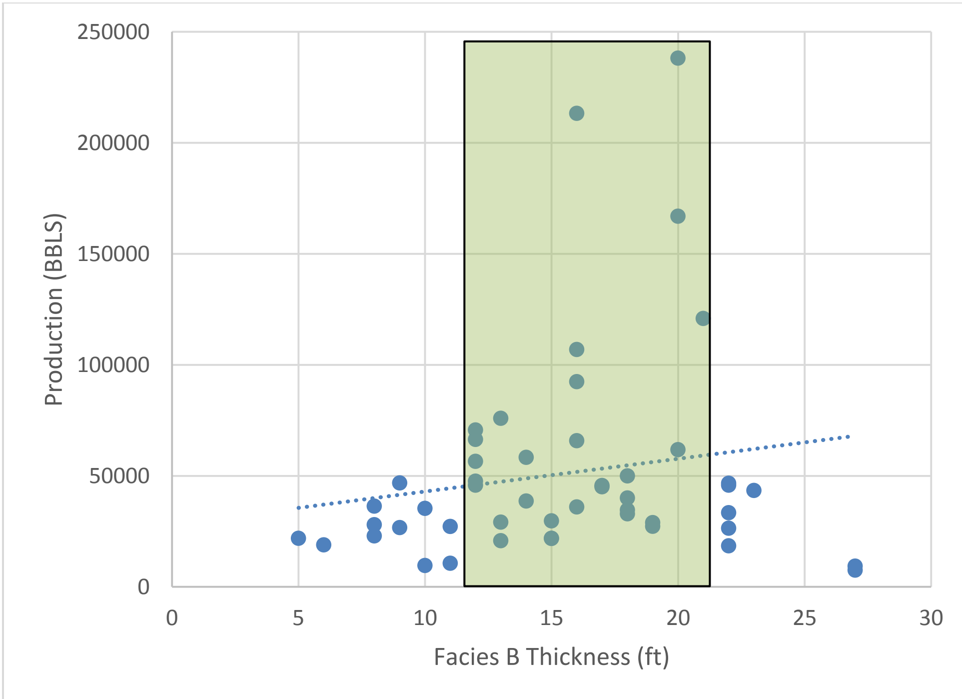

Figure 5.32. Comparison of Facies B thickness with the first 8 months production.

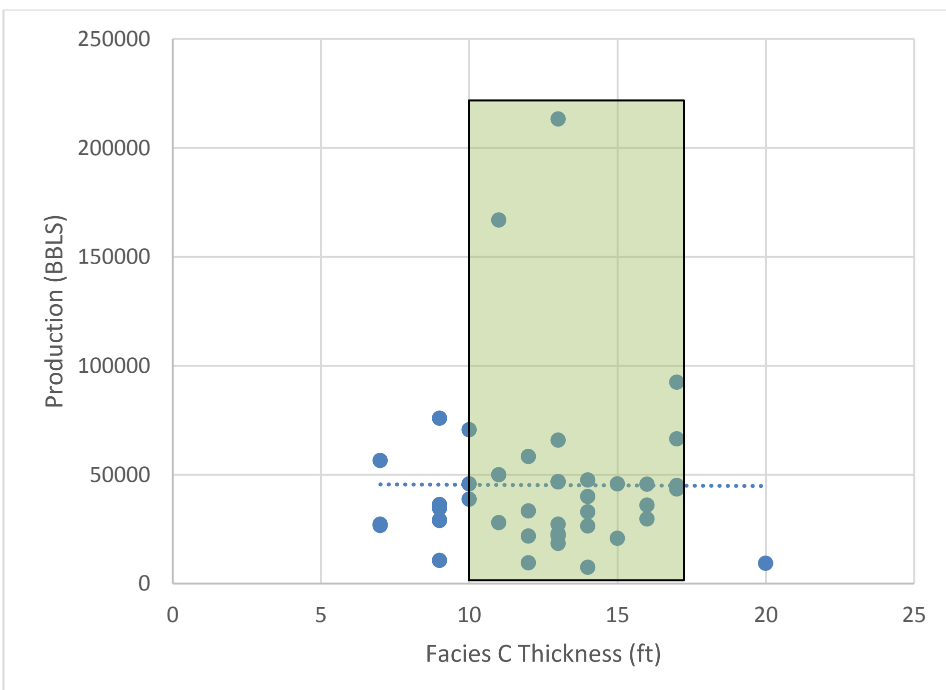

Figure 5.33. Comparison of Facies C thickness with the first 8 months production.

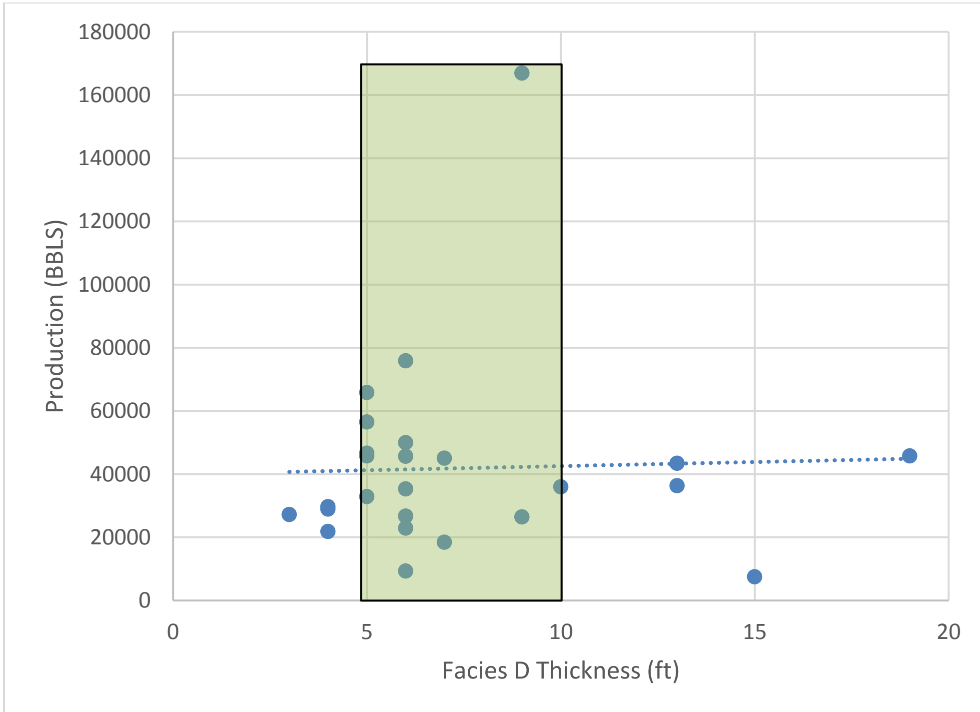

Figure 5.34. Comparison of Facies D thickness with the first 8 months production.

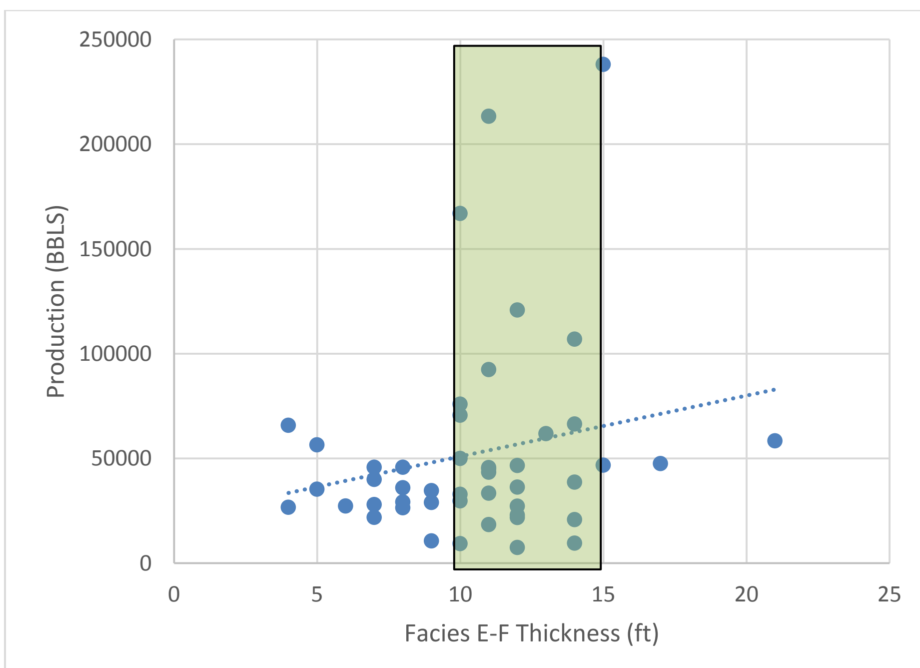

Figure 5.35. Comparison of Facies E-F thickness with the first 8 months production.

5.7. Comparison of Brittleness and Production

The brittleness of facies was compared with production values to investigate the relationship between them. The average brittleness values for each facies were compared with the first 8 months production values (Figure 5.36, 5.37, 5.38, and 5.39). The comparison charts were created by using 6 wells: NELSON FARMS 1-24H, CCU PRAIRIE ROSE 24-31H, DEADWOOD CANYON RANCH 43-28H, DEADWOOD CANYON RANCH 11-5H, LIND 2-1H, and GO-DARRYL-158-98-0904H-1. The locations of each well are shown in Appendix 1.

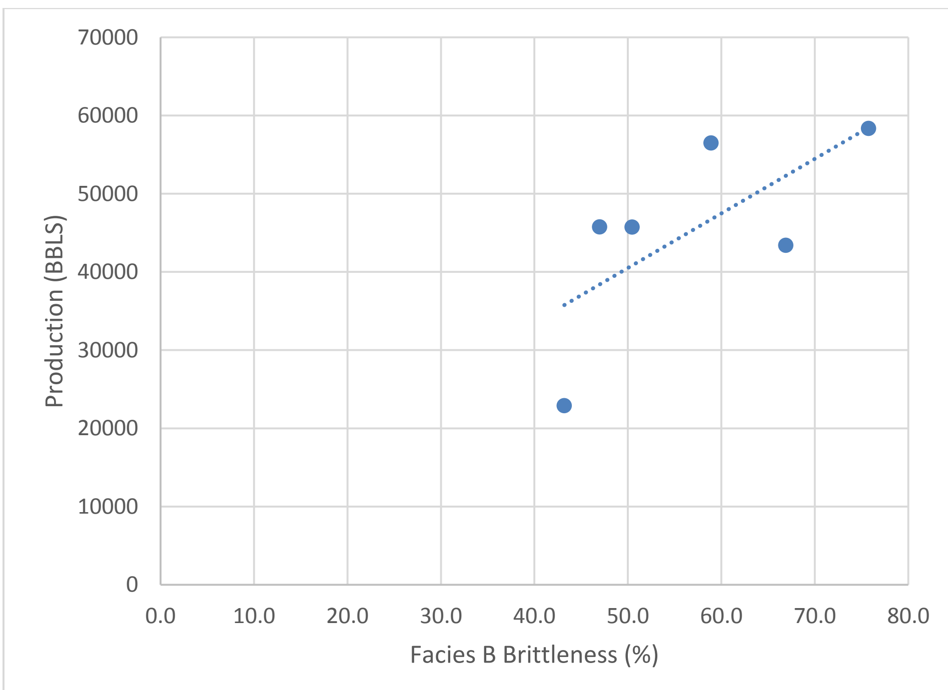

Figure 5.36. Comparison of Facies B brittleness with first 8 months production.

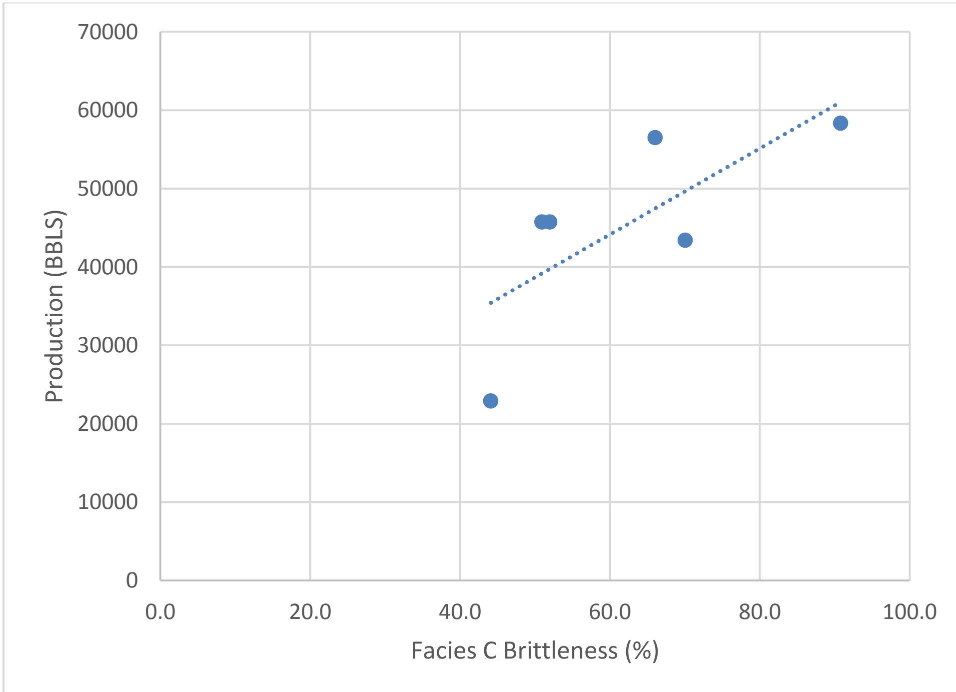

Figure 5.37. Comparison of Facies C brittleness with the first 8 months production.

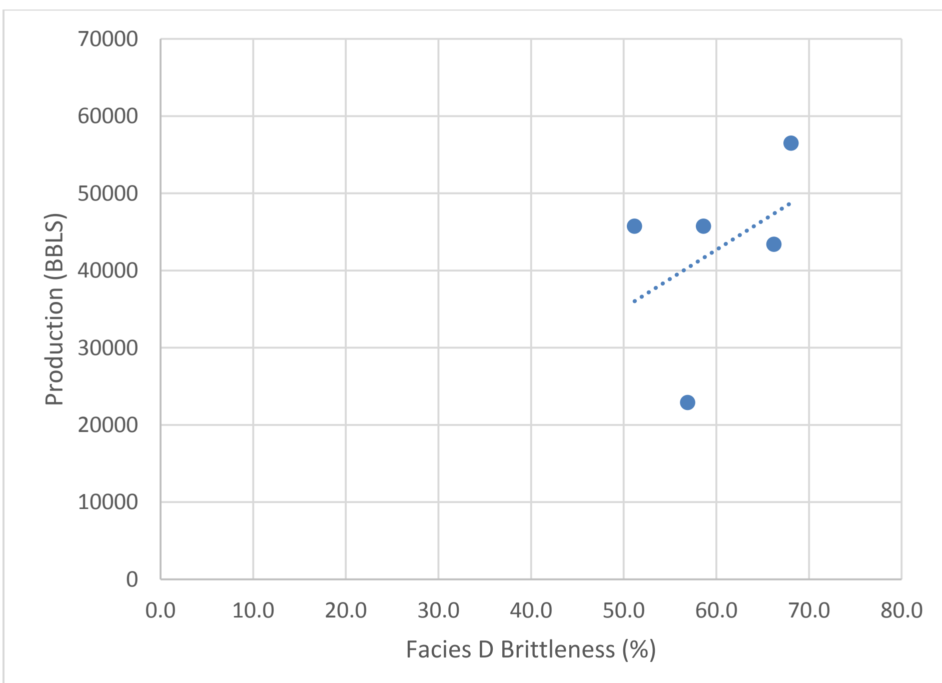

Figure 5.38. Comparison of Facies D brittleness with the first 8 months production.

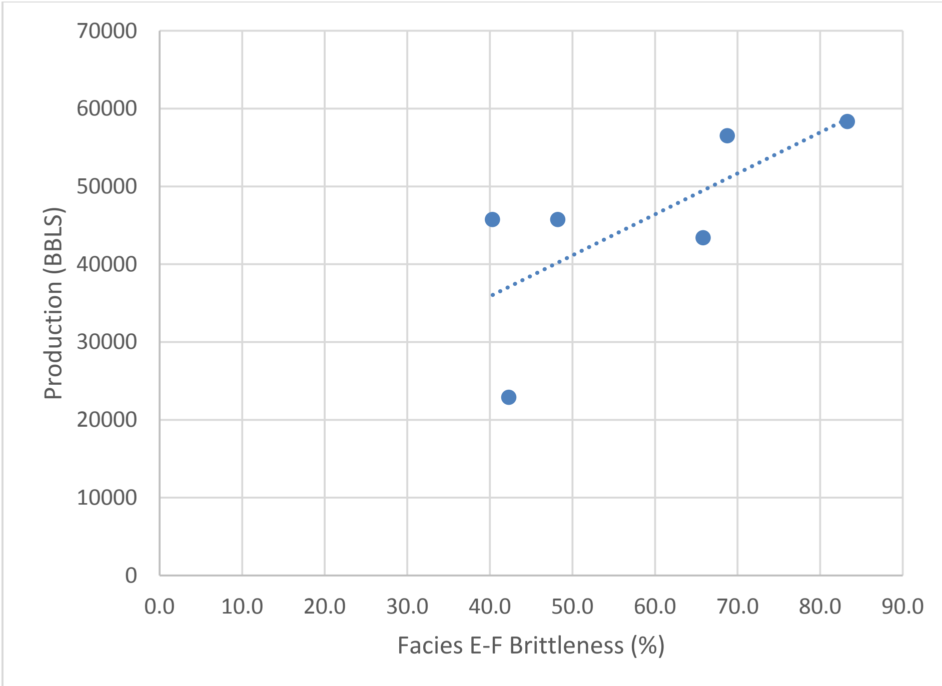

Figure 5.39. Comparison of Facies E-F brittleness with the first 8 months production.

6. DISCUSSION

Shale plays are unconventional reservoirs, and the production requires new technology such as horizontal drilling and hydraulic fracturing. Therefore, research about unconventional reservoirs focuses on the effects of key parameters on drilling and production. For example, Luker 2012 studied Marcellus Shale, which is an unconventional play, by examining mineralogy, TOC and sequence stratigraphy relationship. According to that study, production increases with certain mineralogy such as silica and calcite. Determinant factors on productivity are also tested in this study. This research mainly focused on the effects of thickness and petrophysical and elastic parameters especially the brittleness on productivity. Several cross sections, maps, and comparison charts were created and shown in previous chapters. In this chapter, these figures will be discussed in more detail.

Structural cross sections were plotted to examine the Bakken thickness changes all over the study area. In the central portion of the west-east oriented cross sections, Figure 5.2 and Figure 5.3, there is an uplift of the Bakken due to the Nesson anticline. In the west-east oriented cross-sections, the Bakken thins towards the west and thickens through the middle which also corresponds to the central portion of the Williston Basin. There is not any influence of the Nesson anticline in Figure 5.4. In addition, the Bakken is congruent with the shape of the Williston Basin. According to the south-north oriented cross section in Figure 5.5, the Bakken thins in the south which is close to the Bakken edge, and deepens and thickens through the middle which corresponds to the center of the formation. In the northern part, the thick Bakken interval is continuous although there is an upwelling. This part is not the edge of the formation since the Bakken extends over southern Canada.

Stratigraphic cross sections indicate thickness change and continuity of each facies over the study area. There is a thick Bakken deposition near the center of the basin. The facies become absent through the margins. Facies B, C, and E-F are the most continuous facies in the middle member. The continuity of Facies D is variable in different parts of the study area. It thins and becomes absent through the south. In each cross section, there is Facies D deposition near the center.

Different calculation methods were applied to calculate petrophysical and elastic parameters. Stieber and Clavier methods were used for the shale volume calculation. Since both methods showed similar results, the Stieber method was applied to calculate effective porosity and water saturation. Shale corrected porosity values are consistent with the core data porosity results. The water saturation values calculated from Archie's equation are also compatible with the core data results. Although this equation is a basic water saturation calculation, it is applicable for the Bakken Formation, which is an unconventional reservoir. On the other hand, the Simandoux model overestimates the water saturation (Figure 4.3) and is therefore not suited for the Bakken Formation.

Three kinds of oil-production maps were constructed including the last month of (April 2014) production, the first eight months of production, and total production. According to the April 2014 production map (Figure 5.25), the Westberg and Cabernet fields have the highest oil production values. Both wells from these fields can be considered as recent production wells since they have been producing for 14 and 16 months respectively. As mentioned before, production of unconventional wells tends to decline after an initial high production period. Therefore, both wells will probably experience a decrease in their production rates after the initial production period has passed. According to the map representing the first eight months of production (Figure 5.26), the wells in Sanish, Parshall and Westberg fields have high oil production values. According to the total production map (Figure 5.27), the Sanish and Parshall fields have the highest oil production. Since the facies are thicker in the central part of the formation, this may also increase the potential in productivity. The Sanish and Parshall fields are located where the middle Bakken thickness is changing between 36 – 55 feet, which can be considered as ample thickness.

Lithology and oil zones can be estimated from the consideration of several well logs which include gamma ray, resistivity, porosity, and velocity logs. Well log readings such as, convergent density-neutron porosity, and high resistivity readings are indicative of oil zones. During this study, possible Bakken target zones were estimated by the consideration of these logs in addition to the calculated parameters of water saturation and brittleness. Oil saturation increases as the water saturation decreases. Therefore, low water saturated parts can be interpreted as oil saturated zones as indicated by the water saturation calculations. Since the Bakken is an unconventional reservoir, oil production is fulfilled through the process of horizontal drilling and hydraulic fracturing. The determination of frackable parts is an important step for hydraulic fracturing. An increase in rock brittleness correlates to the frackability of a rock. Thus, for the determination of possible target zones in this study, the zones with higher brittleness were taken into account. Brittleness was also calculated by using mineralogy data showing the mineral percentages. The presence of carbonate minerals such as dolomite, limestone, and calcite add to the brittleness of a rock. Lastly, determined target zones were compared with the horizontal drilling depth, where the oil production is accomplished, to check the accuracy of the estimation.

The well-log parameters with calculated water saturation and brittleness values were plotted together for the Nelson Farms 1-24H well in Ross Field (Figure 5.28). Facies D, at a depth of 9622-9628 ft, has both high resistivity and convergent density-neutron porosity and can be considered a possible target. Calculations also indicate that Facies D has low water saturation (an average 22%) and high brittleness (up to 60%). The amount of carbonate minerals at 9628 ft is 36% dolomite and 10% calcite (Appendix 2). The significant amount of dolomite makes this facies an attractive hydro-fracturing target. According to the well post file from the NDIC website, this well has been drilled horizontally at a depth of 9616-9630 ft. The data from the NDIC confirmed the estimations made to determine oil zone location and productivity.

Petrophysical and elastic parameters were also compared for the Deadwood Canyon Ranch 43-28H well, in Sanish Field, in the efforts to target an oil zone (Figure 5.29). This well has a thick Facies D deposition between 10092-10110 ft where the resistivity is high and density-neutron porosities are convergent. Facies D has a low water saturation with an average of 25%, and high brittleness with up to an average of 61%. In terms of mineralogy, there is 20.54% calcite and 14.29% dolomite found at the depth of 10109.72 (Appendix 3). A 35% carbonate mineral percentage makes this facies an attractive target in terms of hydraulic fracturing. Horizontal drilling at this depth also confirms that this interval is a target zone.

The V. Chapin 32-21 well in Hawkeye Field was also assessed in terms of its production feasibility by examining petrophysical and elastic parameters (Figure 5.30). There are two zones, specifically the lower part of Facies E-F, and the whole of Facies D, which could be deemed an attractive prospect with a high resistivity. Although the lower part of Facies E-F has convergent porosities, and a high brittleness, it also has a high water saturation amount meaning there is a low oil accumulation. Facies D does not have a convergent porosity. It has increasing water saturation and decreasing brittleness corresponding to depth. Thus, these parameters indicate that this well is an undesirable location for oil production.

Thickness values of the whole Bakken and the middle Bakken facies were compared with the first eight months production amounts to check if there is a relationship between them. According to Figure 5.31, production trend increases with the increasing thickness. There is an anomaly of production where the Bakken varies in thickness between 70 ft and 100 ft. This area, which is also marked in the figure, shows a sweet spot for production. To check the detailed relation, each facies thickness was compared with the first eight months production values. The production trend increases in each facies with the increasing thickness except in Facies C. Each chart has anomaly values for a certain depth in terms of production. Figure 5.32 shows that the sweet spot thickness for Facies B changes between 12 – 21 ft. Facies C has an anomaly between 10 – 17 ft in terms of production (Figure 5.33). Production values correlate with Facies D in the depth which changes between 5 – 10 ft (Figure 5.34). Facies E-F where it changes between 10 – 15 in thickness, correlates with the production (Figure 5.35). These sweet spots can be an indicator for the production of oil in the Bakken Formation.

Another comparison was applied between production and brittleness values. The brittleness calculation from log data has been applied for six productive wells. Average brittleness values for each facies were compared with the wells' first 8 months production amounts. According to the production trends in Figure 5.36, 5.37, 5.38, and 5.39, production increases with increasing brittleness.

7. CONCLUSIONS

This research aims to investigate the depositional environment and characterize the reservoir rock properties of the Bakken Formation. Stratigraphy changes of the Bakken members, the middle Bakken facies, and the effects of the petrophysical and elastic properties' on production has been assessed in the northwest part of North Dakota.

Two depositional sequences were described by interpreting digital log data for 86 wells. Facies A, B and C constitute the highstand system tract of the first sequence boundary, Facies D composes the lowstand system tract, and Facies E-F generates the transgressive system tract of the second sequence. Facies A, B, and C were deposited from offshore to middle shoreface environment during the sea level rise. As a result of a sea level drop, Facies D was deposited in the middle shoreface environment. Facies E-F was deposited with the sea level rise in the outer ramp environment.

Petrophysical and elastic properties of the Bakken Formation have been examined by trying different calculation methods to determine the best method to reproduce the core data results for the Bakken Formation. The Stieber shale volume calculation method was applied during the calculation of effective porosity and water saturation. Since the Bakken Formation is a shale play, shale correction was applied for the effective porosity calculation. Archie's equation works better for the water saturation than the Simandoux model. Mineralogy data was used to calculate the brittleness of the Bakken Formation from different equations such as Jarvie (2007) and Wang (2009). Although the core data has a limited depth interval, the brittleness values from core data and log data show similar results. Several formulas were created for the brittleness calculation by using mineralogy and minerals' actual Poisson's ratio and Young's modulus values. The calculated brittleness values were not compatible with the log data brittleness. Similarly, the formula created for the calculation of compressional slowness from mineralogy and minerals' actual compressional slowness values did not show consistency with the log data slowness readings.

Effects of the petrophysical and elastic parameters were investigated on the production. Although the petrophysical parameters are suitable for the presence of oil, brittleness is a key factor for horizontal drilling. Being in a state of high brittleness, increases the frackability of the rock. The wells which produce from the Bakken Formation, have high brittleness values.

The thicker areas of the Bakken Formation indicate suitable areas for high oil production. Sanish and Parshall fields are the most productive oil fields of the Bakken Formation being located close to the central part of the Bakken Formation. Brittleness has an effect on the productivity. Brittleness analysis shows that an increase in brittleness also advances the production of oil.

In conclusion, brittleness is an important factor for oil production where horizontal drilling and hydraulic fracturing are applied. It can be a good determinant parameter on production.

8. FUTURE WORKS

During the brittleness calculation, the parameters, which are mineral percentages and actual Poisson's ratio and Young's modulus, were not enough to obtain close results to calculated brittleness from log data. Taking into consideration the other minerals' elastic values such as K-Feldspar, plagioclase and the adding of porosity values may provide better brittleness results.

During the compressional slowness calculation, the parameters used in the formula, which are mineral percentages and their actual compressional slowness values were insufficient to get close results with slowness readings from the log. Modifications of the formula such as adding porosity values and the slowness values of the liquids may help to get consistent results with the log data readings.

Obtaining seismic sections might help to interpret the distribution and depositional environment of the Bakken Formation. The combination of interpretations from seismic sections and log data will help to draw better depositional framework.

Appendix

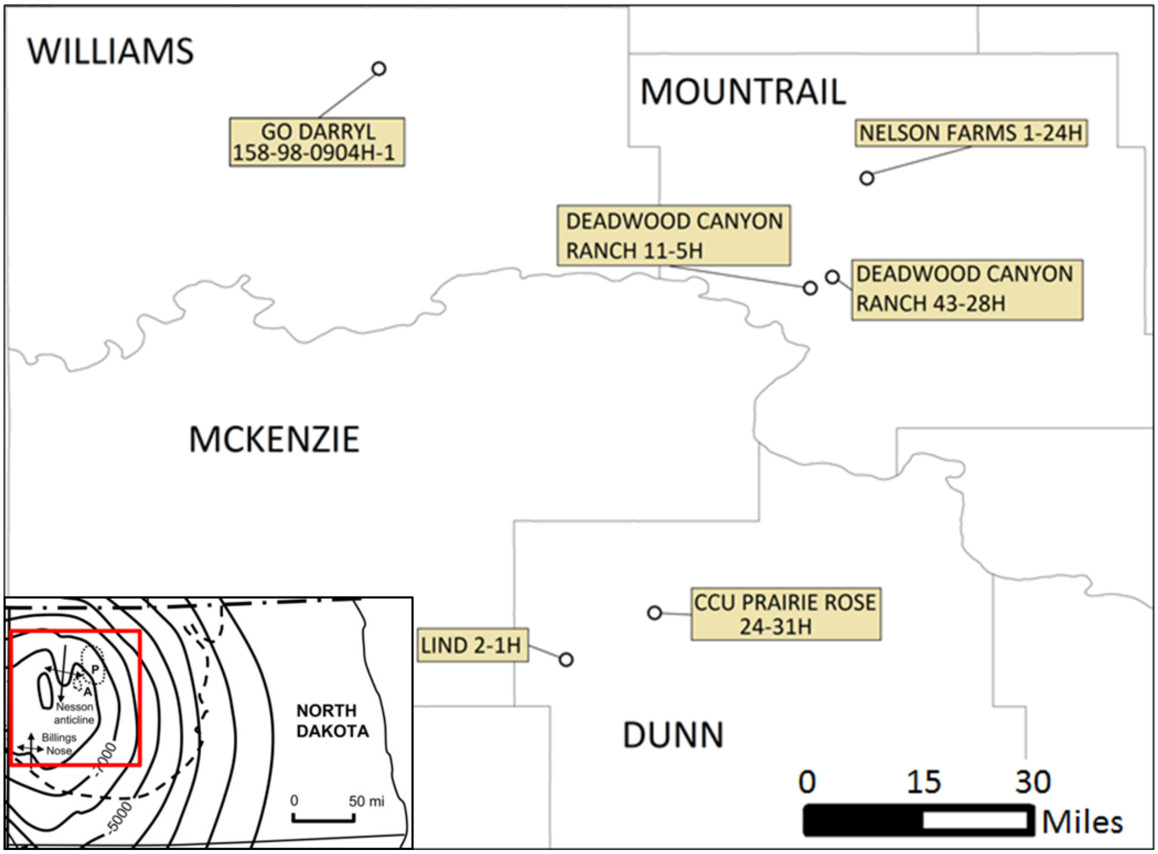

Appendix 1. Calculated brittleness locations for the north-west portion of North Dakota. The red frame in the bottom left shows the map location.

DEPTH	Quartz	K-Feldspar	Na-Feldspar	Calcite	Dolomite	Illite	Mixed layer Clay	15% HCl Acid Solubility
9628	26	2	7	10	36	10	9	45.5
9632.5	37	7	9	0	33	10	4	32.2
9636	19	0	1	76	4	0	0	78.4
9640	11	0	0	88	1	0	0	87.3
9645	43	6	4	10	19	9	9	27.8
9647	41	4	8	11	21	11	4	31.2
9651	23	6	10	31	11	19	0	41
9656	46	7	8	8	20	11	0	27.4

Appendix 2. Mineralogy values of the Nelson Farms 1-24H well in Ross Field (the NDIC website).

DEPTH (FT)	Quartz	K-Feldspar	Plagioclase	Illite/Smectite	Calcite	Dolomite	Pyrite	Kaolinite	Others
10079.1	26.96	2.32	2.14	13.39	12.32	38.04	0.00	0.00	4.82
10081.62	34.46	2.86	2.32	11.61	13.93	29.46	0.71	0.00	4.64
10082.71	37.86	3.57	3.39	15.71	3.21	30.18	0.71	0.00	5.36
10083.07	40.18	3.93	3.21	18.93	2.86	25.00	0.00	0.36	5.54
10095.87	44.64	2.50	1.25	7.14	29.29	10.71	0.54	0.00	3.93
10109.72	40.18	3.57	3.39	11.96	20.54	14.29	0.00	0.36	5.71
10113.57	42.32	3.93	3.39	13.57	14.46	17.14	0.00	0.00	5.18
10120.07	42.86	4.11	3.75	13.93	11.96	18.21	0.54	0.36	4.29
10134.02	36.07	3.21	3.04	17.32	16.61	13.39	4.29	0.71	5.36
10134.98	34.64	3.39	3.21	14.11	25.89	14.29	0.00	0.00	4.46
10135.99	40.18	3.57	3.57	18.57	12.32	15.54	0.54	0.54	5.18
10146.12	46.25	2.14	1.96	34.64	3.04	5.18	0.54	1.79	4.46

Appendix 3. Mineralogy values of the Deadwood Canyon Ranch 43-28H well in Sanish Field (the NDIC website).

References

Ahern, J. L. and Mrkvicka, S. R., 1984, A Mechanical And Thermal Model For the Evolution of the Williston Basin. Tectonics, v. 3, p. 79-102.

Angulo, S. and Buatois, L., 2009, Depositional Setting of the Upper Devonian – Lower Mississippian Bakken Formation of Subsurface Saskatchewan, Integrating Sedimentologic and Ichnologic Data: Frontiers and Innovation, Canadian Society of Petroleum Geologists Convention, Calgary, Proceedings, p. 829–832.

Anna, L. W., Pollastro, R., and Gaswirth, S. B., 2010, Williston Basin Province – Stratigraphic and Structural Framework to a Geologic Assessment of Undiscovered Oil and Gas Resources: Assessment of Undiscovered Oil and Gas Resources of the Williston Basin Province of North Dakota, Montana and South Dakota, U.S. Geological Survey Digital Data Series, p. 17.

Asquith, G. B. and Gibson, C. R., 1982, Basic Well Log Analysis for Geologists, The American Association of Petroleum Geologists, Tulsa, Oklahoma, p. 214.

Asquith, G. and Krygowski, D., 2004, Basic Well Log Analysis, 2nd edition, The American Association of Petroleum Geologists, Tulsa, Oklahoma, Series 16, p. 244.

Attanasi, E. D., Schmoker, J. W., and Quinn, J. C., 1995, Economics and continuous-type oil and gas accumulations in the 1995 National Assessment of U.S. Oil and Gas Resources, United States Department of Interior U.S. Geological Survey, p. 38.

Bellelli, J., 2013, The shale gas ‘revolution’ in the United States: Global implications, options for the EU, Directorate-General For External Policies, Policy Department, p. 18.

Burgess, P. M., 2008, Phanerozoic evolution of the sedimentary cover of the North American craton, in A. D. Miall, ed., The sedimentary basins of theUnited States and Canada: Amsterdam, Netherlands, Elsevier, Sedimentary Basins of the World, p. 31-63.

Burrus, J., Osadetz, K., Wolf, S., Doligez, B., Visser, K., and Dearborn, D., 1996, A Two-Dimensional Regional Basin Model of Williston Basin Hydrocarbon Systems: AAPG Bulletin, v. 80, p. 265–291.

Canter, L., Skinner, O., and Sonnenfeld, M. D., 2009, Facies and mechanical stratigraphy of the middle Bakken, Mountrail County, North Dakota: Abstract, SEPM Rocky Mountain Section meeting, Denver, Colorado.

Carmichael, R. S., 1982, Handbook of Physical Properties of Rocks, CRC Press, Boca Raton, FL, United States, Volume 2.

Crain's Petrophysical Handbook, http://spec2000.net/18-tightoil.htm accessed 7/7/2014.

Crain's Petrophysical Handbook (2), http://www.spec2000.net/05-mineralprops.htm accessed 7/7/2014.

Doveton, J. H., 1994, Geologic Log Analysis Using Computer Methods, The American Association of Petroleum Geologists, Tulsa, Oklahoma, No. 2.

Egenhoff, S., Dolah, A. V., Jaffri, A., and Maletz, J., 2011, Facies Architecture and Sequence Stratigraphy of the Middle Bakken Member, North Dakota, The Bakken-Three Forks Petroleum System in the Williston Basin: The Rocky Mountain Association of Geologists (RMAG), p. 27–47.

Flannery, J., 2006, Integrated analysis of the Bakken Petroleum System, U.S. Williston Basin, Saskatchewan Geological Society, Saskatchewan and Northern Plains Oil & Gas Symposium, p. 138-145.

Gaswirth, S. B., Marra, K. R., Cook, T. A., Charpentier, R. R., Gautier, D. L., Higley, D. K., Klett, T. R., Lwean, M. D., Lillis, P. G., Schenk, C. J., Tennyson, M. E., and Whidden, K. J., 2013, Assessment of Undiscovered Oil Resources in the Bakken and Three Forks Formations, Williston Basin Province, Montana, North Dakota, and South Dakota: USGS National Assessment of Oil and Gas Fact Sheet, 4 p.

Gerhard, L. C., Anderson, S. B., LeFever, J. A., and Carlson C. G., 1982, Geological Development, Origin, and Energy Mineral Resources of Williston Basin, North Dakota, The American Association of Petroleum Geologists Bulletin, v. 66, No. 8, p. 989–1020.

Gerhard, L. C., Anderson, S. B., and LeFever, J. A., 1987, Structural History of the Nesson Anticline, North Dakota, Rocky Mountain Association of Geologists, Williston Basin: Anatomy of a Cratonic Oil Province, p. 337–354.

Gerhard, L. C., Anderson, S. B., and Fischer, D. W., 1990, Petroleum geology of the Williston Basin: AAPG Memoir, v. 51, p. 507-559.

Greaves, G. N., Greer, A. L., Lakes, R. S., and Rouxel, T., 2011, Poisson's ratio and modern materials: Nature Materials, Review Article, p. 823–837.

Hayes, M. D., and Holland, Jr., F. D., 1983, Conodonts of Bakken Formation (Devonian and Mississippian), Williston Basin, North Dakota: AAPG Rocky Mountain Section Meeting, Billings, Montana, September 18, 1983, p. 1341–1342.

Holland, Jr., F. D., Hayes, M. D., Thrasher, L. C., and Huber, T. P., 1987, Summary of the Biostratigraphy of the Bakken Formation (Devonian and Mississippian) in the Williston Basin, North Dakota, in C.G. Carlson, and J.E. Christopher, eds., Fifth International Williston Basin Symposium: Saskatchewan Geological Society Special Publication 9, p. 68–76.

Jin, H., and Sonnenberg, S. A., 2012, Source Rock Potential of the Bakken Shales in the Williston Basin, North Dakota and Montana, AAPG Search and Discovery Article, No: 20156.

Kent, D. M., and Christopher, J. E., 1994, Geological History of the Williston Basin and the Sweetgrass Arch, in G. D. Mossop and I. Shetsen, comp., Geological atlas of the Western Canada sedimentary basin: Calgary, Alberta, Canada, Canadian Society of Petroleum Geologists and Alberta Research Council Special Report 4, p. 421-429.

Kuhn P. P., Primio R., Hill, R., Lawrence J. R., and Horsfield B., 2012, Three-dimensional modeling study of the low-permeability petroleum system of the Bakken Formation, AAPG Bulletin, V. 96, No. 10, p. 1867-1897.

LeFever, J. A., 1991, History of Oil Production from the Bakken Formation, North Dakota, Montana Geological Society: 1991 Guidebook to Geology and Horizontal Drilling of the Bakken Formation, p. 3–17.

LeFever, J. A., 1992, Horizontal drilling in the Williston Basin, United States and Canada *in* Schmoker, J. W., E. B. Coalson, C. A. Brown, eds., Geological studies relevant to horizontal drilling: examples from western north America, Denver, Colorado, Rocky Mountain Association of Geologists, p. 177-197.

LeFever, J. A., 2008, Bakken Formation Map Series: North Dakota Geological Survey, scale 1:1,000,000, 5 sheets.

LeFever, J. A., LeFever, R. D., and Anderson, S. B., 1987, Structural Evolution of the Central and Southern Portions of the Nesson Anticline, North Dakota, Fifth International Williston Basin Symposium, p. 147–156.

LeFever, J. A., Martiniuk, C. D., Dancsok, E. F. R., and Mahnic, P. A., 1991, Petroleum potential of the middle member, Bakken Formation, Williston Basin: 6th International Williston Basin Symposium, Regina, Saskatchewan, October 7–9, 1991, p. 74–94.

LeFever J. A., LeFever, R. D., and Nordeng, S. H., 2011, Revised Nomenclature for the Bakken Formation (Mississippian-Devonian), North Dakota, The Bakken-Three

Forks Petroleum System in the Williston Basin, The Rocky Mountain Association of Geologists (RMAG), p. 11-26.

Luker, A. T., 2012, A Comparison of Sequence Stratigraphy and Mineralogical Variations Associated with Total Organic Carbon in the Marcellus Formation: Washington County, Pennsylvania, University of Houston M.S. Thesis, p. 133.

Mavko, G., Mukerji, T., and Dvorkin, J., 2003, The Rock Physics Handbook, Tools For Seismic Analysis in Porous Media, Cambridge University Press, p. 324.

Meissner, F. F., 1978, Petroleum geology of the Bakken Formation, Williston Basin, North Dakota and Montana: Montana Geological Society 24th Annual Conference, Billings, Montana, September 24–27, 1978, p. 207–227.

Milici, R., and Swezey, C., 2006, Assessment of Appalachian Basin Oil and Gas Resources: Devonian Shale-Middle and Upper Paleozoic Total Petroleum System: U.S. Geological Survey, Reston, Virginia, p.1-70.

Nisbet, E. G. and Fowler, M. R., 1984, A Review of Some Models For the Formation of the Williston Basin, 1984, Saskatchewan Geological Society, Oil and Gas in Saskatchewan, p. 1-3.

Perez, R., 2013, Integration of Surface and Subsurface in the Reservoir Characterization of Unconventional Plays, AAPG Search and Discovery Article, No: 41211.

Pitman, J. K., Price, L. C., and LeFever, J. A., 2001, Diagenesis and fracture development in the Bakken Formation, Williston Basin: Implications for reservoir quality in the middle member: U.S. Geological Survey Professional Paper, v. P1653, p. 1–19.

Pollastro, R. M., Cook, T. A., Roberts, L. N. R., Schenk, C. J., Lewan, M. D., Anna, L. O., Gaswirth, S. B., Lillis, P. G., Klett, T. R., and Charpentier, R. R., 2008, Assessment of undiscovered oil resources in the Devonian-Mississippian Bakken Formation, Williston Basin Province, Montana and North Dakota: USGS National Assessment of Oil and Gas Fact Sheet, 2 p.

Pollastro R. M., Roberts L. N. R., and Cook, T. A., 2010, Assessment of Undiscovered Oil and Gas Resources of the Williston Basin Province of North Dakota, Montana, and South Dakota, U.S. Geological Survey Digital Series DDS-69-W.

Price, L. C., Daws, T. A., and Pawlewicz, M. J., 1986, Organic metamorphism in the Lower Mississippian–Upper Devonian Bakken shales: Part 1. Rock-Eval pyrolysis and vitrinite reflectance: Journal of Petroleum Geology, v. 9, p. 125-162.

Ratner, M. and Tiemann, M., 2014, An Overview of Unconventional Oil and Natural Gas: Resources and Federal Actions, Congressional Research Service, p. 27.

Rider, M. and Kennedy, M., 2011, The Geological Interpretation of Well Logs, 3rd edition, Rider-French Consulting Limited, p. 432.

Schmoker J. W. and Hester, T. C., 1983, Organic Carbon in Bakken Formation, United States Portion of Williston Basin, The American Association of Petroleum Geologists Bulletin, V. 67, No. 12, p. 2165–2174.

Simenson, A., 2010, Depositional Facies and Petrophysical Analysis of the Bakken Formation, Parshall Field, Mountrail County, North Dakota, Colorado School of Mines M.S. Thesis, 219 p.

Simenson, A. L., Sonnenberg, S. A., and Cluff, R. M., 2011, Depositional Facies and Petrophysical Analysis of the Bakken Formation, Parshall Field and Surrounding Area, Mountrail County, North Dakota, The Bakken-Three Forks Petroleum System in the Williston Basin: The Rocky Mountain Association of Geologists (RMAG), p. 48–101.

Sloss, L. L., 1963, Sequences in the cratonic interior of North America: Geological Society of America Bulletin, v. 74, p. 93-114.

Smith, M. G. and Bustin, R. M., 1995, Sedimentology of the Late Devonian and Early Mississippian Bakken Formation, Williston Basin: Montana GS: Seventh International Williston Basin Symposium, p. 103–114.

Smith, M. G. and Bustin, R. M., 1996, Lithofacies and Paleoenvironments of the Upper Devonian and Lower Mississippian Bakken Formation, Williston Basin, Bulletin of Canadian Petroleum Geology, Vol. 44, No 3, p. 495–507.

Sonnenberg, S. A., and Pramudito, A., 2009, Petroleum geology of the giant Elm Coulee field, Williston Basin: AAPG Bulletin, v. 93, No.9, p. 1127–1153.

Sonnenberg, S. A., Vickery, J., Theloy, C., and Sarg, J. F., 2011, Middle Bakken Facies, Williston Basin, USA: A Key to Prolific Production, AAPG Search and Discovery Article, No: 50449.

Thrasher, L. C., 1987, Macrofossils and Stratigraphic Subdivisions of the Bakken Formation (Devonian-Mississippian), Williston Basin, North Dakota, in Carlson C. G., and Christopher, J. E., eds., Fifth International Williston Basin Symposium: Regina, Saskatchewan Geological Society Special Publication 9, p. 53–67.

USGS, 2013, http://certmapper.cr.usgs.gov/data/noga00/natl/graphic/2013/mean_cont_oil_2013.pdf accessed 7/7/2014.

Wang, Z., Wang, H., and Cates, M. E., 2001, Effective Elastic Properties of Solid Clays, Geophysics, vol. 66, no.2, p. 428–440.

Webster, R. L., 1984, Petroleum source rocks and stratigraphy of the Bakken Formation in North Dakota: 1984 Symposium of the Rocky Mountain Association of Geologists, p. 57–81.

Webster, R. L., 1987, Petroleum Source Rocks and Stratigraphy of the Bakken Formation in North Dakota, Williston Basin: Anatomy of a Cratonic Oil Province, Rocky Mountain Association of Geologists, p. 269–285.